BRITZ, HESTER ESNA

APPLICATION OF FLOW-INJECTION ANALYSIS AS PROCESS ANALYZERS

MSc UP 1996

Application of flow-injection analysis as process analyzers

by

Hester Esna Britz

Submitted in partial fulfilment of the requirements for the degree

MAGISTER SCIENTIAE

in the Faculty of Science

University of Pretoria

Pretoria

November 1996

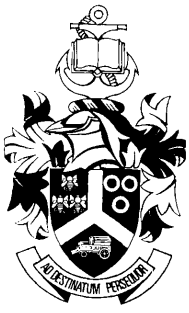

Application of flow-injection analysis as process analyzers

by

Hester Esna Britz

Submitted in partial fulfilment of the requirements for the degree

MAGISTER SCIENTIAE

in the Faculty of Science
University of Pretoria
Pretoria
November 1996

Supervisor: Prof Jacobus F van Staden
Department of Chemistry
University of Pretoria

SYNOPSIS

Flow-injection analysis has developed into a powerful tool for not only substituting tedious manual procedures, but also revolutionising conventional operations in the analytical laboratory. The advantages and disadvantages of flow-injection analysis is discussed briefly. Different quantitative evaluations are investigated to cover the theoretical background of this technique. The influence of various hydrodynamic and geometric factors on dispersion are discussed. Attention is given to the design of the flow-injection system, including instrumental set-up and computerized control and data acquisition. In-line liquid-liquid extraction and dialysis techniques are described. A method for in-line flow injection extraction preconcentration through a passive hydrophylic membrane to determine total phenols in oil is proposed. Methods for the determination of ketones and aldehydes in water and oils are described as well as methods for the determination of alcohols in water and oil.

Toepassing van vloei-inspuit analise as prosesanaliseerders

deur

Hester Esna Britz

Voorgelê ter gedeeltelike voldoening aan die vereistes vir die graad

MAGISTER SCIENTIAE

in die Fakulteit Natuurwetenskappe
Universiteit van Pretoria
Pretoria
November 1996

Studieleier: Prof Jacobus F van Staden
Departement Chemie
Universiteit van Pretoria

SYNOPSIS

Vloei-inspuit analise het ontwikkel in 'n kragtige tegniek wat tydrowende analitiese metodes vervang en ook talle nuwe uitdagings ten opsigte van konvensionele analises aanbied. Die voordele en nadele van vloei-inspuit analise word kortliks bespreek. Die teoretiese agtergrond van vloei-inspuit analise word bespreek deur verskillende kwantitatiewe benaderings te oorweeg. Die invloed van verskillende hidrodinamiese en geometriese faktore op dispersie word ondersoek. Die ontwerp van die vloeisisteem (instrumentele opstelling, gerekenariseerde beheer, gerekenariseerde data opname en gerekenariseerde data manipulasie) word uiteengesit. Aan-lyn vloeistof-vloeistof ekstraksie en dialise word bespreek. 'n Metode vir aan-lyn vloei-inspuit ekstraksie en prekonsentrasie deur 'n passiewe hidrofiliese membraan om totale fenole in olie te bepaal, word voorgestel. Metodes vir die bepaling van ketone en aldehiede in water en olies word beskryf. Metodes vir die bepaling van alkohole in water, wyn en bier en olies word beskryf.

Acknowledgements

I praise our Lord for his love! "He that dwelleth in the secret place of the Most High shall abide under the shadow of the Almighty. I will say of the LORD, He is my refuge and my fortress: my God; in him will I trust." Psalm 91 : 1, 2.

I want to thank my supervisor, prof JF van Staden, for his guidance and endurance. I had the opportunity to be a member of an excellent research group.

Sasol supplied chemicals, samples and financial support for the project.

My parents, Billy and Susan, and the rest of my family, Chris and Jorien, believed in me and gave love and encouragement all the way. You are the best!

The company and support of my friends at the University of Pretoria gave the work meaning. I want to thank you all for listening, giving good advice and sharing in the successes.

I want to thank Mias for his support and encouragement.

Table of Contents

CHAPTER 1

FLOW INJECTION ANALYSIS

1.1 Introduction

Flow-injection analysis, FIA, was originally considered to be a technique for automation of serial assays. This technique has developed into a powerful tool for not only substituting tedious manual procedures, but also revolutionising conventional operations in the analytical laboratory. FIA was formally defined as "Information gathering from a concentration gradient formed from an injected, well-defined one of a fluid, dispersed into a continuous unsegmented stream of a carrier" [1]. FIA constitutes the most advanced form of solution manipulation available to analytical chemists for the mixing of sample, reagents and reaction products and their transport to the measurement point.

FIA is a continuous flow analysis (CFA) method and forms part of automatic methods of analysis. The main features of FIA are as follows.

- Air bubbles are absent.
- The sample is injected directly into the carrier stream.
- The sample may undergo chemical reaction, dialysis, liquid-liquid extraction, etc. during transport before detection.
- The dispersion of the sample during transport can be controlled by changing the physical characteristics of the FIA system.

- The continuous signal from the detector is suitably recorded.

- FIA is a fixed-time automatic method, since neither physical nor chemical equilibrium has been attained when the signal is detected.

1.2 Advantages and disadvantages of FIA

FIA has a simple basis, its equipment is not expensive and rapid, accurate and precise results are produced by this versatile method [2]. The researcher can adapt a specific FIA system easily to suit a different application, without employing (expensive) teams of electronic and mechanical engineers [3]. FIA can be used to obtain excellent and fast results without using glassware (those are replaced by tubes, pumps and valves) and without exposing the analyst to toxic reagents. Reagents and samples are safe from atmospheric gases (CO_2, O_2 and humidity) and contamination. There are two main types of continuous analysis: segmented (SFA) and unsegmented (FIA). Why was FIA chosen for the continuous analysis?

The main difference between SFA and FIA is that SFA makes use of air bubbles. The air bubbles were used to prevent cross-contamination, dilution of the sample and to create turbulent flow in aid to reaching physical and chemical equilibrium before detection. The use of air bubbles results in a pulsating flow and lag in recording the signal. These bubbles had to be introduced and removed reproducibly before detection and continuous separation devices had limited efficiencies. The build-up of static electricity is unwanted. The flow rate is less reproducible than with FIA. SFA systems are too technically complex to miniaturise.

FIA apparatus is suitable for miniaturisation. A low flow rate is used with the FIA systems which means the reagent consumption is low. The use of a wash-out cycle to avoid cross-contamination between samples is not necessary with FIA, as the carrier stream continuously rinses the system. The sample throughput is exceptionally high. FIA produces not only peak height as data, but also peak area, peak width (for FIA gradient methods) and peak-to-peak measurements (for stopped-flow determinations).

FIA analysis may be considered a hybrid of SFA and HPLC (high pressure liquid chromatography). The similarities between FIA and HPLC are obvious:

- both systems can be miniaturised,
- the sample is injected,
- the flow is unsegmented,
- the sample volume is small,
- the same signal profile can be seen and
- no lag phase is present.

However, in HPLC there is always an interface to separate mixtures of substances through the use of a column. Columns are not a usual component of FIA systems. HPLC makes use of high pressure pumps to overcome the hydrodynamic resistance of columns. These columns are packed with fine material to improve the efficiency of the separation process. Generally FIA systems are much simpler and cheaper than HPLC systems.

HPLC and FIA have different scopes of application. The basic aim of an HPLC instrument is to separate and analyse a complex mixture of substances. This is not the aim of FIA! The remarkably high sampling rate makes FIA ideal for rapid determinations of a single species in a large number of samples.

1.3 Process analysers

A chemical manufacturing process can be monitored by measuring only temperature, pressure and flow rate. Timely composition data of the product streams can give additional information and became imperative in modern manufacturing processes:

- It is necessary for the safe operation of a plant, as runaway reactions cause loss of lives and equipment.

- Better quality control of products as required by the consumer can be achieved.

- It can lower quality costs associated with reprocessing, destroying or selling of off-spec material.

- Product performance can be determined during manufacturing. For example, octane numbers for gasoline and other parameters are determined on-line by using near infrared spectral data.

- Stringent regulations are set by the authorities in relation to production and production processes. Data on impurities, solvents and wastewater are needed to ensure that chemical manufacturing is safe for workers, communities near chemical plants and for the environment.

- Stronger economic competition requires a minimisation of energy consumption and a reduction of the amount of raw materials used in the process operation.

There are two approaches to process control. Firstly, samples from the process environment are sampled manually, transported to a centralised analytical laboratory, analysed by qualified technical staff who also process the data obtained and report the results obtained to the plant. Only then can corrective action be taken and plant conditions accordingly adjusted. Such analysis is generally used to measure process efficiency, to identify materials which need to be reworked or discarded or to assess the charge for the next stage in a multistage batch synthesis.

Secondly, Process Analytical Chemistry (PAC) can be implemented. PAC analysers are situated in or immediately next to the manufacturing process. These analysers can be operated automatically or by non-technical staff such as process operatives. Real or near-real-time data produced can now be used for process control and optimisation.

The application of analytical science to the monitoring and control of industrial chemical process is called Process Analytical Chemistry (PAC) [4,5]. PAC has been applied in the petroleum and petrochemical industries since the 1950s. This field is rapidly developing in all areas of chemical production: petroleum, fine chemicals, commodity chemicals, petrochemicals, biotechnology, food, pharmaceuticals, etc.

The differences between off-line analysis, at-line analysis, on-line analysis and in-line analysis need attention.

Off-line analysis:

- The sample is manually removed.
- The sample is transported to the measurement instrument located in a specialised central laboratory.
- Highly qualified technical staff is used for carrying out the analysis.
- The sample frequency is relatively low.

- The sample preparation is complex.
- The analysis is flexible and complex.
- Expensive instruments and skilled staff can be used for more than one type of analysis.
- Administration costs are high.
- The work has to be prioritised.
- Processes in chemical manufacturing plants have to be designed to accommodate the time delay, resulting in longer cycle times and reduced plant utilisation.
- This process is known as time-delay monitoring.

At-line analysis:

- The sample is manually removed.
- The sampling process is faster than with off-line analysis.
- The measurement is carried out on a dedicated analyser at the sampling site, which may result in low equipment utilisation.
- Method development work has to be done, as the laboratory analysis cannot be simply transferred to the plant floor.
- The sample preparation is simplified.

- The measurement technique is modified to permit the use of robust, reliable instrumentation to cope with the production environment.

- The data are known to the production personnel.

- Priorities can be controlled by production personnel.

- At-line analysis produces close-time data.

On-line analysis:

- Uses fully automated analyser systems.

- The sample is automatically sampled.

- A dedicated analyser automatically analyses this sample.

- The feedback to the process stream for adjustment and corrective action is automatic.

- The sample throughput is high.

- On-line analysers require minimum downtime.

- The method development is time consuming and expensive.

- A 24 hour troubleshooting or maintenance resource is required.

- The system requires electrical classification.

- On-line analysis produces real-time data.

In-line analysis:

- The analysing probe is situated inside the plant as part of the process stream.
- The analysis is done inside the process stream.
- The processor outside the stream makes an automatic adjustment according to the feedback from the analysing probe.
- The system requires minimum downtime.
- The method development is time consuming and expensive.
- A 24 hour troubleshooting or maintenance resource is required.
- The system requires electrical classification.
- In-line analysis produces real-time data.

Many of the salient features that have established FIA as an indispensable tool for laboratory analysis are often quoted as prerequisites for process analysers: speed of response, high sample frequency and dependable instrumentation. Many of the procedures carried out in the microconduits of the manifold are miniaturised reproductions of the large-scale manipulations performed in process plants. There are also similarities between the control, acquisition and communication functions of the FI computer and the central process computer.

The sample presentation must be effective and in many cases filtration and the control of biofouling is required. The number of reported applications of process FIA remains low despite the versatility and potential of the technique and is in part due to industrial confidentiality. The reported chemical production applications are collated in Table 1.1 and the distribution of FIA methods by area of application is shown in Fig 1.1 [6].

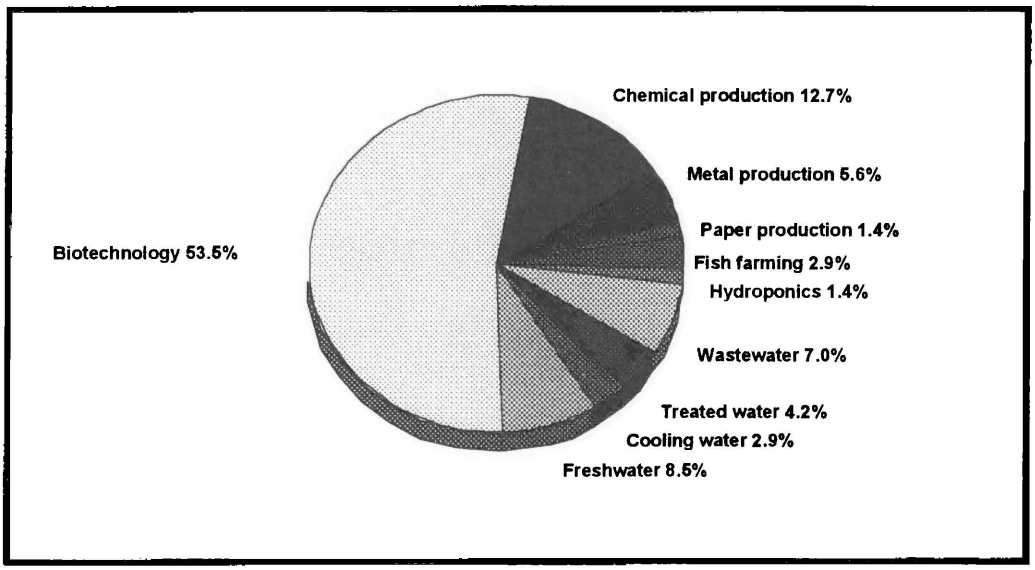

Figure 1.1 - The distribution of FIA methods by area of application [6].

FIA has been successfully applied to several other fields: metal production [16-19], paper production [20], fish farming [21,22], hydroponic cultivation [23], wastewater monitoring [24-28], treated water monitoring [29-31], power-plant/cooling water monitoring [32,33], freshwater monitoring [34-39] and biotechnology [40-76].

Analyte	Comments	Reference
(i) Sulphuric acid, ammonia and caustic solutions	-	7
(ii) Sulphide in di-isopropanolamine solutions	-	8
(iii) HCl in concentrated hydrochloric acid	-	9
(iv) Azo dyes	-	10
(v) Sulphite in KCl brine	On-line monitoring of industrial process streams	11, 12
(vi) Salicylic and acetylsalicylic acids in pharmaceutical preparations	Continuous monitoring of tablet dissolution tests	13
(vii) Morphine	-	14
(viii) Hydrogen cyanide in process gas streams	On-line monitoring of industrial process gas streams	15

Table 1.1 - Reported chemical production applications [6].

1.4 Aim of this study

Phenols, alcohols and carbonyls are present in the light oil mixtures in the Synthol process. The concentration of these compounds present influence some of the synthesis processes. At the moment these type of samples are analysed by gaschromatography. Gaschromatography is used for detailed, precise analyses, but is time consuming. Conventional methods of analysing these samples are time consuming. Often a fast analysis, which gives a global estimate of the concentration of a compound, is necessary.

FIA has an exceptionally high sample throughput and is ideal for fast assays. A small sample is injected into a carrier stream, sample preparation takes place automatically in a mixing system, reagents are added automatically and the final product is carried to a detection system. The effective control of sample dispersion, flow rate of the carrier and reagent streams and the chemical kinetics play important roles in the optimisation of the flow dynamics of such a system. The system is computer controlled and data acquisition is automatic.

In this project methods for determining phenol, carbonyls and alcohols in light oil mixtures are automated and the prospects for application as process analysers are investigated.

1.5 References

1. Růžička J, Hansen EH, ***Flow Injection Analysis***, first edition, John Wiley and Sons, New York, 1981.
2. Fang Z, ***Flow Injection Separation and Preconcentration***, Weinheim, New York, 1992.
3. Valcárcel M, Luque de Castro MD, ***Flow-Injection Analysis Principles and Applications***, John Wiley and Sons, New York, 1987.
4. Callis JB, Illman DL, Kowalski BR, ***Anal. Chem.***, **59,** 1987, 624A.
5. Rube MT, Eustace DJ, ***Anal. Chem.***, **62**, 1990, 65A.
6. McLennan F, Kowalski BR, ***Process Analytical Chemistry***, Chapman & Hall, London, 1996.
7. Schick KG, ***ISA Trans. Adv. Instr.***, **39,** 1984, 279.
8. van der Linden WE, ***Anal. Chim. Acta***, **179**, 1986, 91.
9. van Staden JF, ***Fres. Z. Anal. Chem.***, **328**, 1987, 68.
10. Gisin M, Thommen C, ***Trends Anal. Chem.***, **8**, 1989, 62.
11. MacLaurin P, Parker S, Townshend A, Worsfold PH, Barnett NW, Crane M, ***Anal. Chim. Acta***, **238**, 1990, 171.
12. MacLaurin P, Worsfold PJ, Townshend A, Barnett, NW, Crane M, ***Analyst***, **116**, 1991, 701.
13. López Fernández JM, Luque de Castro MD, Valcárcel M, ***J. Auto. Chem.***, **12**, 1990, 263.
14. Barnett NW, Rolfe DG, Bowser TA, Paton TW, ***Anal. Chim. Acta***, **282**, 1993, 551.
15. Olson DC, Bysouth SR, Dasgupta PK, Kuban V, ***Process Quality and Control***, **5**, 1994, 259.
16. Lynch TP, Kernoghan NJ, Wilson JN, ***Analyst***, **109**, 1984, 843.
17. Bergamin H, Krug FJ, Zagatto EAG, Arruda EC, Coutinho CA, ***Anal. Chim. Acta***, **190,** 1986, 177.
18. Jones EA, Hemmings MJ, ***S. Afr. J. Chem.***, **42**, 1989, 6.
19. Taylor MJC, Barnes DE, Marshall GD, ***Anal. Chim. Acta***, **265**, 1992, 71.
20. Nyman J, Ivaska A, ***Talanta***, **40**, 1993, 95.

21. Muraki J, Higuchi K, Sasaki M, Korenaga T, Tôei K, ***Anal. Chim. Acta***, **261**, 1992, 345.
22. Ariza AC, Linares P, Luque de Castro MD, Valcárcel, ***J. Auto. Chem.***, **14**, 1992, 181.
23. Clinch JR, Worsfold PH, Casey H, Smith SM, ***Anal. Proc.***, **25**, 1988, 71.
24. Gisin M, Thommen C, ***Trends Anal. Chem.***, **8**, 1989, 62.
25. van Staden JF, ***Anal. Chim. Acta***, **261**, 1992, 453.
26. Pedersen KM, Kümmel M, Søeberg H, ***Anal. Chim. Acta***, **238**, 1990, 191.
27. Benson RL, McKelvie ID, Hart BT, Hamilton IC, ***Anal. Chim. Acta***, **291**, 1994, 233.
28. Pilloton R, Mignogna G, Fortunato A, ***Anal. Letters***, **27**, 1994, 833.
29. Chen D, Luque de Castro MD, Valcárcel M, ***Anal. Chim. Acta***, **230**, 1990, 137.
30. Benson RL, Worsfold PJ, Sweeting FW, ***Anal. Chim. Acta***, **238**, 1990, 177.
31. Benson RL, Worsfold PJ, ***Sci. Tot. Env***, **135**, 1993, 17.
32. Balconi ML, Sigon F, Borgarello M, Ferraroli R, Realini F, ***Anal. Chim. Acta***, **234**, 1990, 167.
33. MacLaurin P, Worsfold PJ, Norman P, Crane M, ***Analyst*** **118**, 1993, 617.
34. Worsfold PJ, Clinch JR, Casey H, ***Anal. Chim. Acta***, **197**, 1987, 43.
35. Clinch JR, Worsfold PJ, Casey H, ***Anal. Chim. Acta***, **200**, 1987, 523.
36. Benson RL, Worsfold PJ, Sweeting FW, ***Anal. Proc.***, **26**, 1989, 385.
37. Casey H, Clarke RT, Smith SM, Clinch JR, Worsfold PJ, ***Anal. Chim. Acta***, **227**, 1989, 379.
38. Blundell NJ, Hopkins A, Worsfold PJ, Casey H, ***J. Auto. Chem.***, **15**, 1993, 159.
39. Clinch JR, Worsfold PJ, Sweeting FW, ***Anal. Chim. Acta***, **214**, 1988, 401.
40. Recktenwald A, Kroner KH, Kula MR, ***Enzyme Microb. Technol.***, **7**, 1985, 146.
41. Recktenwald A, Kroner KH, Kula MR, ***Enzyme Microb. Technol.***, **7**, 1985, 607.
42. Nalbach U, Schiemenz H, Stamm WW, Hummel W, Kula MR, ***Anal. Chim. Acta***, **213**, 1988, 55.
43. Nikolajsen K, Nielsen J, Villadsen J, ***Anal. Chim. Acta***, **214**, 1988, 137.
44. Künnecke W, Kalisz HM, Schmid RD, ***Anal. Letters***, **22**, 1989, 1471.
45. Stamm WW, Pommerening G, Wandrey C, Kula MR, ***Enzyme Microb. Technol.***, **11**, 1989, 96.

46. Brand U, Reinhardt B, Rüther F, Scheper T, Schügerl K, ***Anal. Chim. Acta***, **238**, 1990, 201.
47. Künnecke W, Schmid RD, ***J. Biotechnol.***, **14**, 1990, 127.
48. Lüdi H, Garn MB, Bataillard P, Widmer HM, ***J. Biotechnol.***, **14**, 1990, 71.
49. Stamm WW, Kula MR, ***J. Biotechnol.***, **14**, 1990, 99.
50. Worsfold PJ, Whiteside IRC, Pfeiffer HF, Waldhoff H, ***J. Biotechnol.***, **14**, 1990, 81
51. Chung S, Wen X, Vilholm K, de Bang M, Christian G, Růžička J, ***Anal. Chim. Acta***, **249**, 1991, 77.
52. Christensen LH, Nielsen J, Villadsen J, ***Anal. Chim. Acta***, **249**, 1991, 123.
53. Filippini C, Sonnleitner A, Fiechter A, Bradley J, Schmid R, ***J. Biotechnol.***, **18**, 1991, 53.
54. Forman LW, Thomas BD, Jacobson FS, ***Anal. Chim. Acta***, **249**, 1991, 101.
55. Freitag R, Fenge C, Scheper T, Schügerl K, Spreinat A, Antranikian G, Fraune E, ***Anal. Chim. Acta***, **249**, 1991, 113.
56. Kracke-Helm HA, Brandes L, Hitzmann B, Rinas U, Schügerl K, ***J. Biotechnol.***, **20**, 1991, 95.
57. Nilsson M, Håkanson H, Mattiasson B, ***Anal. Chim. Acta***, **249**, 1991, 163.
58. Ogbomo I, Kittsteiner-Eberle R, Englbrecht U, Prinzing U, Danzer J, Schmidt HL, ***Anal. Chim. Acta***, **249**, 1991, 137.
59. Peris-Tortajada M, Maquieira A, López E, Ors R, ***Analusis***, **19**, 1991, 266.
60. Scheper T, Brandes W, Grau C, Hundeck HG, Reinhardt B, Rüther F, Plötz F, Schelp C, Schügerl K, Schneider KH, Giffhorn F, Rehr B, Sahm H, ***Anal. Chim. Acta***, **249**, 1991, 25.
61. Schügerl K, Brandes l, Dullau T, Holzhauer-Rieger K, Hotop S, Hübner U, Wu X, Zhou W, ***Anal. Chim. Acta***, **249**, 1991, 87.
62. Degelau A, Freitag R, Linz F, Middendorf C, Scheper T, Bley T, Müller S, Stoll P, Reardon KF, ***J. Biotechnol.***, **25**, 1992, 115.
63. Englbrecht U, Schmidt HL, ***J. Chem. Tech. Biotechnol.***, **53**, 1992, 397.
64. Nilsson M, Håkanson H, Mattiasson B, ***J. Chromatogr.***, **597**, 1992, 383.

65. Pfeiffer HF, Waldhoff H, Worsfold PJ, Whiteside IRC, ***Chromatographia***, **33**, 1992, 49.

66. Becker T, Kittsteiner-Eberle R, Luck T, Schmidt HL, ***J. Biotechnol.***, **31**, 1993, 267.

67. Becker T, Schuhmann W, Betken R, Schmidt HL, Leible M, Albrecht A, ***J. Chem. Tech. Biotechnol.***, **58**, 1993, 183.

68. Busch M, Höbel W, Polster J, ***J. Biotechnol.***, **31**, 1993, 327.

69. Carlsen M, Johansen C, Min RW, Nielsen J, Meier H, Lantreibecq F, ***Anal. Chim. Acta***, **279**, 1993, 51.

70. Gründig B, Strehlitz B, Kotte H, Ethner K, ***J. Biotechnol.***, **31**, 1993, 277.

71. Middendorf C, Schulze B, Freitag R, Scheper T, Howaldt M, Hoffman H, ***J. Biotechnol.***, **31**, 1991, 395.

72. Nilsson M, Mattiasson G, Mattiasson B, ***J. Biotechnol.***, **31**, 1993, 381.

73. Ogbomo I, Steffl A, Schuhmann W, Prinzing U, Schmidt HL, ***J. Biotechnol.***, **31**, 1993, 317.

74. Scheper T, Brandes W, Maschke H, Plötz F, Müller C, ***J. Biotechnol.***, **31**, 1993, 345.

75. Schügerl K, Brandes L, Wu X, Bode J, Ree JI, Brandt J, Hitzmann B, ***Anal. Chim. Acta***, **279**, 1993, 3.

76. Steube K, Spohn U, ***Analyst***, **287**, 1994, 235.

CHAPTER 2

THEORETICAL BACKGROUND

2.1 Introduction

Usually a specific FIA manifold is optimized only through experimentation. The peak height (or peak area), h, and the return time, T', are the signal parameters that determine the sensitivity and the sample throughput of the analytical method. Quantitative relations have been mathematically derived to describe the influence of various physical parameters on the signal, but can only be applied in a few specific cases. Different injection systems, connectors, dead volumes, design of the flow-cell, etc. may cause deviations from these mathematical relations. Not only do the physical parameters of the manifold influence the signal, but chemical reactions taking place between the sample and stream components also contribute to dispersion.

2.2 Dispersion of sample and reagent zones

Dispersion is the dilution undergone by a sample volume injected into the flowing stream. The dispersion is characterized by the concentration profile adopted by a zone or plug inserted at a given point in the system without stopping the flow.

Whenever a mixture or sample, reagent and diluent are homogenized, dispersion takes place. FI dispersion is different in the sense that it is reproducible and controllable. The injected zone undergoes partial dispersion into the carrier stream and this is caused by convection and by molecular diffusion.

The conduits are thin (generally 0.3 to 1.5 mm i.d.) and no air segments are present in the system, which means no turbulence is produced. At first is was assumed that turbulent flow was necessary to avoid cross-contamination between successive samples [1], but the Reynolds number is always much less than 2 000, meaning transport takes place by laminar flow [2]. Dispersion caused by convection can be made very reproducible and a reproducible readout can be achieved before physical or chemical equilibration has been reached.

The dispersion is time-dependent, which means an injected sample will have mixed to different extents at different points along the flow-line. Two mechanisms cause dispersion: convective transport and diffusional transport. Molecules at the conduit tube walls have a zero linear velocity and molecules at the centre have twice the average velocity. This results in a parabolic profile and the mechanism causing it is called convective transport. Diffusional transport manifests as axial and radial diffusion, caused by concentration gradients resulting from the above parabolic flow profile.

The diffusion process of an injected sample can be devided into four different stages during transport to the detector. The reactor length, L, and the flow rate, q, will determine the peak profile. During stage one the undiluted sample is introduced into the carrier stream. The peak profile has a rectangular shape. Convective transport changes this situation, so that the zone profile is now parabolic. The front of the parabolic flow profile can be seen as a vertical portion on the peak profile and the signal shows a "tail" as the last part of the flow profile. This situation occurs when t_a, the travel time, is short.

$$t_a = \frac{L}{2\bar{u}}$$

where t_a = travel time (sec)

L = overall tube length (cm)

$\bar{u}$ = mean linear velocity (cm/sec)

During the third stage radial diffusion changes the peak profile to a slanted portion, a longer peak time (t′) and a longer "tail" portion.

During the fourth stage radial diffusion yields a symmetrical peak. The travel time must be long (or the flow rate must be low) to obtain these Gaussian peaks.

$$t' = T - t_a = \frac{\Delta t}{2}$$

where t' = peak time (sec)

T = residence time (sec)

t_a = travel time (sec)

Δt = baseline-to-baseline time (sec)

and $$T = \frac{L}{\bar{u}}$$

where T = residence time (sec)

L = overall tube length (cm)

$\bar{u}$ = mean linear velocity (cm/sec)

$$\bar{t}_r = \frac{reactor.volume}{flow-rate} = \frac{\pi R^2 l}{q}$$

where $\bar{t}_r$ = reduced mean residence time

R = tube radius (mm)

q = flow-rate (ml/min)

A longer residence time results in an increase in diffusion.

$$D = D_{injection} + D_{transport} + D_{detector} + D_{connectors}$$

where $D_{injection}$ = dispersion due to sample volume and geometric aspects of system

$D_{transport}$ = dispersion due to flow rate and reactor geometry

$D_{detector}$ = dispersion due to flow-cell geometry (shape and dimensions)

$D_{connectors}$ = dispersion due to connectors.

The total dispersion can be divided into the contributions of the different parts of the FIA system: injection, transport, detector and connectors.

2.3 Quantitative evaluation of dispersion

2.3.1 Taylor's model

$$C = f(t) = \frac{m}{r^2} \cdot \frac{1}{4\pi . Dt} \exp\left[\frac{-(x - L)^2}{4Dt}\right]$$

and

$$C = \frac{C_0 V_i}{q\sigma . (2\pi)^{\frac{1}{2}}} . \exp\left[\frac{(t - t_r)^2}{2\sigma^2}\right]$$

where m = the injected solute mass ($m = C_0 V_i$),

σ = the parameter corresponding to the standard deviation (Gaussian distribution)

x = the axial distance from the injection point.

Conditions for the model to be applicable are:

- The flow rate has to be low
- The reactors have to be very long
- $V_i \langle\langle V_r$; the injected volume must be negligible compared to the reactor volume
- $\frac{L}{q} \rangle\rangle \frac{r^2}{14.44D}$
- $t \rangle\rangle \frac{r^2}{14.44.D}$

Most FIA manifolds do not fulfill these conditions, but the Aris-Taylor modification is more applicable to ordinary FIA systems [3].

2.3.2 Tanks-in-series model

$$C = \frac{1}{(\bar{t}_r)_N}\left(\frac{t}{(\bar{t}_r)_N}\right)^{N-1} \frac{1}{(N-1)!}\exp\left[\frac{-t}{(t_r)_N}\right]$$

where $(\bar{t}_r)_N$ = the mean residence time of an element of fluid in a given tank [4,5]. Analogous to liquid chromatography, the profile of C = f(t) becomes more Gaussian if N is larger. Above mathematical relation can be used when the flow is modelled to pass sequentially through a large number (N) of "tanks" where instanteneous mixing occurs. This model is an improvement on the Taylor model [6], but it is still not ideal, especially for short reactors (meaning short N values).

2.3.3 Mixing chamber model

This model was developed by improving the tanks-in-series model [7,8].

$$\underset{\text{sample}}{A} + \underset{\text{reagent}}{nB} \rightarrow \underset{\text{product}}{P}$$

- Reaction rates are not treated as variables, which means the chemical reactions should be fast
- The sample reaches the mixing chamber undiluted.
- The analyte and reagent mix immediately inside the chamber.
- No further dilution occurs between the mixing chamber and the detector.

The reagent (B, concentration C_b^0) acts as a circulating carrier stream. The initial concentration of the analyte in the sample, (A), is C_{as}^0. A volume, V_s, is injected directly into the gradient chamber (volume V_g). The analyte mixes and reacts immediately with the reagent. The concentrations of the reagent (C_{bg}) and sample (C_{ag}) in the chamber will be determined by the relative concentrations of A and B and on the flow-rate. Three stages can be distinguished in this process.

Stage one. When the sample begins to enter the chamber (time t_0), it mixes and reacts immediately and completely with the reagent (time t_1-t_i ; $C_{as} \approx 0$). The chemical reaction is taken into account for the first and third stages, i.e. when the sample enters the chamber, filled with reagent and when the reagent enters the chamber, filled with sample. In both cases, the reaction is instantaneous and complete.

The decrease in the reagent concentration due to chemical reaction and dilution is given by:

$$-\frac{dC_{bg}}{dt} = \frac{qC_{as}^{0}}{nV_g} + \frac{qC_{bg}}{V_g}$$

and

$$C_{bg} = \left(\frac{c_{as}^{0}}{n} + C_{bg}^{0}\right)\exp\left(-\frac{qt}{V_g}\right) - \frac{c_{as}^{0}}{n} \quad \text{(valid between } t_0 \text{ and } t_1\text{)}.$$

where C_{bg} = reagent concentration (M)

t = time (sec)

C^{0}_{as} = initial sample concentration (M)

V_g = volume of chamber

Stage two. ($t_i < t < t_2$) The rest of the sample enters the chamber and its initial concentration inside the chamber increases:

$$\frac{dC_{ag}}{dt} = \frac{q}{V_g}C_{as}^{0} - \frac{qC_{ag}}{V_g}$$

and

$$C_{ag} = C_{as}^{0}\left\{1 - \exp\left[-\frac{q}{V_g}(t - t_1)\right]\right\} \quad \text{is valid between } t_i \text{ and } t_2,$$

where C_{ag} = sample concentration in chamber (M)

q = flow rate (ml/min)

V_g = volume of chamber

C^{0}_{as} = initial sample concentration (M)

Stage three. Reagent enters the sample-filled chamber and the sample concentration in the chamber decreases due to mass flow and chemical reaction:

$$-\frac{C_{ag}}{dt} = \frac{q}{V_g} C_{ag} + n\frac{q}{V_g} C_b{}^0$$

and

$$C_{ag} = C_{ag,\max} \exp\left[-\frac{q}{V_g}(t - t_2)\right] - nC_b{}^0\left\{1 - \exp\left[-\frac{q}{V_g}(t - t_2)\right]\right\}$$

is valid between t_2 and t_3 (end-point).

where $C_b{}^0$ = undiluted reagent concentration in flowing stream (M)

C_{ag} = sample concentration in chamber (M)

q = flow rate (m*l*/min)

V_g = volume of chamber.

The concentration of the sample in the mixing chamber increases to reach a maximum value at t_2 after which the concentration decreases again. The rate of decrease of the sample concentration in the chamber depends on $C_{as}{}^0$ relative to $C_b{}^0$, as can be seen in the above mathematical expression.

The same expressions can be derived for a situation where the carrier stream contains no reagent and the injected sample is only diluted in the chamber ($C_b{}^0 = C_{bg} = 0$).

2.3.4 General model

$$D\left(\frac{\delta^2 C}{\delta l^2}+\frac{\delta^2 C}{\delta r^2}+\frac{1}{r}\frac{\delta C}{\delta r}\right)=\frac{\delta C}{\delta t}+u_0\left(1-\frac{r^2}{R^2}\right)\frac{\delta C}{\delta l}$$

where D = molecular diffusion coefficient (cm^2/sec)

C = concentration (mol/*l*)

l = partial tube length (cm)

r = partial tube radius (mm)

R = tube radius (mm)

u_0 = maximum linear velocity (cm/sec)

$\frac{\delta^2 C}{\delta l^2} \Rightarrow$ axial diffusion

$\left(\frac{\delta^2 C}{\delta r^2}+\frac{1}{r}\frac{\delta C}{\delta r}\right) \Rightarrow$ radial diffusion

$\frac{\delta C}{\delta t} \Rightarrow$ build-up of matter

$u_0\left(1-\frac{r^2}{R^2}\right)\frac{\delta C}{\delta l} \Rightarrow$ convective transport (parabolic velocity profile)

A differential volume of the flow was considered, a mass balance was applied and concentration gradients and flow profiles were incorperated into above equation.

2.3.5 Růžička's dispersion coefficient

$$D=\frac{C_0}{C}$$

Dispersion can be expressed as the dilution of the sample from the point of injection (C_0) to detection (C) in a FIA manifold [9].

$$D_{max} = \frac{k_0 h_0}{k_1 h_{max}} = \frac{h_0}{h_{max}}$$

where D_{max} = dispersion at signal maximum

$D>1$

k_0, k_1 = proportionality constants

$k_0=k_1 \Rightarrow$ when the relationship between response and concentration is linear

h_0 = magnitude of the response (potential, pH, absorbence or fluorescence intensity) recorded when the sample solution is used as the carrier

h_{max} = maximum response recorded of sample injected into a carrier.

It can be seen that the larger the value of D_{max}, the smaller the value of h_{max}, resulting in a lower sensitivity.

2.3.6 Vanderslice's expressions

$$D = \frac{C_0}{C}$$

This equation has two numerical solutions [3]:

$$t_a = \frac{109 R^2 D^{0.025}}{f}\left(\frac{L}{q}\right)^{1.025} \quad \text{and} \quad \Delta t = \frac{35.4 R^2 f}{D^{0.36}}\left(\frac{l}{q}\right)^{0.64}$$

where t_a = travel time (sec)

Δt = baseline-to-baseline time (sec)

q = flow-rate (ml/min)

f = Vanderslice's accommodation factor.

R = tube radius (mm)

D = molecular diffusion coefficient (cm^2/sec)

L = overall tube length (cm)

The travel time and Δt can now be predicted by using the physical characteristics of the FIA system. The magnitude of the response, however, cannot be calculated using these equations.

$$t_a = \frac{(t_a)_t}{f}$$

and

$$t = (\Delta t)_t . f$$

where t_a = experimental travel time (sec)

Δt = experimental baseline-to-baseline time (sec)

$(t_a)_t$ = theoretical t_a data (sec)

$(\Delta t)_t$ = theoretical Δt data (sec)

Clearly, f, the accommodation factor, rectifies the difference between the experimental t_a and Δt values and the theoretical data.

2.4 Influence of various factors on dispersion

2.4.1 Sample volume

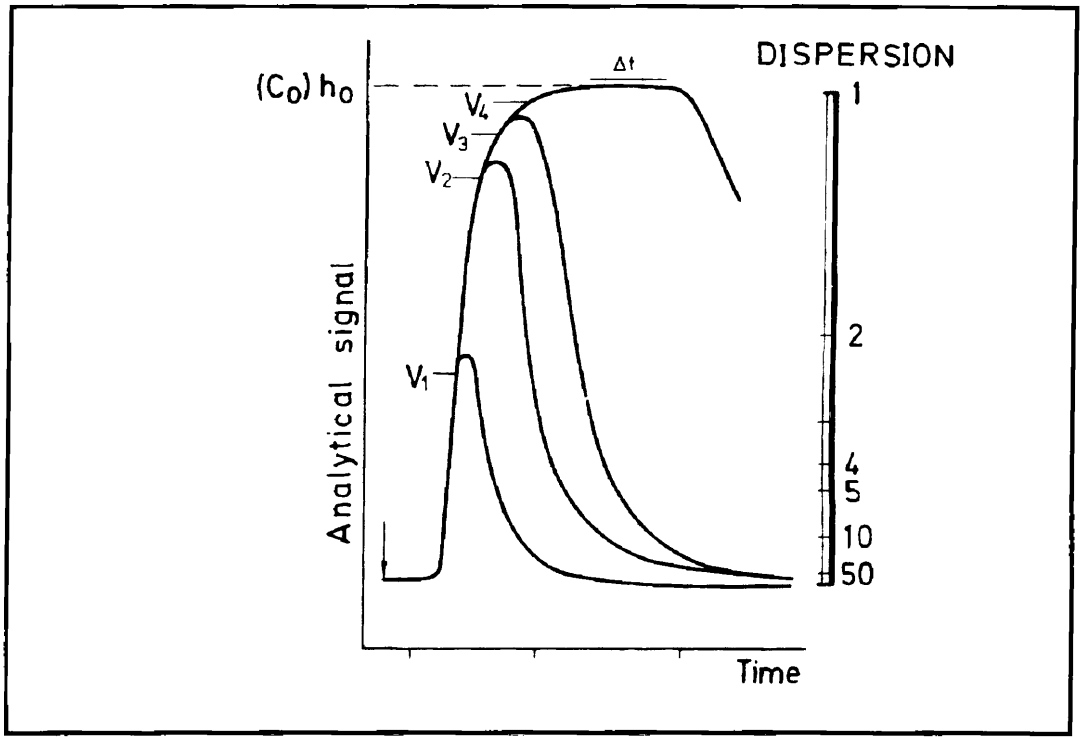

Figure 2.4.1A - Superimposed curves obtained when increasing volumes of a dye ($V_1<V_2<V_3<V_4$) were injected into an ordinary FIA system.

$$D = \frac{k}{V_i}$$

where k = proportionality constant

V_i = injected sample volume

A larger sample volume has no influence on the travel time, but definitely increases the residence and baseline-to-baseline times. In extreme cases where the sample volume is very large (V_4), a part of the sample (Δt) will be undiluted (D=1).

2.4.2 Hydrodynamic factors

2.4.2.1 Flow rate

$$t_a = \frac{k}{q^{0.125}}$$

and

$$\Delta t = \frac{k'}{q^{0.64}}$$

where t_a = travel time (sec)

Δt = baseline-to-baseline time (sec)

k, k′ = constants that are not influenced by the flow rate (including f)

q = flow rate (m*l*/min)

$$D = ku^{1/2}$$

and

$$D = k'q^{1/2}$$

where D = dispersion coefficient (cm^2/sec)

k, k′ = constants

u = linear flow velocity (cm/sec)

q = flow rate (m*l*/min)

$u \propto q$

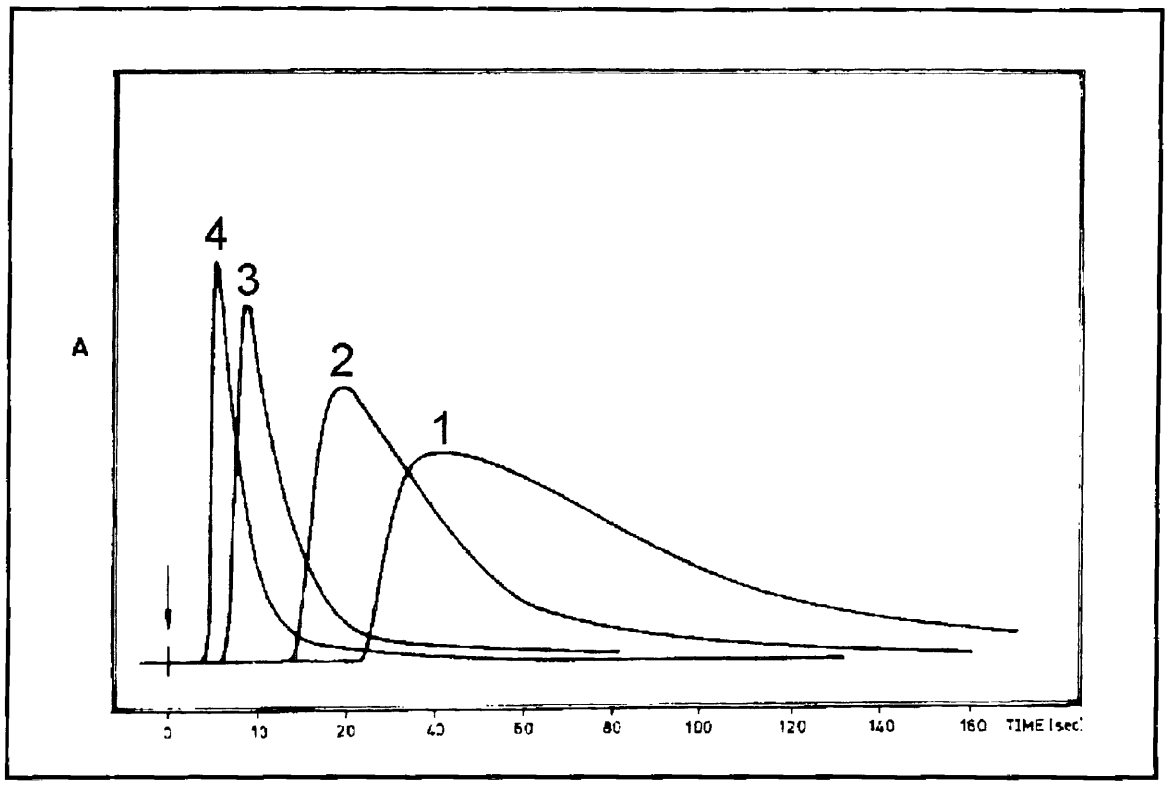

Figure 2.4.2.1A - Superimposed signals obtained when different flow rates are used in a FIA system [10].

L = 100 cm
d = 0.5 mm
1 q = 0.57 ml/min
2 q = 0.95 ml/min
3 q = 2.00 ml/min
4 q = 3.00 ml/min

An increase in flow rate results in a decrease in the values of D, t_a, the residence time and the peak width.

2.4.3 Geometric factors

2.4.3.1 Straight tubes

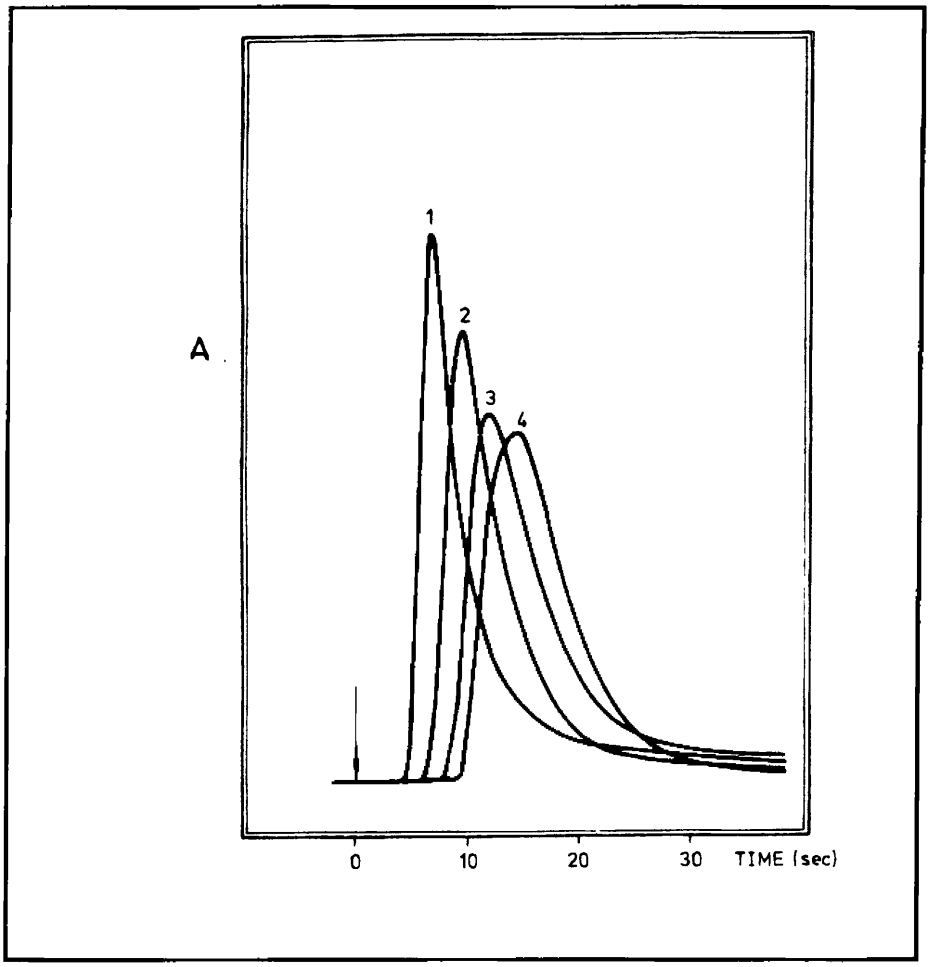

Figure 2.4.3.1A - Superimposed signals obtained when different reactor lengths are used.

d = 0.50 mm
q = 2.0 ml/min
1 L = 50 cm
2 L = 100 cm
3 L = 150 cm
4 L = 200 cm

An increase in reactor length results in an increase in the values of D, t_a and the peak width.

$$t_a = kL^{1.025}$$

and

$$\Delta t = k'L^{0.64}$$

and

$$D = kL^{1/2}$$

where t_a = travel time (sec)

k, k′ = constants

L = tube length (cm)

D = dispersion coefficient (cm^2/sec)

Above expressions (Vanderslice and Růžička) are proven correct by results shown in Fig. 2.4.3.1A.

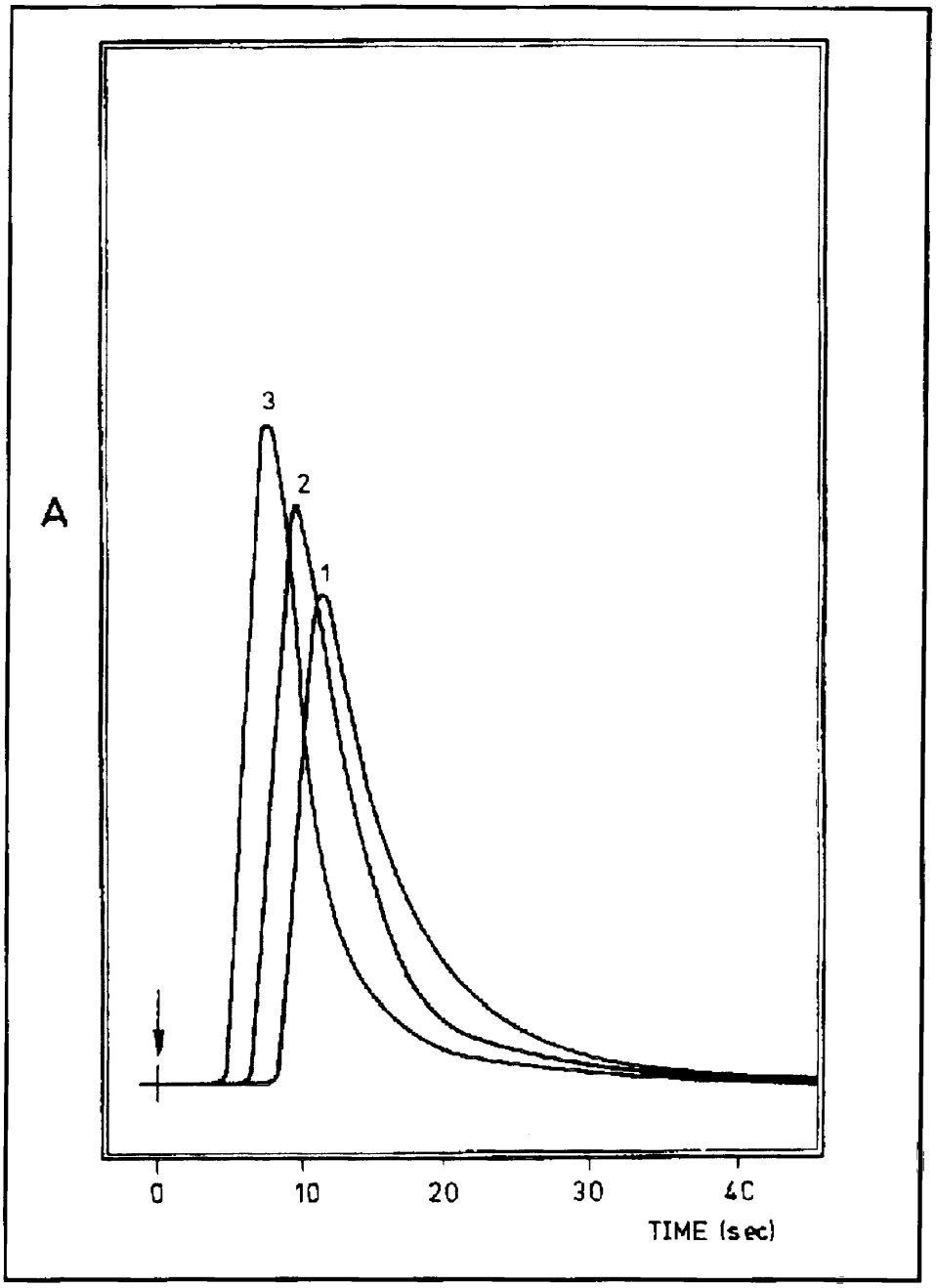

Figure 2.4.3.1B - Superimposed signals obtained when different reactor diameters are used.

L = 100 cm

q = 20 m*l*/min

1 = 0.70 mm d

2 = 0.50 mm d

3 = 0.35 mm d

The dispersion, travel time, residence time and peak width increase with increasing tube diameter.

$$t_a = kd^2$$

and

$$\Delta t = k'd^2$$

where t_a = travel time (sec)

Δt = baseline-to-baseline time (sec)

k, k′ = constants

d = tube diameter (mm)

Results shown in Fig. 2.4.3.1B are according to these predictions made by Vanderslice.

2.4.3.2 Coils

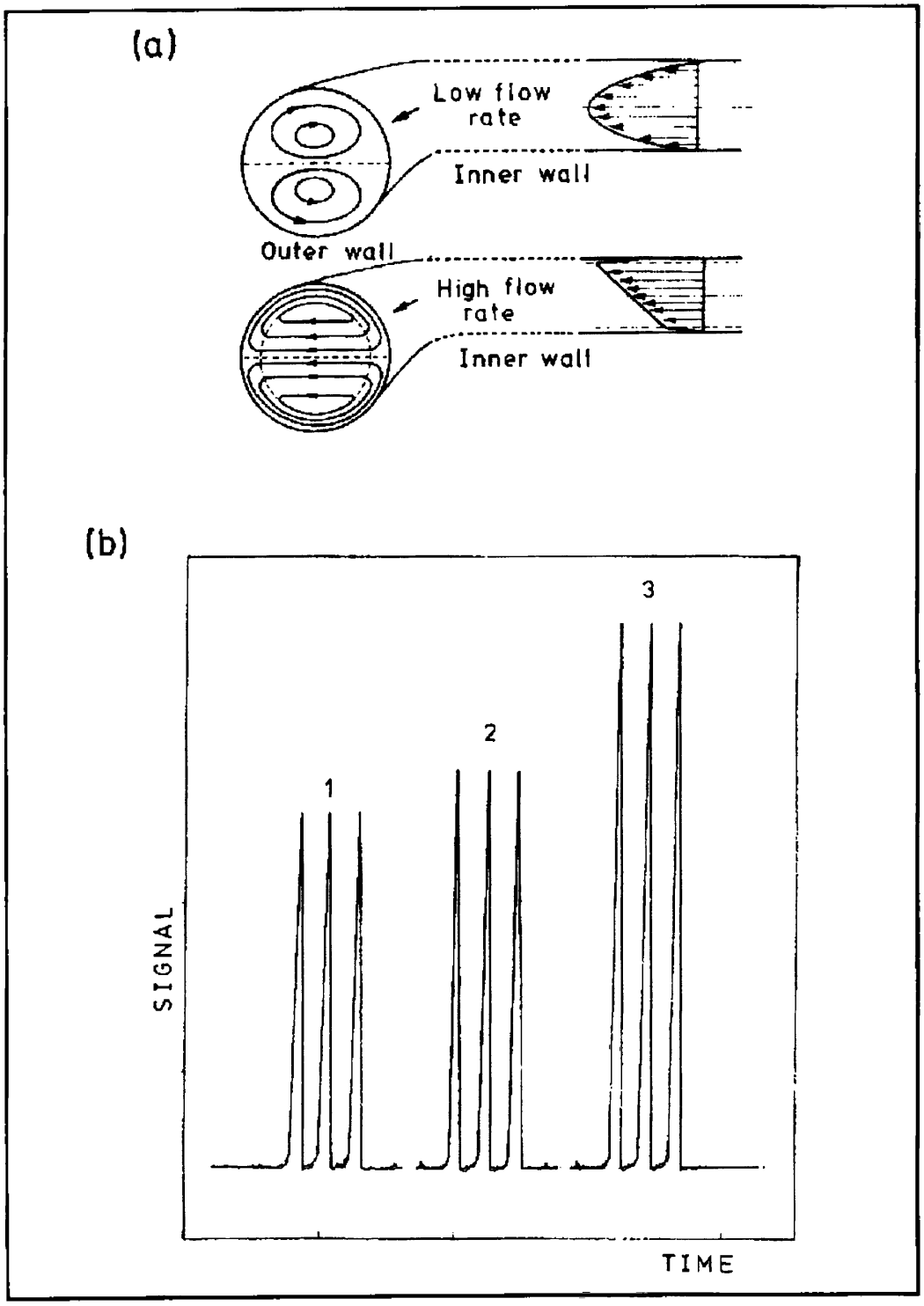

Figure 2.4.3.2A - (a) Secondary flow [11] resulting from the centrifugal force in a coiled reactor.

(b) Response for different reactors:

1 - reactor consisting of straight tubing

2 - reactor consisting of a coil (diameter = 26 mm)

3 - reactor consisting of a coil (diameter = 4 mm)

It is clear that the dispersion decreases with decreasing reactor coil diameter.

$$\lambda = \frac{coil.diameter}{tube.diameter}$$

where λ = coiling.

2.4.3.3 Knotted reactors

Knotted reactors reduce the dispersion, because the knots have the same effect as intensified coils.

2.4.3.4 Normal packed tubes

$$\tau = \frac{tube.diameter}{particle.diameter}$$

To minimize the axial dispersion, the particle size of the packed tube must be smaller (the dispersion is linearly related to the particle size if $5<\tau<50$). When a packed reactor is incorporated into the system, FIA looses its advantages of being simple and inexpensive, since higher pressures must be used to pump the reagents.

2.4.3.5 Single bead string reactors

To construct a single bead string reactor (SBSR), a Teflon tube is packed with glass beads [12,13]. The use of a SBSR increases the radial diffusion. The flow rate can be varied over the range 0.2-1.5 ml/min without changing the dispersion coefficient. Unlike a system where a packed tube is used, the sample throughput is high and different streams can be easily merged.

2.5 Types of dispersion

Three types of FIA techniques can be distinguished [14].

D<3: Limited dispersion can be achieved when a large sample is transported, without a chemical reaction taking place, at a high flow rate, over a short distance through a small, thin reactor. These conditions result in a high sample throughput and an excellent analytical sensitivity.

3<D<10-15: A chemical reaction will increase the dispersion coefficient and to accommodate a reaction long tubes, low flow rates, various channels and mixing points are used. A higher dispersion coefficient implies a lower analytical sensitivity.

D>10-15: The carrier reagent and the sample are mixed so well that chemical equilibrium is reached in some cases. The sample throughput is low and in some cases, a mixing chamber is used.

2.6 Influence of chemical kinetics on dispersion

Dispersion is influenced by the physical and chemical characteristics of a specific method. In ordinary FIA systems, the response is recorded before chemical equilibrium is reached and the kinetics of a reaction will definitely influence the dispersion coefficient.

$$\underset{\text{sample}}{A} + \underset{\text{carrier}}{B} \xrightarrow{k_1} \underset{\text{measured substance}}{C}$$

D becomes smaller when the reaction rate constant, k_1, is higher. This is true in cases where a property of the reaction product is measured.

D increases when the reaction rate constant, k_1, is higher in cases where a property of a reactant is measured.

$$D_c = D_{p+c} - D_p$$

where D_c = kinetic contribution to dispersion

D_{p+c} = total dispersion in the presence of one of the reactants

D_p = dispersion in the absence of one of the reactants [15].

$$D\left(\frac{\delta.^2 C}{\delta.l^2} + \frac{\delta.^2 C}{\delta.r^2} + \frac{1}{r}\frac{\delta.C}{\delta.r}\right) - k(C)^n = \frac{\delta.C}{\delta.t} + u_0\left(1 - \frac{r^2}{R^2}\right)\frac{\delta.C}{\delta.l}$$

where k = the rate constant

n = the reaction order

The term $-k(C)^n$ is added to the above convective-diffusional transport equation to take into account the decrease in concentration of a reactant.

2.7 References

1. Růžička J, Hansen EH, ***Anal. Chim. Acta***, **78**, 1975, 145.
2. Růžička J, Hansen EH, Zagatto EA, ***Anal. Chim. Acta,*** **88**, 1977, 1.
3. Vanderslice JT, Stewart KK, Rosenfeld AG, Higgs DJ, ***Talanta***, 1981, **28**, 11.
4. Růžička J, Hansen EH, ***Anal. Chim. Acta***, **99**, 1978, 37.
5. Betteridge D, ***Anal. Chem.***, **50**, 1978, 832A.
6. Painton CC, Mottola HA, ***Anal. Chim. Acta***, **154**, 1983, 1.
7. Pardue HL, Fields B, ***Anal. Chim. Acta***, **124**, 1981, 39.
8. Pardue HL, Fields B, ***Anal. Chim. Acta***, **124**, 1981, 65.
9. Růžička J, Hansen EH, Zagatto EA, ***Anal. Chim. Acta***, **88**, 1977, 1.
10. Gómez-Nieto MA, Luque de Castro MD, Martin A, Valcárcel M, ***Talanta***, **32**, 1985, 319.
11. Tijssen A, ***Anal. Chim. Acta***, **114**, 1980, 71.
12. Reijn JM, van der Linden WE, Poppe H, ***Anal. Chim. Acta***, **123**, 1981, 229.
13. Reijn JM, van der Linden WE, Poppe H, ***Anal. Chim. Acta***, **126**, 1981, 1.
14. Růžička J, Hansen EH, ***Flow Injection Analysis***, Wiley, New York, 1981.
15. Painton CC, Mottola HA, ***Anal. Chim. Acta***, **53**, 1981, 1713.

CHAPTER 3

DESIGN OF THE FLOW INJECTION SYSTEM

3.1 Introduction

A FIA system has four basic components: a propelling system, an injection system, a transport system and a detection system. The aim is to design a system which flow does not pulsate, has narrow tubes, which can be easily adjusted for different analyses and which can yield a fast, sensitive and reproducible response to quantify the analyte's concentration.

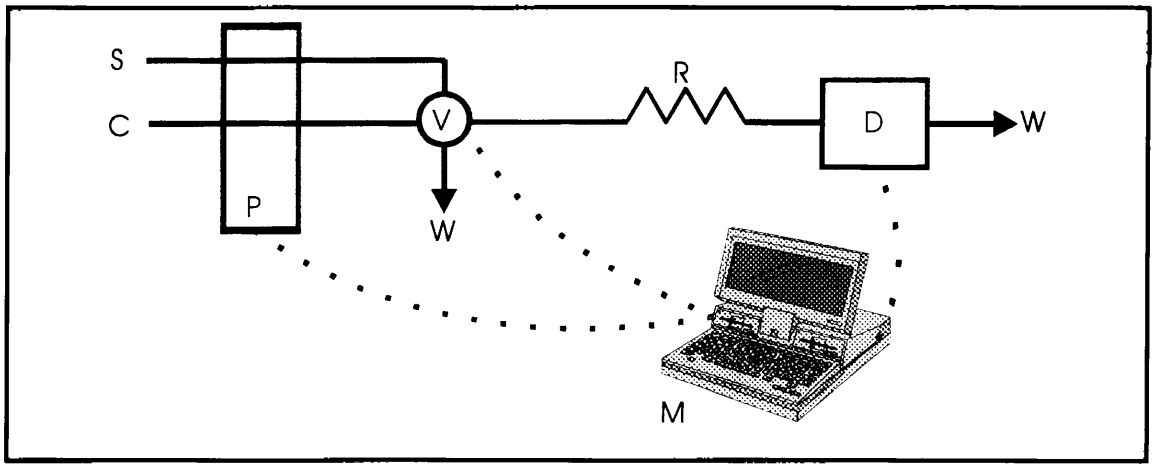

Figure 3.1A - Arrangement of a FIA system

S = sample
C = carrier solution
P = peristaltic pump
V = rotary valve
W = waste
R = reactor
D = detector
M = computer for data acquisition and device control

3.2 Instrumental set-up

3.2.1 Propelling systems

3.2.1.1 Peristaltic pumps

The timing in a FIA method must be very reproducible and the flow rates in the system need to be constant and pulseless. Peristaltic pumps contribute to one very important aspect of FIA: it is simple and easy to manage. It is the most widely used propelling system and by far less expensive than high pressure HPLC pumps.

A peristaltic pump consist of a drum bearing rollers on which tubes are arranged. The rollers cause successive flexions which pump fluids through the tubes. This method of propelling fluids through a FIA system does not deliver a pulse-free flow and the flow rate is not stable because of the slow deterioration of the pump tubing (especially when organic solvents and acids are pumped). A pulse-dampening system, like a separator can be built into the system to improve the pulsating flow.

Some other pumps use gas-pressure, a hydrostatic head or a motor-driven piston burette, but these pumps are less frequently found in FIA. The gas-pressure pump delivers a pulseless flow, but the flow is less controllable than with a peristaltic pump and bubbles are formed in the flow. When gravity-based pumps are used, the liquid's level in the reservoir must be constant to obtain a constant flow rate. These pumps were used in a few theoretical studies.

The reciprocating piston pump can be used succesfully, but has a limited number of available channels (one or two). Syringe pumps have been used, but the sample throughput is lower and it is less versatile compared to peristaltic pumps [2].

3.2.1.2 Pump tubing

Type of solution	Tubing material
aqueous solution	PVC, Tygon
dilute ethanol solutions	PVC, Tygon
dilute acids and bases	PVC, Tygon
concentrated acids and bases	fluoroplasts ("Acidflex" from Technicon)
alcohols	modified PVC ("Solvaflex" from Technicon)
lower alcohols	silicone rubber
formaldehyde, acetaldehyde	PVC, Tygon
acetone	silicone rubber
acetic acid and anhydride	silicone rubber
aliphatic hydrocarbons	modified PVC ("Solvaflex" from Technicon)
aromatic hydrocarbons	fluoroplasts ("Acidflex" from Technicon)
chloroform	fluoroplasts ("Acidflex" from Technicon)
carbon tetrachloride	modified PVC ("Solvaflex" from Technicon)

Table 3.2.1.2A - Tubing material used for different classes of liquids and solutions [1].

The reproducibility of the flow rate can be improved by operating the peristaltic pump and tubing correctly. The compression band presses the pump tubes against the roller. The correct pressure is needed to deliver a reliable flow of reagents and is achieved by first connecting the pump tubes to the rest of the FIA system and releasing the pressure band until the flow stops. The pressure is now adjusted until all streams in the system are flowing and tightened by one extra turn of the pressure band screw.

This setting has to be done often, because of the aging of the pump tubing. Setting the pressure band too tightly results in a very short lifetime for the pump tubing. Whenever the system is not in use, the pressure on the pump tubes must be released by loosening the pressure band and by loosening the tubes from the rollers. At the end of a series of analyses, the system must be thoroughly rinsed with water.

3.2.1.3 Flow rate

The flow rate is changed by changing the pump tubes or by varying the rotation speed of the pump, but not by varying the pressure of the pressure band on a specific set of tubing. The flow rate must be measured and not only calculated by using the colour codes on the tubing. By using higher rotation speeds and shorter pump tubes, the pulsation can be damped.

3.2.1.4 Sample and reagent volumes

The flow rate is measured by determining the weight or volume of liquid pumped in a given period. The flow is measured close to the detector. The flow rate can also be measured by the air-gap method and the electromagnetic method. The volume of the sample injected is determined by the volume of the sample loop and by the flow rate of the sample stream when the rotory valve is used (See 3.2.2).

3.2.2 Injection system

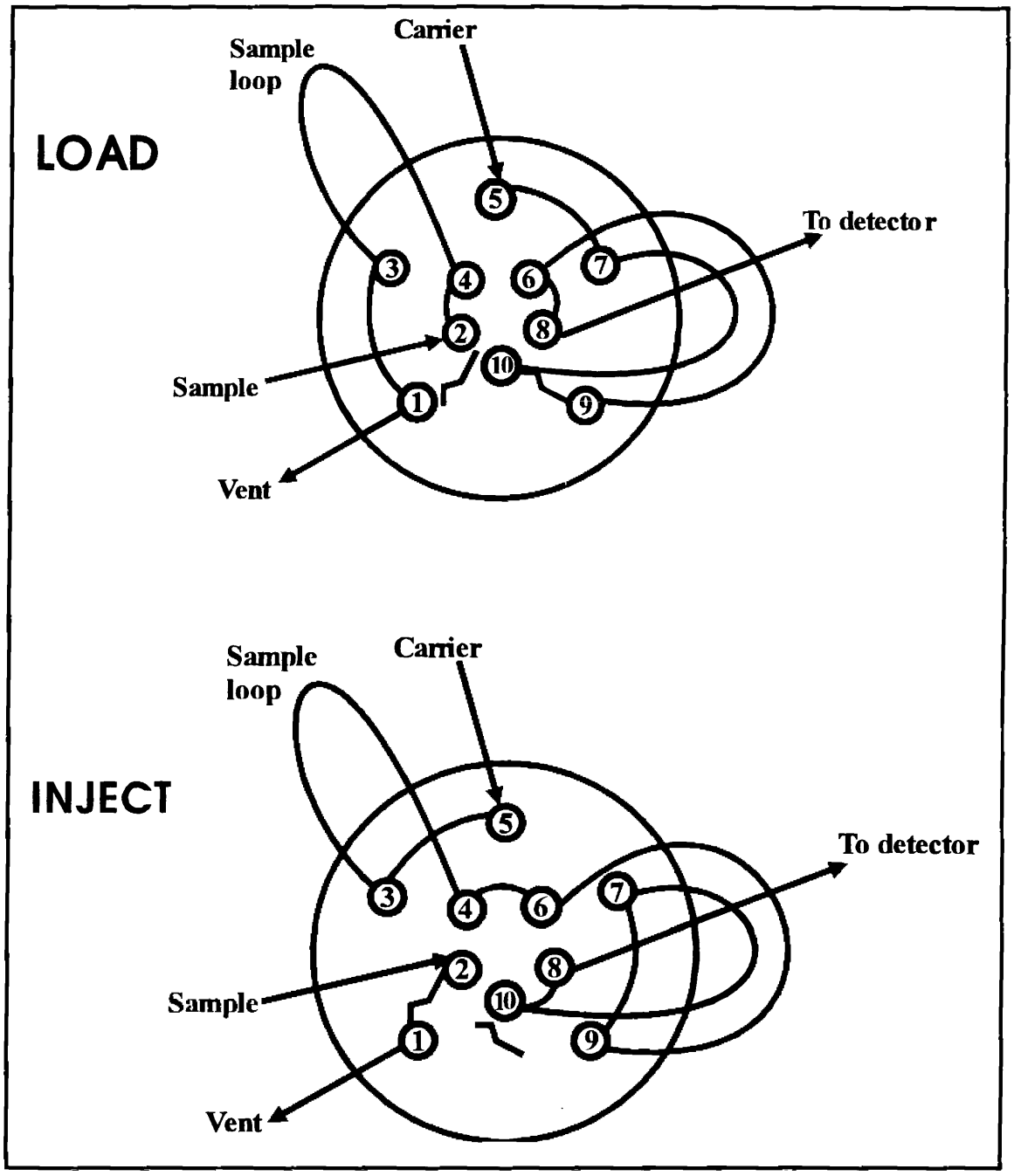

Figure 3.2.2A - Schematic diagram of a 10-port injector valve.

In early FIA systems, the sample was introduced into the carrier stream by injection. Although the sample is introduced by rinsing the sample loop with the carrier nowadays (rotary valves), the analytical technique is still called "flow injection analysis".

Rotary valves are the most frequently used injection systems. Valves in FIA are used as injection systems and to perform other functions like separation or preconcentration.

There are various valve designs. The ten-port valve (Figure 3.2.2A) consists of two layers and has channels engraved on the surface of the rotor and the stator. In the **LOAD** position the sample fills the sample loop by entering at port 2, flowing from port 4 to port 3 and exiting the valve through port 1. The carrier stream enters the valve at port 5, flows through ports 7, 10, 9, 6 and exits the valve at port 8. In the **INJECT** position, the sample is flushed to the detector when the carrier stream enters the valve at port 5, flows via ports 3, 4, 6, 9, 7, 10 and exits at port 8. This method of sample injection is highly reproducible. It can now be seen that the volume of the sample loop and the flow rate of the carrier will determine how much sample is injected into the system.

Other methods of sample introduction are the proportional injector, solenoid valve and the multi-injection system. These systems introduce reproducible sample volumes and can be widely applied in FIA.

3.2.3 Transport conduits and mixing reactors

3.2.3.1 Tubing

The different components in a FIA system are connected by transport conduits. PTFE tubing is used commonly and although special connectors must be used, the tubing is resistant to most diluted acids and organic solutions. Usually tubing with 0.3 to 0.7 mm internal diameter is used. When the tube walls are thinner than 0.5 mm, they do not have sufficient mechanical strength. Tubes with small internal diameters produce lower dispersion, but run the risk of blocking when suspended articles are present in the flow. While making connections, dead volumes, leaks and the introduction of air bubbles should be avoided.

3.2.3.2 Connectors

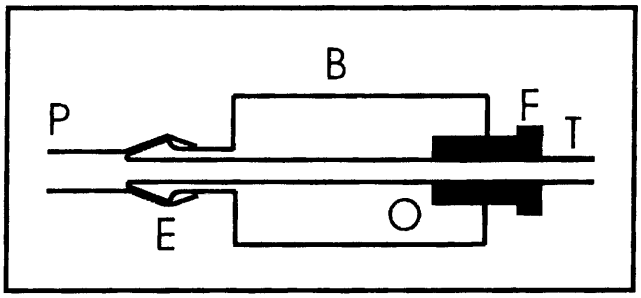

Figure 3.2.3.2A - A connector with a push-fit connector and a threaded fitting connection [3].

P = plastic tubing
E = male end with slip-proof design
B = connector body
O = rubber O-ring
F = threaded fitting
T = PTFE tubing

Push-fit connections are used where no high pressure in the flow is expected. These connections are easy to make, but have a tendency to leak. The ends of the PTFE tubing must be flanged and fitted with rubber O-rings when connections are made using the threaded connectors. Usually these connectors are made of "Perspex" blocks, but these can only be used when the carrier stream is aqueous and when no concentrated acid or bases are used. In cases where the carrier stream and/or sample consists of organic solutions, these connectors must be made of more resistant material. In the case where xylene and concentrated aqueous solutions of bases are used, the connectors were made of a polymer, called "Ertalon". These connectors can be made to suit any application e.g. merging of reagents and connecting pump tubing to the transport system, which means a variety of designs are available. The connection must not have a dead volume or else it acts as a mixing chamber and this adds to broadening of the peaks.

3.2.3.3 Reactors

A length of open tubing can act as reactor between the valve and the detector. Reactors improve the mixing of two reactants or the mixing of the reactant and the sample. The tubes can be coiled helically and even knotted to improve radial diffusion. The coiled reactor consists of a length of tubing helically wound around a cylinder. The diameter of the cylinder influences the dispersion and needs to be optimized. The single bead string reactor can be used effectively as a mixing reactor, but it is less flexible than the coiled and knotted reactors [4]. A packed reactor results in high flow resistance and is not very often used.

When more thorough mixing is required a mixing chamber can be used. Different designs are available, e.g. mixing point, minichamber and a well-stirred mixing chamber, which can improve the sample throughput.

3.2.4 Detector

Detectors often used for FIA detection are the UV/visible spectrophotometer, atomic absorption and ICP spectrometer, chemiluminescence and electrochemical detectors. To convert an ordinary detector to a flow injection detector, the detector must have a small volume, low noise and fast and linear response.

The detection limit of a detector is the lowest concentration which can be measured with a specific statistical risk factor. The detector can measure a reaction product (when the sample and reagent do not give a response) or the disappearence of the carrier stream (which gives a response) when the sample reacts with it. The spectrophotometer is the most frequently used detector and the conventional cuvette is replaced with a flow-cell.

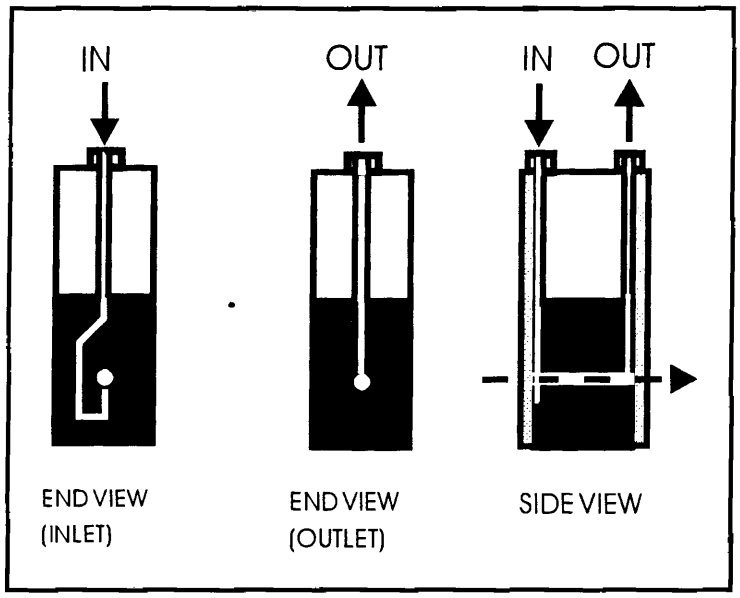

Figure 3.2.4A - A spectrophotometric flow-cell.

The flow-cell is made of quartz or glass and has an internal volume of 80 µl. When bubbles are present in the flow, a three-point flow-cell can be used, called a debubbler. A difference in the refractive indexes of the sample and the carrier can result in a displacement in the baseline. This phenomenon is called the "Schlieren effect". This can be overcome by adding a salt which will not interfere with the analysis to the solution with the lowest refractive index. The light source must be stable, because the amount of absorption is measured as the fraction of the incident light that is transmitted.

Fluorimetry, chemiluminescence, refractometry and atomic spectrometry are other optical detectors that have been used succesfully in FIA systems. There are only a few substances which have fluorescent properties and these kind of detectors do not have a wide range of application. When chemiluminescence detection systems are used, the distance between injection and detection should be as short as possible, since the measurement is made right after the reagents and sample have started mixing. This is necessary, because the intensity of the emission is usually higher at the beginning of the reaction.

Small sample volumes, tolerance of high salt concentrations, less interference effects, high sensitivity, high sample throughput and easy automation are advantages of the atomic spectrometry techniques [5]. An ICP as detection system is ideal when high sensitivity and sample throughput are needed.

Electrochemical detectors are selective, sensitive and give linear responses over wide concentration ranges. Different types are available: conductimetric and capacitometric detectors are based on the properties of the bulk solution and amperometric, polarographic, coulometric and potentiometric detectors are based on the properties of the solute. Only the detectors based on the properties of the solute are selective. The detector measures activity on the surface of the electrode and it is a local measurement.

There are three types of electrochemical detectors: the annular detector, the wire-type and the cascade-type detector. This classification is according to the geometry of the system. Potentiometric techniques include redox detectors, glass electrodes, ion-selective electrodes and potentiometric stripping analysis.

3.3 Computerized control and data acquisition

3.3.1 Data output

The FlowTEK [6] package (obtainable from MINTEK) for computer-aided flow analysis was used throughout for device control and data acquisition. The software can control a series of FIA components: the peristaltic pump, the rotary valve (load and inject) and the detector. The data is obtained as peak height, peak width, peak time and concentration. This means that calibration curves and a number of analysis can be done by simply writing a procedure with the assistance of the FlowTEK software. The data are saved in specific files and can be retrieved for later use.

3.3.2 Interface board

Data acquisition and device control were achieved using a PC30-B interface board (Eagle Electric, Cape Town, South Africa) and an assembled distribution board (MINTEK, Randburg, South Africa).

3.4 References

1. Válcárcel M, Luque de Castro MD, ***Flow-Injection Analysis Principles and Applications***, John Wiley and Sons, New York, 1987.
2. Rüžička J, Hansen EH, ***Flow-Injection Analysis***, Second Edition, John Wiley & Sons, New York, 1988.
3. Fang Z, ***Flow Injection Separation and Preconcentration***, Weinheim, New York, 1993.
4. Reijn JM, van der Linden WE, Poppe H, ***Anal. Chim. Acta***, **123**, 1981, 229.
5. Gallego M, Luque de Castro MD, Valcárcel M, ***Atomic Spectrosc.***, **6**, 1985, 16.
6. Marshall GD, van Staden JF, ***Anal. Instrum.***, **20**, 1992, 79.

CHAPTER 4

IN-LINE LIQUID-LIQUID EXTRACTION

4.1 Introduction

Liquid-liquid extraction is done to remove interferences and to preconcentrate an analyte. By automating this process, the analyst does not have to cope with the (toxic) odours from the organic solutions used. The phase transfer factor in FIA is much higher with liquid-liquid extraction than with dialysis and diffusion.

To automate the extraction process a phase segmentor, extraction coil and phase separator have to be built into the ordinary FIA system [1,2]. Determinations can also be made without phase separation.

In-line liquid-liquid extraction has been applied in various types of determinations: molybdenum in plants [2], cadmium in urine [3], caffeine in pharmaceuticals [1], vitamin B1 in pharmaceuticals [4], codeine in acetylsalicylic acid tablets [5], extraction constants [6], polycyclic organic compounds in oils [7,8], perchlorate in serum and urine [9], anionic surfactants [10], cationic surfactants [11], lead and cadmium [10,12], gallium(III) [13], procyclidine in tablets [14,15], orthophosphate [16], metal ions [17] and potassium [18].

4.2 Instrumentation

4.2.1 Phase segmentors

It is important to keep in mind that the FIA system (including the tubing and connectors) has to be adapted to be resistant to organic solvents. The fast deterioration of the pump tubing when the water-solvent mixture contains more than 30% organic solvent is enhanced by the repeated distortion of the tubing by the pump rollers. Displacement pumps or tubing made from inert material (fluoroplasts, silicone rubber or modified PVC) can be used to circumvent this problem.

The segmentor must mix the two different phases used in the liquid-liquid extraction. Merging segmentors were built in the T, Y and W configurations [11]. Pulsations in the flow and the smoothness of the segmentor bores determine the regularity of the segmentation. With the ideal segmentor, both the length and regularity of the segments can be controlled.

Merging segmentors do not give reproducible segmentation for different aqueous phase flow rates. The coaxial segmentor has a "falling drop" design and provides repeatable segmentation for higher total flow rates. This segmentor consists of a small chamber (glass or Perspex) with an inlet and an outlet. The outlet has a conical shape. The organic solution drops into the chamber, moves to the outlet and the drop is transported by the aqueous stream. All-glass chambers produce the lowest %RSD values in the segment lengths [19]. The chamber walls and the flat end of the inlet capillary must be cleaned regularly to maintain the segmentor's performance.

4.2.2 Extraction coils

The extraction coil is the part of the liquid-liquid extraction system where the actual transfer from the analyte takes place. The coil consists of PTFE tubing wound helically around a cylinder. The completeness of the mass transfer is determined by the extraction time (depending on the tube diameter, tube length and the flow rate).

Usually the phase transfer is improved by decreasing the flow rate [20]. When the flow rate is too low the extraction factor is very high, but the dispersion of the sample plug increases.

When Teflon tubing is used, the organic phase wets the walls of the tubing and the aqueous phase forms bubbles. With glass tubes the situation is exactly the opposite. It is better to have the analyte initially in the bubble phase to avoid cross-contamination between samples. When the interfacial area to initial volume ratio is high (in the bubble containing the analyte) the extraction is good.

4.2.3 Phase separators

Gravitational phase separators are based on the differences in densities of the organic and aqueous phases. The glass T-configuration phase separator is an example of this type of separators, where the segmented flow enters the separator from the horizontal side and the separated phases leave the separator in opposite directions, through the vertical sides. The phase originally containing the analyte is extracted at a slightly higher flow rate than the phase pumped to the detector. In the case where the organic phase (containing the extracted analyte) is pumped to the detector, the aqueous phase will be pumped at a slightly higher flow rate, ensuring that no aqueous phase will contaminate the flow-cell. This type of separator is simple, but cannot be used for two phases with similiar densities.

A sandwich-type gravitational separator has been designed [21] and no membrane is necessary for separation, but the applications seem to be limited. The sandwich-type membrane phase separator portrays better performance than the gravitational separator [10]. This separator consists of two blocks (resistant to both the organic and the aqueous phases) with grooves and a membrane sandwiched between the two blocks.

The efficiency of phase separation is influenced by the membrane area used for the separation, the porosity of the membrane, the volume formed by the grooves in the separator, the angle at which the flow meets the membrane and the pressure across the membrane. The mechanical strength of the membrane must be kept in mind when increasing the membrane area available for extraction.

It was found that the volume formed by the grooves must be at least four times larger than the volume of one of the segments in the aqueous phase. If the chamber is too large, the dispersion is very high. Separation better than 99% can be achieved using sandwich-type membrane separators, but a small fraction of organic solution is still present in the aqueous phase. The aqueous phase cannot be used for detection. A separator with three chambers, using a hydrophilic and a hydrophobic membrane can be used when the organic and the aqueous phases are needed for detection.

For the membrane type of separators, the two phases need not have a difference in densities and the separator is easier to manipulate. The lifetime of the membrane is limited.

Hydrophobic membranes are chosen when the organic phase are used for detection. PTFE membranes are used most frequently and the pore size determines the mass transfer across the membrane. Larger pore size may result in intrusion of the phase which is not used for detection.

Columns were used successfully for liquid-liquid extraction [22]. The column was packed with absorbent paper from babies' diapers. A small volume of aqueous sample was injected into a continuous flow of organic solvent, the aqueous phase was absorbed by the column and the organic phase was rinsed to the detector. This system cannot be used for preconcentration purposes, but is effective when the main object is to remove interferences from the aqueous phase.

4.3 Theoretical aspects of flow injection liquid-liquid extraction

4.3.1 Mechanism of phase transfer

The phase transfer takes place at the interface between the two phases. In FIA the phases are not highly dispersed, but high extraction coefficients can still be achieved. It was found that a film is formed on the sides of the tube, for example when PTFE tubing is used, a film of the organic solvent is formed and the thickness increases with increasing flow rate, but disappears when the flow is stopped. This film can increase the transfer efficiency of the analyte into the organic phase [23].

4.3.2 Dispersion in flow injection liquid-liquid extraction

Dispersion takes place before phase segmentation, during extraction, in the phase separator or after phase separation during the transport to the detector. The dispersion before and after liquid-liquid extraction must be minimized when high sensitivities are required and this is done by the same methods as in ordinary FIA systems. Merging of samples before segmentation should be done carefully to limit dilution effects. High transfer factors are achieved by using long extraction coil lengths. This cannot increase dispersion, because the flow is segmented. When a film is formed, however, this can increase the dispersion.

Assuming that the analyte is extracted from the aqueous phase into the organic phase (which has formed a film), the analyte is again transported into the organic segment by molecular diffusion and convection. When the aqueous plug is introduced mass transfer takes place from the aqueous plug to the organic film that still contains analyte from the first aqueous segment. This results in axial dispersion of the analyte. In coiled extraction conduits, radial dispersion decreases the axial dispersion.

4.4 Manifolds for liquid-liquid extraction

4.4.1 Sample introduction

The sample volume can be varied by adjusting the volume or the sampling time. Volume based sampling is used when a small sample volume is needed and the sensitivity need not be high. In liquid-liquid extraction large sample volumes are used, especially in systems where preconcentration, high phase ratios and reduced analyte dispersion are necessary.

The sample throughput decreases when a large sample volume is used. When the analyte is preconcentrated on a column, in a filter or in an acceptor solution, the enrichment factor (EF) will increase linearly with an increase in sampling time if the collection capacity of the column is not exceeded. In liquid-liquid extraction EF is only determined by the phase ratio and the phase transfer factor. The sampling time will influence EF only when the sample volume is very small. When volume-based sample injection is used, the sample is introduced into a non-segmented stream which is segmented at a later stage.

4.4.2 Segmentation and extraction

Usually liquid-liquid extractions are done by using segmented flow. This is not a strict rule and solvent circulation has been successfully applied in extractions [24]. A small volume of organic solvent is trapped in a closed loop and the extractant is circulated. The closed loop contains the segmentor, extraction coil, phase separator and the detector. EF depends on the number of cycles of the extractant.

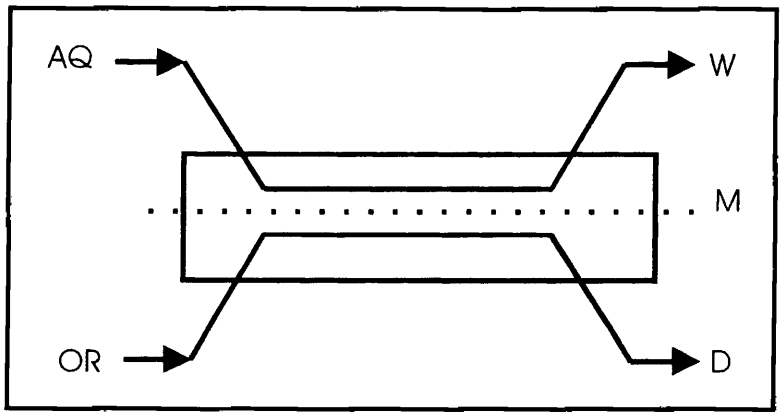

Figure 4.4.2A - A sandwich-type membrane extraction module.

AQ = aqueous phase
OR = organic phase
M = membrane
D = detector
W = waste

A sandwich-type membrane extraction module can be used for non-segmented liquid-liquid extraction. The two phases are pumped separately. When a PTFE membrane is used, the analyte is extracted from the aqueous stream into the hydrophobic membrane and then transferred into the organic stream. The phase transfer efficiency is about 18% and this technique can be used when concentrated samples have to be analysed.

4.4.3 Phase separation

Different phase separators were described in section 4.2.3. As was mentioned earlier, liquid-liquid extractions can be done without phase separation [25,26,27]. Phase separation can be avoided by using computer software to distinguish the analyte signals. The optical fibres are situated in the capillary flow-cell transmitted light from and to a spectrophotometer. The light is transmitted perpendicular to the flow direction to reduce interferences from differences in the refractive indexes from the two phases. Analyte concentrations can be monitored in both phases. The use of a capillary flow-cell will cause a loss in sensitivity.

4.4.4 Derivatization

Derivatization is used to enhance the sensitivity and/or selectivity of a method. The chemical reagents are added either immediately after sample injection or during segmentation. The chemical reaction can also take place in the extraction coil or the reagents can be added to the separated phase containing the analyte.

4.5 Coupling of liquid-liquid extraction systems to spectrophotometers

4.5.1 General

The spectrophotometer is the most popular detector used in liquid-liquid extraction FIA systems, because any flow rate and flow direction through the flow-cell can be used. The position of the flow-cell in the FIA manifold is not fixed and the quartz flow-cell is resistant to organic solvents. The glass/quartz flow-cell is hydrophilic and means that it can be contaminated with aqueous phase when the carrier stream consists of the organic phase.

As mentioned earlier, flame atomic absorption spectrometers, electrothermal atomic absorption spectrophotometers, ICP spectrometers and gas and liquid chromatographs can be used successfully as detectors in FIA systems.

4.5.2 Typical manifolds

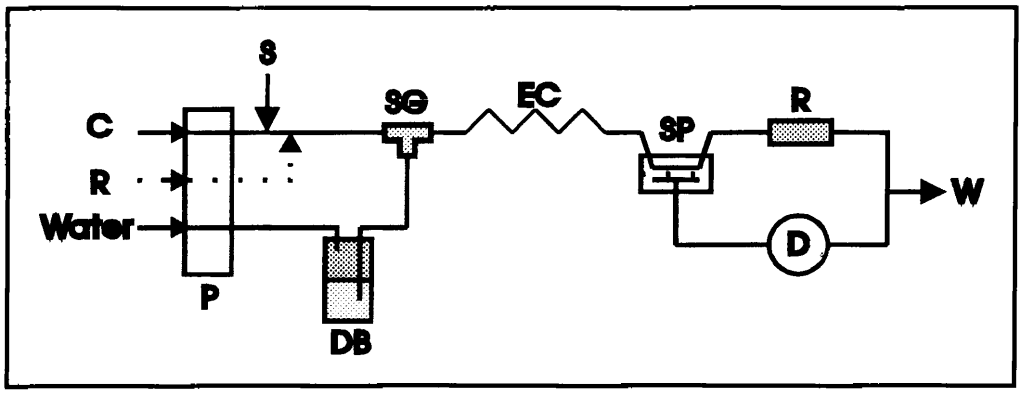

Fig.4.5.2A - FIA manifold for liquid-liquid extraction spectrophotometry [28].

P	=	**pump**
DB	=	**displacement bottle**
C	=	**carrier**
R	=	**reagent**
S	=	**sample**
SG	=	**phase segmentor**
EC	=	**extraction coil**
SP	=	**phase separator**
R1	=	**restrictor or impedance coil**
D	=	**detector**
W	=	**waste**

A typical FIA manifold used for liquid-liquid extraction can be seen in Fig. 4.5.2A. The sampling is volume-based, the reagent is added before segmentation, the segmentor is a merging tube segmentor and the organic solvent is propelled by making use of a displacement bottle. The extraction coil is connected to a sandwich-type membrane separator. The separated phase is transported directly to the detector. The flow of the sample waste is controlled by making use of a restrictor.

4.5.3 Performance of flow injection liquid-liquid extraction spectrophotometric systems

The sample throughput of liquid-liquid extraction spectrophotometric systems is high, usually in the range 30-60 h^{-1}. A precision of 1-2% is usually achieved. When samples are not preconcentrated, sample volumes are in the range of 100-500 µl.

A few examples of typical FI liquid-liquid extraction spectrophotometric procedures are the determinations of anionic and cationic surfactants [10,11], molybdenum [2] and lead [10].

4.6 References

1. Karlberg B, Thelander S, ***Anal. Chim. Acta***, **98**, 1978, 1.
2. Bergamin H, Medeiros JX, Reis BF, Zagatto EAG, ***Anal. Chim. Acta***, **101**, 1978, 9.
3. Burguera JL, Burguera M, ***Anal. Chim. Acta***, **153**, 1983, 207.
4. Karlberg B, Thelander S, ***Anal. Chim. Acta***, **114**, 1980, 129.
5. Karlberg B, Johansson PA, Thelander S, ***Anal. Chim. Acta***, **104**, 1979, 21.
6. Johansson PA, Karlberg B, Thelander S, ***Anal. Chim. Acta***, **114**, 1980, 215.
7. Rossi TM, Shelly DC, Warner IM, ***Anal. Chem.***, **54**, 1982, 2056.
8. Shelly DC, Rossi TM, Warner IM, ***Anal. Chem.***, **54**, 1982, 87.
9. Gallego M, Valcárcel, ***Anal. Chim. Acta***, **169**, 1985, 161.
10. Kawase J, Nakae A, Yamanaka M, ***Anal. Chem.***, **51**, 1979, 1640.
11. Kawase J, ***Anal. Chem.***, **52**, 1980, 2124.
12. Klinghoffer O, Ruzicka J, Hansen EH, ***Talanta***, **27**, 1980, 169.
13. Imasaka T, Harada T, Ishibashi N, ***Anal. Chim. Acta***, **129**, 1981, 195.
14. Fossey L, Cantwell FF, ***Anal. Chem.***, **54**, 1982, 1693.
15. Ogata K, Taguchi K, Imanari T, ***Anal. Chem.***, **54**, 1982, 2127.
16. Ogata K, Taguchi K, Imanari T, ***Bunseki Kagaku***, **31**, 1982, 641.
17. Nord L, Karlberg B, ***Anal. Chim. Acta***, **145**, 1983, 151.
18. Kina K, Shirashi J, Ishibashi N, ***Talanta***, **25**, 1978, 295.
19. Kuban V, Danielsson LG, Ingman F, ***Anal. Chem.***, **62**, 1990, 2026.
20. Nord L, Backstrom K, Danielsson LG, Ingman P, Karlberg B, ***Anal. Chim. Acta***, **194**, 1987, 221.
21. de Ruiter G, Wolf JH, Brinkman UAT, Frei RW, ***Anal. Chim. Acta***, **192**, 1987, 267.
22. Toei J, ***Talanta***, **36**, 1989, 36.
23. Nord L, Karlberg B, ***Anal. Chim. Acta***, **164**, 1984, 233.
24. Atallah RH, Ruzicka J, Christian GD, ***Anal. Chem.***, **59**, 1987, 2909.
25. Canete F, Rios A, Luque de Castro MD, Valcárcel M, ***Anal. Chem.***, **60**, 1988, 2354.

26. Canete F, Rios A, Luque de Castro MD, Valcárcel M, ***Anal. Chim. Acta*, 224**, 1989, 169.

27. Mesa JAG, Linares P, Luque de Castro MD, Valcárcel M, ***Anal. Chim. Acta*, 235**, 1990, 441.

28. Fang Z, ***Flow Injection Separation and Preconcentration***, Weinheim, New York, 1993.

CHAPTER 5

DIALYSIS

5.1 Introduction

Dialysis is the selective separation of species through a semi-permeable membrane that separates two fluids. In batch procedures the process is allowed to develop until mass transfer equilibrium is reached.

Dialysis membranes play an important in automated sample preparation and in the deliverance of a processed sample under a well defined and interference-free condition. This separation technique is simple, repeatable, reliable, compatible and requires little or no pretreatment of sample. The sample colour and turbidity do not interfere with the detection system and usually the membrane interface is inert. Dialysis membranes can be used in continuous flow, flow injection, stopped-flow, sequential injection and process analysis modes. In continuous flow or flow injection systems coupled with dialysis the timing must be carefully controlled, since the system is not allowed to reach mass transfer equilibrium.

Ions or molecular constituents have different mobilities in a liquid phase when transported across a membrane (semi-permeable) into a second liquid phase. The donor and acceptor phases are separated by a membrane and this membrane is selectively penetrated by solutes and the mass transfer takes place because of the existence of a concentration gradient of the transferable solute present between the two phases. The membrane also acts as a barrier readily permeable to the donor solvent and the smaller analyte solute molecules.

At first FIA was used for analysis of agricultural samples, but application in the field of clinical chemistry soon followed. The analysis of blood serum and urine samples demanded a few changes in the original design of FIA manifolds. The sample volume was limited, the samples were different from the standards, interferences from large molecules (e.g. proteins) had to be removed by dialysis or dilution and organic molecules (fat and proteins) deposited on the walls of the tubes. Haemodialysis is used to treat chronic and acute uraemia and to remove poisons from the blood-stream.

Dialysis is not often applied in industrial procedures, as it is a slow process (driven by concentration differences) and it is not highly selective. Chemically similiar species or species with similiar molecular size cannot be fully separated by dialysis. Dialysis in continuous flow is not efficient (the efficiency is in the range 1-4%), but is used for separation and dilution.

The efficiency of dialysis as a separation technique is governed by the diffusion rate of solutes through the membrane and the stagnant films of fluid on either side of the membrane and the properties of the membrane. When sensitivity is necessary, the low efficiency of the solute transfer can be a serious limiting factor in a FIA method. Liquid dialysis was applied successfully in the determination of inorganic phosphates and chlorides in blood serum [1] and in the turbidimetrical determination of inorganic sulphate in urine [2].

Usually dialysis is not applied in cases where preconcentration of the analyte is necessary. By changing the membrane's nature or by using an ion-exchange membrane (Donnan dialysis), the analyte can be preconcentrated to an extent.

5.2 Theoretical aspects of dialysis

Continuous dialysis is influenced by the membrane area used for dialysis, the membrane thickness, the residence time, the sample-mixing time, the flow rate, temperature, concentration of solutions and the viscosity of the solutions. The first mathematical models were derived to describe mass transfer across membranes in haemodialysers considering both semi-infinite, parallel plate dialysers and cylindrical tube units [17,18]. Haemodialysers containing blood and dialysate streams separated by a semi-permeable membrane were studied. The convective diffusion equations were solved for the two fluids for arbitrary interfacial concentration distributions by linking the two solutions via a continuity-of-flux boundary condition at the membrane surfaces. The true interfacial concentration distribution equations yielded by this process were substituted for the arbitrary distributions and they produced a set of complete solutions for the concentration fields in both fluid phases.

These equations were solved assuming the following:

- the donor fluid enters the system in laminar flow at a uniform concentration,
- the dialysate has a constant bulk concentration at all axial positions in the dialyser,
- the donor fluid is Newtonian,
- both the fluids are homogeneous and have constant physical properties,
- mass transport through the membrane is purely diffusive,
- the membrane permeability and dialysate-side mass transfer coefficients are constant,

- the solute partition coefficients between the fluids and membrane are not the same or equal to unity,

- the axial diffusion in the donor fluid is negligible compared to axial convection,

- steady state conditions exist and

- diffusion in the donor fluid is Fickian.

The convective equations were solved for a constant surface concentration and the results were generalized to varying surface concentration conditions using the Duhamel Theorem. The variables were then separated to yield an equation with eigenvalues and eigenfunctions. The equations were transformed via the Kummer's equation after introducing some variables into the equation and a Sturm-Liouville system was constituted in the mathematical modeling. Sherwood numbers were used to predict that the mass flux takes place mainly at the dialyser's inlet. The model was applied to Kiil haemodialysers.

Theoretical models were proposed to describe mass transfer in on-line dialysers [3]. The models were derived assuming laminar flow and equal hydrostatic pressure on both sides of the membrane. The mass transfer across infinite parallel plate dialysers with co-flow between sample and detector streams was described [3].

Analytical solutions were obtained with coupled diffusion and membrane transfer equations for plug flow in both channels and used the finite difference approximation method to obtain numerical solutions for laminar flow conditions. The two numerical solutions described plug and parabolic flows in both channels. The analytical parallel-plate dialyser model consists of two parallel channels of infinite width separated by a dialysis membrane.

The sample enters at the top (donor) channel and the analyte is transferred through the membrane to the bottom recipient detector (acceptor) channel. The transport in the x-direction is caused by the liquid flow and the transport in the y-direction is caused by molecular diffusion (Fick's law).

The transport in the z-direction is not taken into account, as the width is infinite. The donor fluid enters the dialyser at x = 0 and C_d^0 is the concentration of the analyte in the recipient channel and C_s^0 is the concentration of the analyte in the donor channel.

$$u_j(r)\frac{\partial C_j}{\partial x} = D_j \frac{\partial^2 C_j}{\partial r^2}$$

where u = linear flow velocity

r = radial distance from the tube center

C_j = concentration at a particular point in the channel

x = distance along the tube axis

j = subscript used for sample and detector channels

D_j = diffusion coefficient of the solutes moving through the membrane

The boundary conditions for both streams are

$$C_j = C_i \text{ at } x = 0 \text{ for } 0 \leq r \leq a$$

and

$$\frac{\partial C}{\partial r} = 0 \quad \text{at} \quad r = -\frac{a_i}{2}$$

It was assumed that the permeation is proportional to the concentration differences between the two sides of the membrane.

$$\pm D_j\left(\frac{\partial C_i}{\partial r}\right)(r = a_j, x) = P[C_{w(s)}(r = a_s, x) - C_{w(d)}(r = a_d, x)]$$

where P = permeability in m.s-1

$C_{w(s)}$ = concentration of the sample zone on the membrane surface (donor side)

$C_{w(d)}$ = concentration of the dialysate on the membrane surface.

The mathematical treatment was subdivided into two sections to describe plug flow and parabolic flows [3]. The plug flow equation was solved by Fourier series expansion and the solving of a Sturm-Liouville system.

$$u_i(r) = u_{i,(\max)}\left[1 - \left(\frac{2r_i}{a_i}\right)^2\right]$$

The velocity profile of two dimensional laminar flow is given by the equation above. Four different parallel plate dialysers were evaluated to compare the theoretical results with the experimental results for the dialysis of zinc(II) [3].

$$\frac{D_A}{v_s} = \frac{[(C_s)_1 - (C_s)_2]}{(C_s)_1}$$

where D_A = composite mass transfer diffusion coefficient

v_s = donor channel flow rate

$(C_s)_1$ = concentration of analyte in donor channel entering the dialyser

$(C_s)_2$ = concentration of analyte in donor channel exiting the dialyser [8].

The operating efficiency of a dialyser can be described by the above equation if $(C_d)_1=0$. The efficiency in absolute value is related to the flow rate of the donor phase. $(C_d)_1$ is the analyte concentration where the acceptor stream enters the dialyser and $(C_d)_2$ is the concentration of the analyte where the acceptor stream exits the dialyser.

The mass transfer diffusion coefficient includes all the physical parameters of the system, e.g. membrane surface, membrane area, membrane porosity, membrane thickness, temperature, electrical effects, pressure, flow rates of solution, geometry, viscosity and turtuosity of the membrane.

$$P = \frac{C_d}{C_s}$$

where P = phase transfer factor in dialysis = dialysis factor

C_d = output concentration of the detector channel

C_s = initial sample channel concentration

The mass transfer efficiency can be calculated by multiplying the dialysis factor with 100. There are several factors that influence the dialysis factor, e.g. solute concentrations, relative flow direction of donor and acceptor streams, sample volume, flow rate, membrane properties, channel length and temperature.

The rate at which a compound diffuses through a semi-permeable membrane is dependent on differential transport governed by Fick's law [7] of molecular diffusion. This law can only be applied when the pore diameter of the membrane is much larger than the diameter of the diffusing solute.

5.3 Dialysers

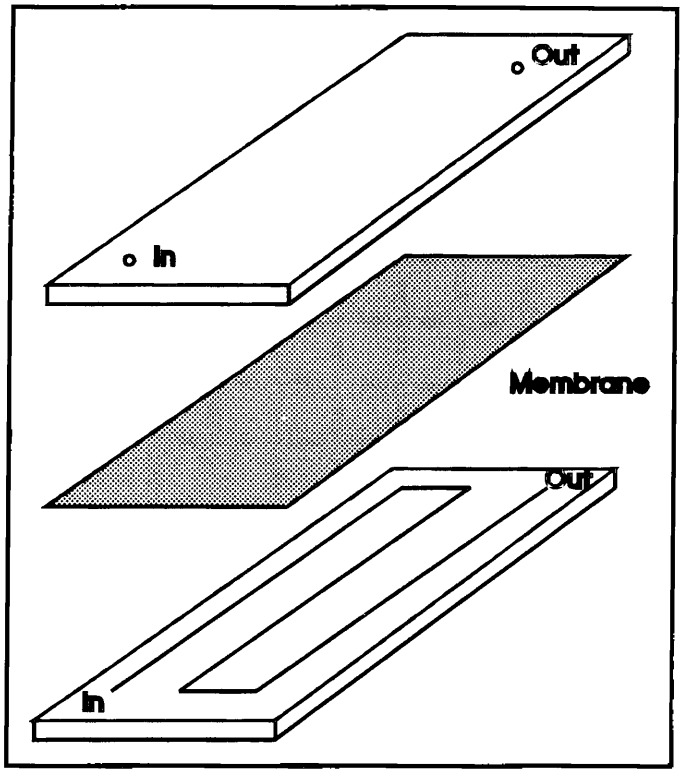

Figure 5.3A - Sandwich-type dialyser unit

The oldest unit used for dialysis is the circular form [19], but the sandwich-type dialyser is most frequently used in FIA (Fig. 5.3A). The dialyser consists of two blocks made from material that is chemical and mechanically resistant and these blocks are held together by screws. Grooves (mirror images of each other) are engraved on the blocks and the donor and acceptor streams flow through these grooves separated by a membrane. The membrane surface on each plate is extremely finely machined to ensure a positive membrane barrier, to prevent leakage and to prevent cross-contamination. The holes for the clamping screws are aligned perfectly to prevent leakage or damage to the fitted membrane. The dialyser is designed to spread the clamping load over the whole block and to prevent distortion and leakage when the dialyser unit is assembled and fitted with a membrane.

The reason why the channels are winded is to save space. A flow restrictor is incorporated into the channel with the lower pressure to balance the pressures on both sides of the membrane. The channels have a semi-tubular form and have the same depth and width as the rest of the manifold to reduce any disturbance of the sampling zone. The channels of the dialyser can be filled with glass beads to reduce dispersion by increasing the radial diffusion of the sampling zone [20]. These glass beads also act as support for the membrane.

5.4 Dialysis membranes

The physical characteristics of membranes will influence the selectivity of the analytical method [8,9,16]. Dialysis processes are classified as passive or active (Donnan) and the nature of the membrane determines this classification [8]. During passive dialysis a neutral membrane differentiates between separations on a molecular scale, allowing species with in a given range of molecular mass to diffuse across a neutral membrane. During active dialysis the ions are transferred across an ion-exchange membrane. This membrane is subjected to membrane fouling that can effect the diffusion rate.

Membranes used in FIA systems must have high transfer factors even when the contact times are very short and they have to maintain their performance. There are three types of membranes: the microporous, homogeneous and ion-exchange membranes.

When homogeneous membranes are used, the transfer takes place by molecular diffusion. Ion-exchange membranes are porous (like the microporous membranes), but the pores have ions attached to them. Ion-exchange membranes are used to perform preconcentration by Donnan dialysis. The membrane consists of film forming polymers with anions or cations fixed to the pore walls.

Mass transfer occurs via an ionic reaction/diffusion and the separation efficiency depends on the solubility and diffusivity of the membrane and the ion-exchange properties of the membrane. A membrane can also be asymmetric and solutes can move from one side through the membrane to the other side, but the transfer is much more difficult in the opposite direction.

Membranes are typically made of cellophane, cellulose acetate, polycarbonate, polyvinyl chloride, polyamides, polysulphone, polyvinylidene fluoride, copolymers of acrylonitrile and vinyl chloride, polyacetal, polyacrylate, poly electrolyte complexes, cross linked polyvinyl alcohols as well as acrylic copolymers.

Cellophane swells when it is covered with water and it can contain up to 50% water to form a hydrogel. This gel acts as a sponge with fixed pore size (ranging from 3-5 nm). Membranes have to be uniform in thickness, elasticity and permeability to guarantee optimum performance.

Before fitting a membrane in a dialyser, the membrane is thoroughly rinsed with distilled water and not allowed to dry after this treatment.

5.5 Manifolds for flow-injection dialysis

5.5.1 Basic configuration

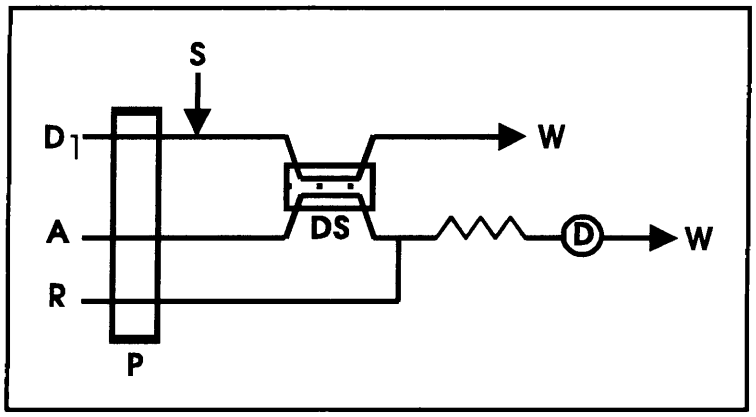

Figure 5.5.1A - Basic configuration of manifold for on-line dialysis [15].

D_1 = donor sample carrier
A = acceptor stream
R = reagent
S = sample
DS = membrane dialyser
D = detector
W = waste

In Fig. 5.5.1A a volume-based sampling FIA manifold is shown. Usually the reagent is added to the acceptor stream.

5.5.2 Manifolds with dialysers as sample loops

The dialyser can be placed in the sample loop to increase the dialysis periods under static conditions. This specific design was used in the determination of salicylic acid [4] and in studies of drug-protein binding [5].

5.6 Coupling of on-line dialysis to spectrophotometric systems

Usually the acceptor stream is coupled to the spectrophotometer after merging with the reagents. Physical interferences, like colloidal or suspended materials, are removed by dialysis and the analyte is diluted.

An interesting liquid dialysis process was used for the determination of glucose and urea in blood serum and urine [10]. The dialyser was fitted with a Cuprofan membrane (membrane area of 8.1 cm^2) and the influence of the flow rate in the sample channel and dialyser was studied. An enzyme reactor was used and the reaction products hydrogen peroxide and ammonia were detected photometrically and potentiometrically.

Gas-dialysis can be used to determine the ammonia content in blood and this was applied to diagnose liver coma and Reye's syndrome. A FIA method where the sample is injected into a sodium hydroxide carrier solution was proposed [11]. Ammonia is released and diffuses through a Teflon membrane and reacts with an indicator and the increase in the basic form of the indicator is measured photometrically. A good sample throughput of 60 h^{-1} and relative standard deviation of 1.3% were achieved. Carbon dioxide, certain carbonyl compounds and fluoride were determined by making use of dialysis [12,13,14]. A detergent was added to improve the diffusion at the membrane during the fluoride determination.

Dialysis improves the sensitivity, stability and lifetime of ion-selective electrodes when coupled with electrochemical detectors [10,6]. Usually colloidal or suspended materials do not interfere with atomic absorption detection and that is why dialysis is not frequently coupled with the AAS detector.

5.7 References

1. Hansen EH, Růžička J, ***Anal. Chim. Acta***, **87**, 1976, 353.
2. van Staden JF, Basson WD, ***Lab. Pract.***, **29**, 1980, 1279.
3. Bernhardsson B, Martins E, Johansson G, ***Anal. Chim. Acta***, **167**, 1985, 111.
4. Chang QL, Meyerhoff ME, ***Anal. Chim. Acta***, **186**, 1986, 81.
5. Macheras PE, Koupparis MA, ***Anal. Chim. Acta***, **185**, 1986, 65.
6. van Staden JF, ***Anal. Letts.***, **19**, 1986, 1407.
7. Fick A, ***Pogg. Ann.***, **94**, 1855, 59.
8. Valcárcel M, Luque de Castro MD, ***Non-chromatographic continuous separation techniques***, Royal Society of Chemistry, London, 1991.
9. Lazaro F, Luque de Castro MD, ***Analusis***, **16**, 1988, 216.
10. Gorton L, Ogren L, ***Anal. Chim. Acta***, **130**, 1981, 45.
11. Svensson G, Anfält T, ***Clin. Chim. Acta***, **119**, 1982, 7.
12. Baadenhuijsen H, Seuren-Jacobs HEH, ***Clin. Chem.***, **25**, 1979, 443.
13. Marstorp P, Anfält T, Andersson L, ***Anal. Chim. Acta***, **149**, 1983, 281.
14. Macdonald AMG, Wu GP, ***9th International Symposium on Microchemical Techniques***, Amsterdam, 1983.
15. Fang Z, ***Flow Injection Separation and Preconcentration***, Weinheim, New York, 1993.
16. van Staden JF, van Rensburg A, ***Analyst***, **115**, 1990, 1049.
17. Cooney DO, Davis EJ, Kim S-S, ***Chem. Eng. J***, **8**, 1974, 213.
18. Cooney DO, Kim S-S, Davis EJ, ***Chem. Eng. Sci.***, **29**, 1974, 1731.
19. ***Gradco catalogue***, Gradco, Winchester, England, 1974, 47.
20. Olsson B, Lundback H, Johansson G, ***Anal. Chim. Acta***, **167**, 1985, 123.

CHAPTER 6

DETERMINATION OF PHENOL

6.1 Introduction

Phenolic compounds are present in various stages in the industrial processing of oil from coal. Phenols can be precursors in gum formation that lead to possible blockage and damage of engines. One of the main targets in the processing of oil is to remove most of the phenols.

Many procedures have been developed for the determination of phenol. Distillation and gas chromatography are amongst the most popular used in South African petroleum industries. However, in the process environment a quick and reliable on-line procedure for the determination of total phenols in oil is a necessity. The concept of flow injection analysis has established itself as an analytical technique which, when automated, is suitable for increasing sample output [1,2].

Membranes are extremely useful for in-line separations in flow-through dialysers as part of flow injection systems [3]. The nature of the membrane (that is the type of membrane, membrane surface, membrane porosity and membrane thickness used) determines the features of the transfer across the membrane and, therefore, the nature and size of the ions and molecules diffusing through it.

The classification of dialysis processes as passive or active (Donnan) also depends on the nature of the membrane. In the passive process a neutral membrane differentiates between separations on a molecular scale with a precision of molecular order allowing species within a given range of molecular mass to diffuse across a neutral membrane.

In active (Donnan) dialysis, the ions with a given type of charge are transferred across an ion-exchange membrane. Hydrophobic microporous membranes such as PTFE, Durapore or isotactic polypropylene are normally used for the filtering of gas streams in gas-diffusion flow injection systems [4,5] or as supported liquid membranes (SLMs) in flow injection manifolds [6-8]. SLMs provide a flexible and selective approach to the separation and enrichment of chemical species. The extraction of the desired species from the donor aqueous solution into the thin organic layer on the SLM occurs simultaneously with its back-extraction into the second acceptor aqueous solution in the FIA manifold.

6.2 Uses of phenol

Synthetic phenol was prepared on industrial scale during the outbreak of World War I, as it was needed as raw material for the manufacture of picric acid (2,4,6-trinitrophenol). Phenol is now used in a variety of products, for example Bakelite resin and adhesives for binding plywood. It also serves as starting material for the synthesis of chlorinated phenols and of the food preservatives BHT (butylated hydroxytoluene) and BHA (butylated hydroxyanisole).

Pentachlorophenol, a wood preservative is prepared by reaction of phenol with excess chlorine. The herbicide 2,4-D (2,4-dichlorophenoxyacetic acid) is prepared from 2,4-dichlorophenol and the antiseptic agent hexachlorophene is prepared from 2,4,5-trichlorophenol. The food preservative BHT is prepared by Friedel-Crafts alkylation of *p*-methylphenol (*p*-cresol) with 2-methylpropene in the presence of acid and BHA is prepared similarly by alkylation of *p*-methoxyphenol [9].

6.3 Properties of phenol

Low-molecular mass phenols are water soluble and have high boiling points because of intermolecular hydrogen bonding. Phenols are acidic. They are weak acids that can dissociate in aqueous solution to give H_3O^+ plus a phenoxide anion, ArO^-.

The acidity value of phenol is pK_a = 10.00, which is much more acidic than ethanol (pK_a = 16.00). Phenols are more acidic than alcohols because the phenoxide anion is resonance-stabilized by the aromatic ring. Sharing of the negative charge on oxygen with the ortho and para positions of the aromatic ring results in an increased stability of the phenoxide anion relative to undissociated phenol.

The value of $\Delta G°$ for the dissociation of phenol is low. The acidity values of nitro-subsitituted phenols approach the acidity of carboxylic acids. Phenols with electron-withdrawing substituents are more acidic because these substituents stabilize the phenoxide ion by delocalizing the negative charge. A phenolic compound can be separated from a mixture by basic extraction into aqueous solution, followed by reacidification.

Phenols undergo alcohol-like reactions (ester formation with acid chlorides or acid anhydrides), electrophilic aromatic substitution reactions (Kolbe-Schmitt carboxylation reaction), oxidation reactions (formation of quinones) and the Claisen rearrangement (formation of an allylphenol).

6.4 Choice of analytical method

Aminoantipyrine condenses with aromatic amines in the presence of an acid oxidizing reagent and also with phenols in the presence of alkaline oxidizing reagents [10]. This provides a sensitive test for phenolic compounds. A chloroform extraction can be used to enhance the sensitivity of the method, but proved to be laborious. When potassium persulphate is used, the fading of the coloured product can be prevented. The effect of temperature on the reaction was investigated and the colour was found not to be stable above 50°C [11].

Friedstad *et al.* [12] described a manual and automated method for determination of phenols by oxidative coupling with 3-methyl-2-benzothiazolinone hydrazone (MBTH). The MBTH method is based on the coupling of phenol with MBTH in an acidic medium using ammonium cerium(IV) sulphate as an oxidant.

The coupling with phenol takes place in the para position, but if this position is occupied, the reagent will react at a free ortho position. This reaction is less dependent on the position of the substituent group than is that with 4-aminoantipyrine (4-AAP). However, the colours (red to violet) produced by different phenolic compounds do not have their absorbance maxima at the same wavelength, but have a maxima ranging from 460 to 595 nm. The automated method gave the same results for both the 4-AAP and MBTH methods. With the MBTH method, aliphatic aldehydes and aromatic amines, however, interfered with the phenol determination.

Hexamine cobalt(III) tricarbonato cobaltate (III) can also be used for quantitative determination of phenol [13], but tartaric acid and citric acid interfere with the redox titration.

A steam distillation in a semimicro Kjeldahl apparatus can be used to remove interferences during the phenol determination using 4-AAP [14]. This can be used for phenol determination in wastes, disinfectants and antitoxins (added as preservatives), but this technique is not suitable for the flow injection determination of phenols in oil. The bromometric flow injection voltammetric method [15] and oven ring techniques [16] for phenol determination are sensitive, but time consuming.

Mohler and Jacob [17] made a comprehensive comparison of several sensitive methods for the determination of phenol and concluded that the 4-AAP method offered the highest speed of analysis at the greatest accuracy and precision.

Möller and Martin [18] adapted the 4-AAP method for the direct flow injection determination of phenol in water. The method was based on the condensation of phenols with 4-AAP with subsequent oxidation by $K_2S_2O_8$ in a buffered alkaline ($NaHCO_3$, H_3BO_3 and KOH) medium. An extraction manifold was also used to enhance the sensitivity and selectivity of the phenol determination.

Gonzalo *et al.* [19] used a hydrophobic silicone rubber membrane for the separation of phenols from kerosene into a basic acceptor stream that contained the 4-AAP reagent. The chemistry involved in their flow injection approach was the same as that reported by Möller and Martin [18].

Passive semipermeable hydrophilic membranes also provide a promising approach for the separation and controllable on-line dilution of analytes [20-22]. By using a time regulated system, analyte from a moving donor aqueous solution was fed via the passive hydrophilic membrane to a stationary acceptor solution in a diffusion process where separation and controllable diluton occurred simultaneously. It was possible with the establishment of a suitable concentration gradient [20-22] to increase the mass transfer efficiency of analyte for determination.

A promising new feature of passive semipermeable hydrophilic membranes is the ability of selective extraction-diffusion of neutral organic compounds from organic solvents to aqueous solutions when converted to ionic compounds.

During this investigation, the reaction between phenolic compounds and 4-aminoantipyrine in the presence of $K_2S_2O_8$ as oxidizing reagent was used to determine phenols in oil mixtures (Fig. 6.4A).

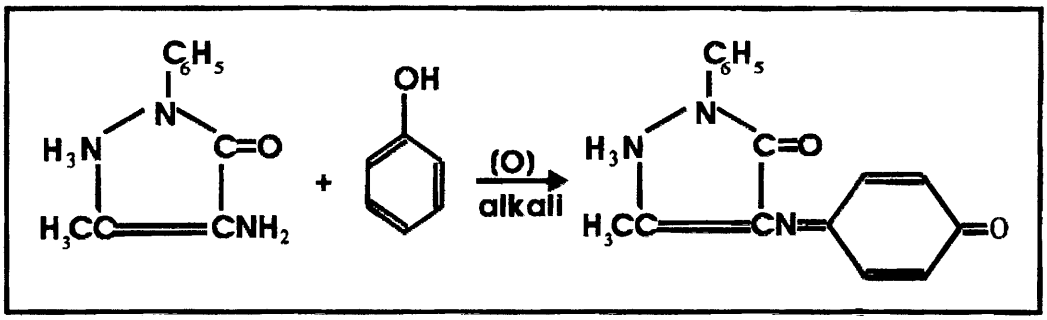

Figure 6.4A - The reaction used in the determination of phenols.

The phenols were extracted and preconcentrated from a xylene solution or oil samples by using a passive hydrophilic Spectrapor membrane. In this case, the membrane was used to enhance the sensitivity of the phenol determination and to remove interferences.

The phenols deprotonated after diffusion to the basic acceptor stream and the preconcentrated phenolate was injected into a carrier stream containing 4-aminoantipyrine as colour reagent. The carrier stream then merged with the oxidant stream, followed by detection at 500 nm.

6.5 In-line flow injection extraction preconcentration through a passive hydrophilic membrane. Determination of total phenols in oil by flow injection analysis (FIA).

6.5.1 Experimental

6.5.1.1 Reagents and solutions

A stock solution of phenol containing 1 000 mg/*l* was prepared by dissolving the appropriate amount of phenol (Merck) in xylene. Working standard solutions were prepared by suitable dilution with the same xylene. A buffer solution was prepared by dissolving 23 g $NaHCO_3$, 27 g H_3BO_3 and 35 g KOH in 1 *l* deionized water.

The 4-aminoantipyrine (4-AAP) reagent was prepared by dissolving 2.0 g 4-AAP and 22 g NaCl in 80 m*l* buffer solution and diluting to exactly 500 m*l* with deionized water. The oxidizing reagent was prepared by dissolving 25 g $K_2S_2O_8$ in 1 *l* deionized water adjusting the pH to 11 with KOH.

6.5.1.2 Apparatus

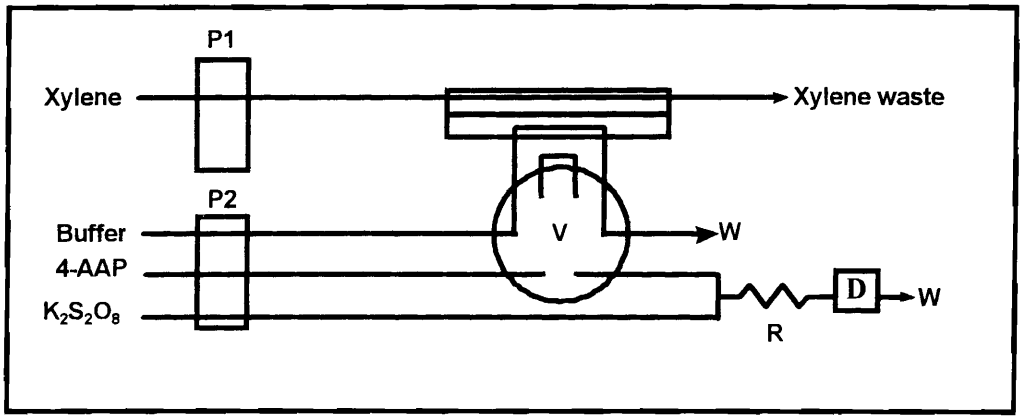

Figure 6.5.1.2A - The flow injection system used for the determination of phenol in oils.

P_1 = Ismatec peristaltic pump
P_2 = Gilson Minipuls peristaltic pump
V = VICI Valco valve
W = waste
R = reactor
D = detector

A flow injection system outlined in Fig. 6.5.1.2A was constructed from the following components: a Gilson Minipuls peristaltic pump (used to pump the reagents), an Ismatec peristaltic pump (used to pump the xylene or oil samples), a VICI Valco 10-port multi-functional sampling valve, a dialyser unit with Spectrapor membrane connected to the sample loop of the 10-port VICI Valco valve and a Unicam 8625 UV-visible spectrophotometer equipped with a 10-mm Hellma flow-through cell (volume 80 μl) for detection at 500 nm.

Data acquisition and device control were achieved using a PC30-B interface board (Eagle Electric, Cape Town, South Africa) and an assembled distribution board (MINTEK, Randburg, South Africa). The FlowTEK [23] software package (obtainable from MINTEK) for computer-aided flow analysis was used throughout for device control and data acquisition.

The system consists of four lines: the xylene donor stream that contains the phenol or oil sample, the buffer solution, the buffered 4-AAP colour reagent and the $K_2S_2O_8$ stream.

A Spectrapor cellulose membrane, through which molecules with molecular mass smaller than 6 000 to 8 000 dalton can diffuse, was used. The membrane was rinsed with deionized water and fitted immediately in the dialyser. This membrane portrayed optimum performance when it was never allowed to dry.

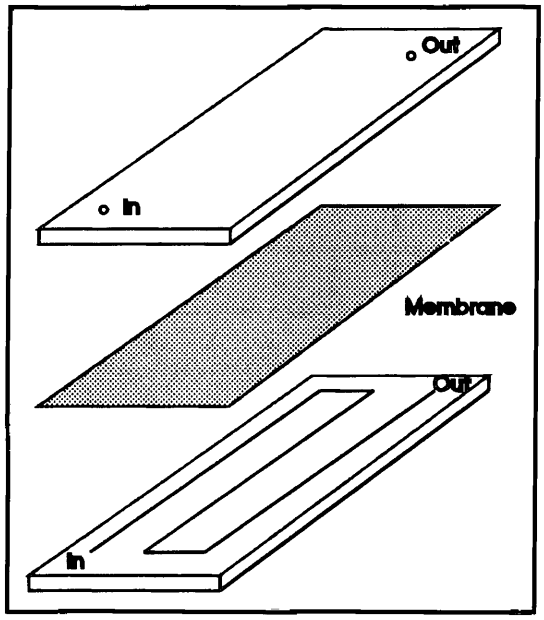

Figure 6.5.1.2B - Aluminium extraction preconcentration cell.

The dimensions of the aluminium extraction preconcentration cell can be seen in Fig. 6.5.1.2B. The groove (1mm x 0.5 mm x 280 mm) provides a preconcentration volume of 140 μl. Teflon tubing (0.76 mm id.) was used. The pump tubing was made of Tygon, except the Acidflex tubing that was used to pump the xylene.

6.5.1.3 Procedure

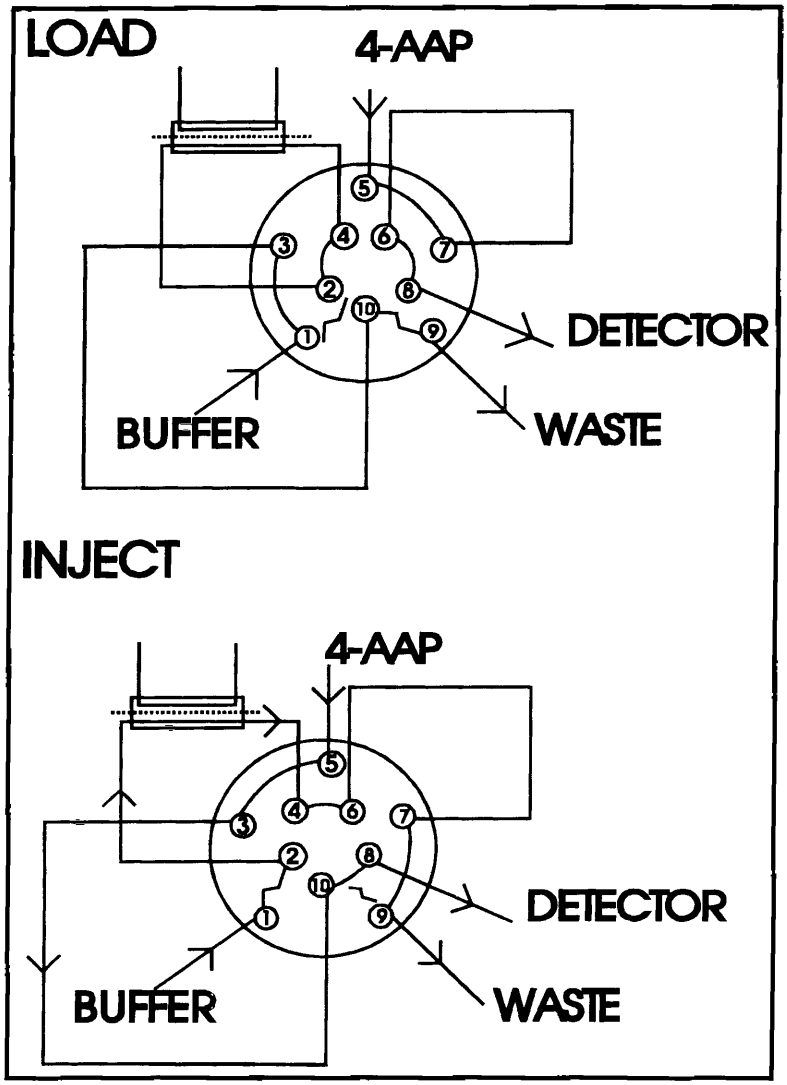

Figure 6.5.1.3A - In-line extraction preconcentration valve configuration.

The in-line extraction preconcentration valve configuration is outlined in Fig. 6.5.1.3A. The dialyser was rinsed with buffer solution for 30 seconds by switching the valve to the **INJECT** position (Fig. 6.5.3.1A (b)). With this configuration the buffer stream was pumped (using the valve port sequences 1→2→4→6→7→9) via the acceptor channel of the membrane to waste rinsing the membrane.

The buffered 4-AAP colour reagent stream was pumped (using the valve port sequences 5→3→10→8) through the detector to waste. When the valve switched to the **LOAD** position (Fig. 6.5.3.1A (a)), preconcentration of the phenolate into the buffer solution occurred inside the closed stationary part (between valve ports 2 and 4) of the valve system as illustrated in Fig. 6.5.3.1A (a). At the same time the xylene stream was pumped at constant flow rate on the donor side of the membrane, the buffer solution (using valve port sequences 1→3→10→9) to waste and the buffered 4-AAP reagent stream (using valve port sequences 5→7→6→8) via the detector to waste. The buffer that contains the preconcentrated phenol was then rinsed to the holding coil between valve ports 6 and 7 by switching the valve to the **INJECT** position for 2 seconds.

When the valve was again switched to the **LOAD** position (Fig. 6.5.3.1A (a)), the sample was rinsed to the detector by the buffered 4-AAP reagent (via the valve port sequence 5→7→6→8). The buffered 4-AAP reagent was used as blank for the analysis. The refraction indexes of the buffer and the buffered 4-AAP solutions were compared and it was necessary to add NaCl to the buffered 4-AAP solution to equal the refractive indexes.

Wavelength scans of the maximum absorbance for the red coloured reaction products for the different phenols gave a wavelength of 505 nm for phenol, 508 nm for o-cresol and 502 nm for m-cresol. A wavelength of 500 nm was selected as the optimum to determine the total value of the different phenols involved.

Hydrophobic microporous and passive hydrophilic membranes were evaluated. The process of membrane extraction with a continuous hydrophobic membrane, such as the polyvinylidene difluoride (Durapore) membrane, can be divided into three broad steps [6-8, 24,25]. In the first step the aqueous sample containing the analyte is brought into contact with the membrane where some of the analyte is extracted into the surface of the membrane. In the second part the analyte that is dissolved in the membrane diffuses across the membrane wall to the membrane/extractant interface.

The extraction mechanism involved in hydrophobic microporous membranes were discussed in detail [24,25]. Due to the hydrophobic nature of these membranes, they favour the extraction of organic species including organic solvents into the hydrophobic membrane. As a result of the hydrophobicity of the membrane large quantities of xylene leaked into the aqueous buffered 4-AAP acceptor stream that caused a lot of difficulties in the detection system.

The pressure of the donor stream was set as low as possible, but even stopping the xylene stream's flow for the preconcentration period, did not solve the problem. It was therefore clear that the hydrophobic Durapore (polyvinylidene difluoride) membrane was not suitable for the extraction and other options should be looked at.

A passive Spectrapor hydrophilic membrane was then investigated, where mass transport of phenol through the membrane occurred mainly by diffusion. Separation and preconcentration of the phenol to the basic acceptor stream were probably enhanced by the following mechanisms.

The passive hydrophilic membrane had a repelling effect on the organic xylene and oil solvents. At the same time the phenol analyte in the xylene (or oil) donor stream was converted to phenolate anions by the basic acceptor stream promoting the transfer of phenolate through the passive hydrophilic membrane. Although the preconcentration time was longer, the problem of transfer of xylene into the aqueous acceptor stream was solved.

6.5.2 Method optimization

6.5.2.1 Physical parameters

6.5.2.1.1 Flow rate

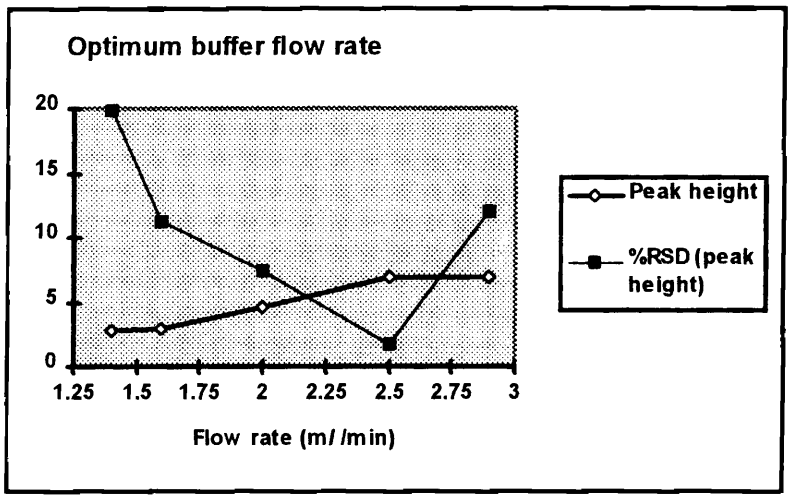

Figure 6.5.2.1.1A - Optimum buffer flow rate (peak heights were used in calculations).

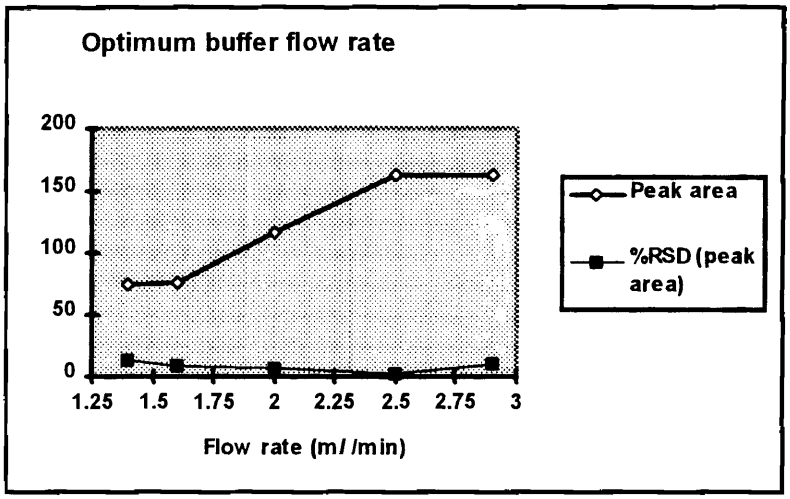

Figure 6.5.2.1.1B - Optimum buffer flow rate (peak areas were used in calculations).

The efficiency of the preconcentration step depends upon the flow rates of both the donor xylene and acceptor buffered 4-AAP streams. The system was optimized and the best mass transfer of phenolate was obtained when the flow rate of the xylene stream was 1 ml/min.

The results in Fig. 6.5.2.1.1A clearly indicate an optimum flow rate of 2.5 ml/min. for the buffered 4-AAP stream. The dispersion decreased with an increasing flow rate resulting in an increase in peak height, but unfortunately the %RSD also increased. These results are according to Vanderslice's expressions that states that the dispersion, travel time and peak width decrease with increasing flow rate (See Chapter 2, 2.3.6).

6.5.2.1.2 Line length

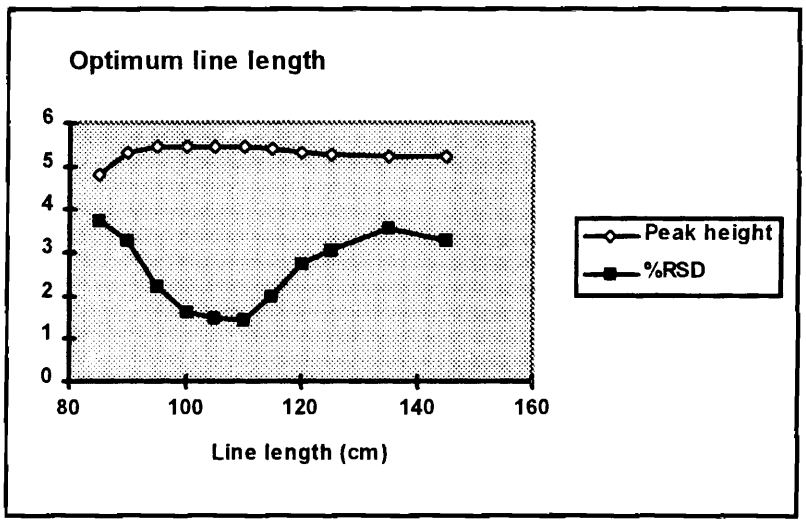

Figure 6.5.2.1.2A - Optimum reactor length (peak heights used in calculations).

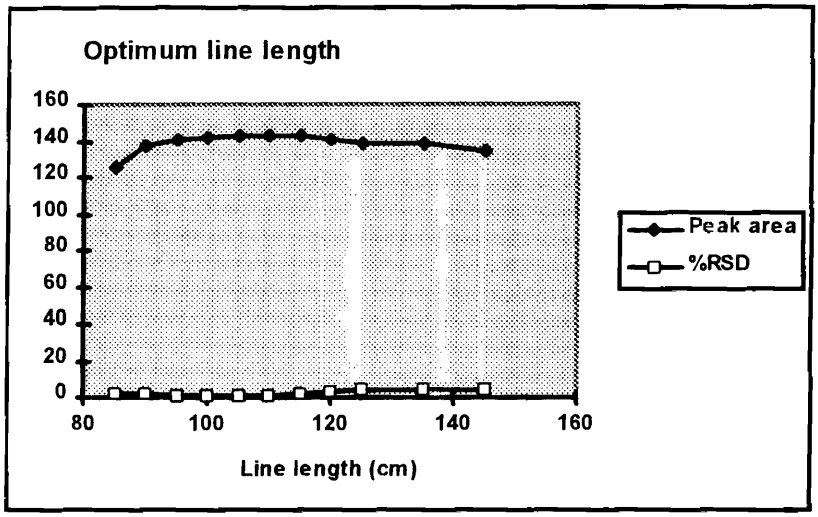

Figure 6.5.2.1.2B - Optimum reactor length (peak areas were used in calculations).

Initial reaction development already started in the acceptor channel of the flow injection system with the conversion of phenol to the phenolate ion. Oxidation and final colour development occurred in the reactor mixing coil, before the final product was transported to the detector. Line lengths between 85 and 145 cm were evaluated. The results obtained, are illustrated in Fig. 6.5.2.1.2A. An optimum reactor length of 110 cm was chosen as compromise between response and precision. The increasing dispersion coefficient with increasing reactor length is consistent with Ruzicka's expression (See Chapter 2, 2.4.3.1).

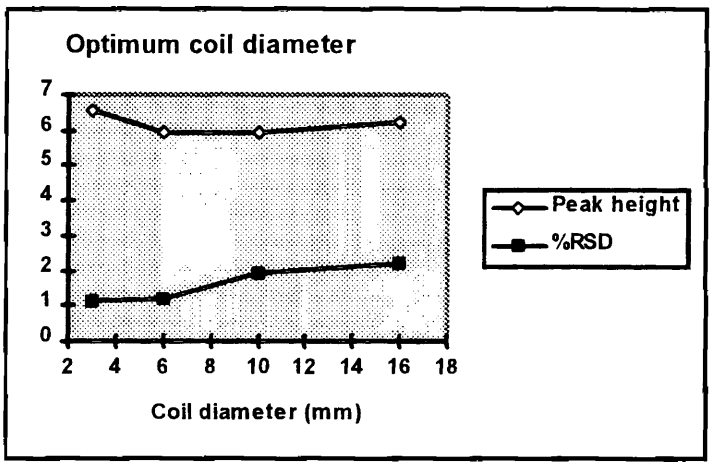

Figure 6.5.2.1.2C - Optimum reaction coil diameter (peak heights were used for calculations).

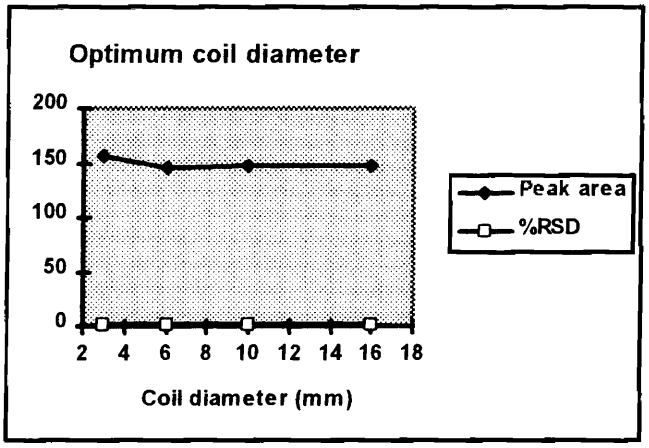

Figure 6.5.2.1.2D - Optimum coil diameter (peak areas were used for calculations).

The optimum coil diameter was 3 mm. The smaller the coil diameter, the smaller the dispersion (See Chapter 2, 2.4.3.2).

6.5.2.1.3 Sampling volume

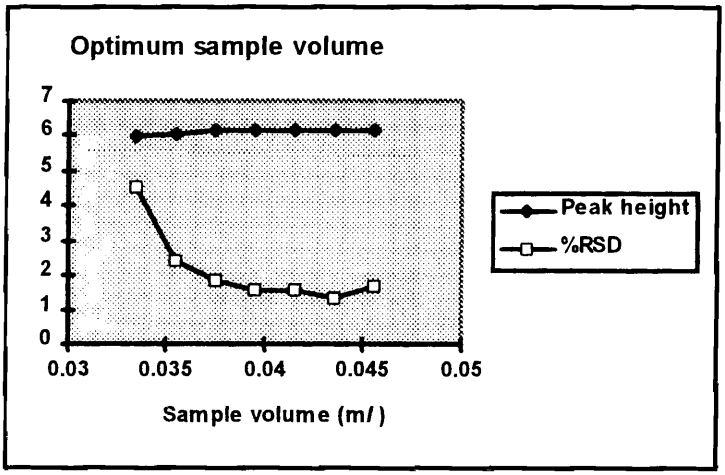

Figure 6.5.2.1.3A - Optimum sample volume (peak heights were used in calculations).

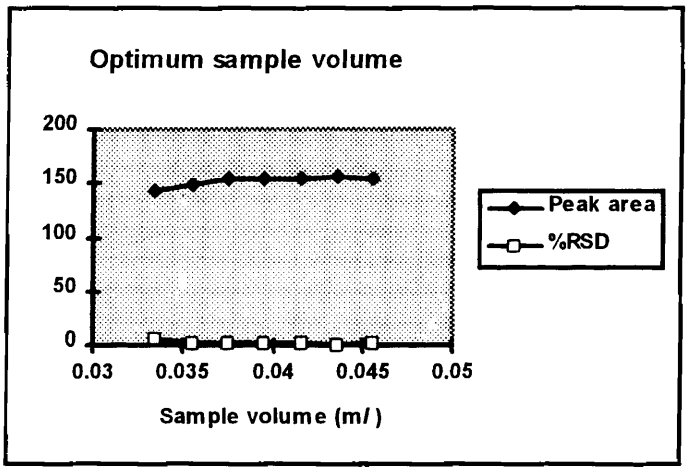

Figure 6.5.2.1.3B - Optimum sample volume (peak areas were used in caculations).

The sampling volume of the extracted phenolate analyte plays a crucial role in the response and precision of the proposed system. Sampling volumes between 33 and 45 μl were investigated. The results obtained are given in Fig. 6.5.2.1.3A and B. The response increases with an increase of sample volume up to a volume of 44 μl. The decrease observed at 45 μl is probably due to boundary effects. The optimum sample volume of 44 μl also gave the best precision and was selected for the proposed system. The results obtained when peak heights were used in the calculations correlate well with the results obtained when peak areas were used.

6.5.2.2 Chemical parameters

6.5.2.2.1 Buffer pH

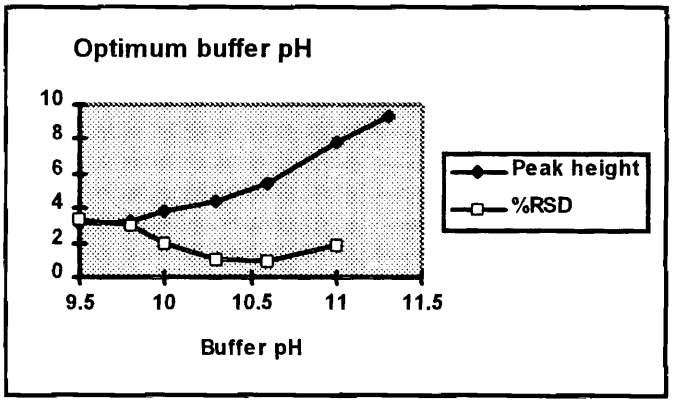

Figure 6.5.2.2.1A - Optimum buffer pH (peak heights were used in calculations).

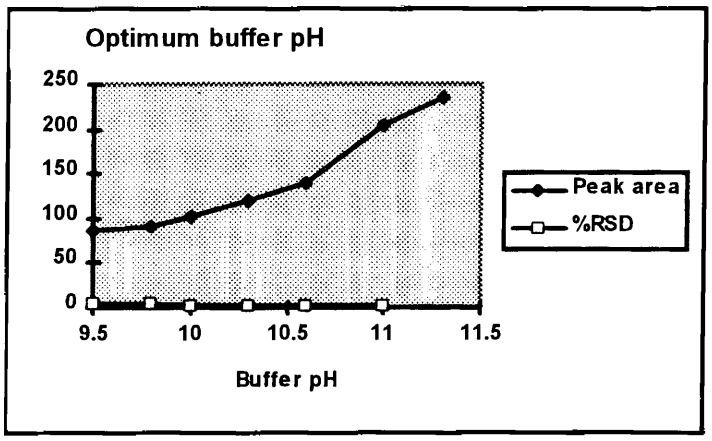

Figure 6.5.2.2.1B - Optimum buffer pH (peak areas were used in calculations).

The pH of the buffered 4-AAP solution was evaluated and the results are outlined in Fig. 6.5.2.2.1A and B. The following conditions had to be considered during the evaluation. The reaction was only successful in a narrow pH range, as a red precipitate formed at a high pH value. The pH had to be high enough to deprotonate the phenol for maximum mass transfer efficiency through the membrane.

The 4-AAP reagent was oxidized to a red compound at a pH below 8. However, at pH values above 8 the colour of this compound changed to yellow with that of the phenol-4-AAP product remaining red. The best results (sensitivity and precision) were obtained with an optimum buffer pH of 10.6 (Fig. 6.5.2.2.1A and 6.5.2.2.1B).

6.5.3 Evaluation of the method

6.5.3.1 Linearity

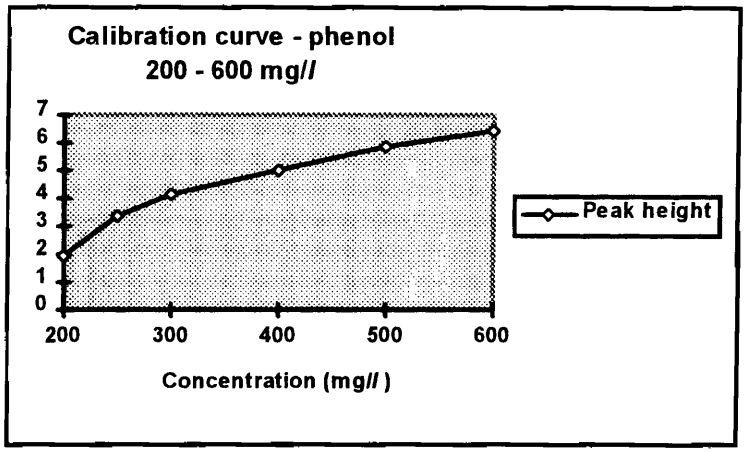

Figure 6.5.3.1A - Calibration curve of phenol in xylene in the range 200 to 600 mg/l.

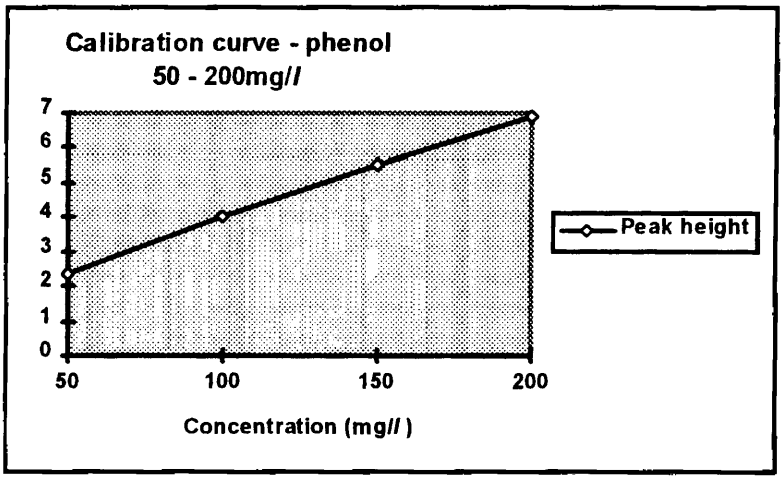

Figure 6.5.3.1B - Calibration curve of phenol in xylene in the range 50 to 200 mg/l.

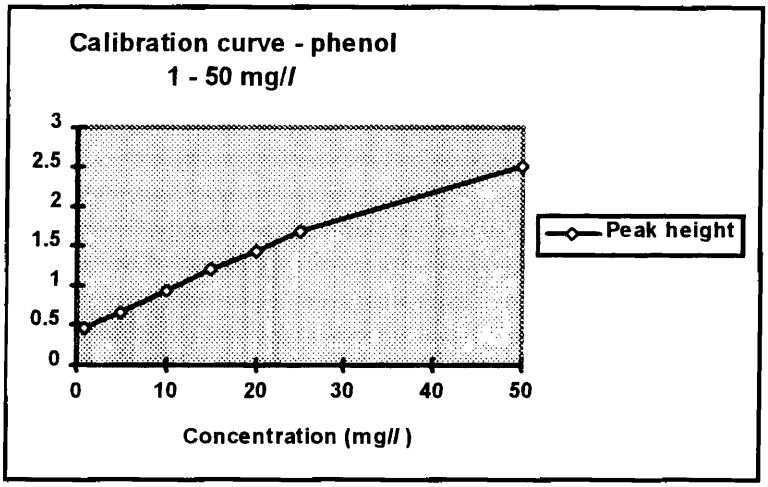

Figure 6.5.3.1C - Calibration curve of phenol in xylene in the range 1 to 50 mg/l.

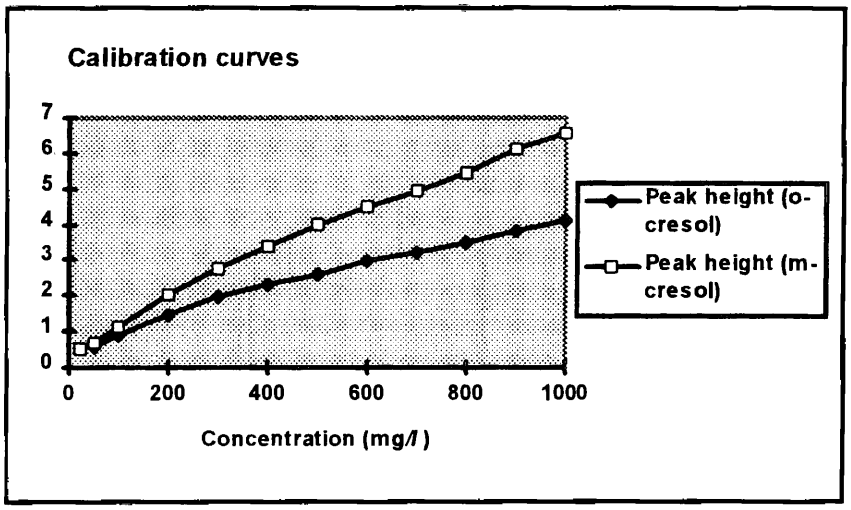

Figure 6.5.3.1D - Calibration curves of o-cresol and m-cresol.

Range (mg/*l*)	Preconcentration time in seconds	Correlation coefficient (r^2)	Relationship between peak height (y) and phenol concentration (x) in mg/*l*.	Relative standard deviation (%)
200 to 600	100	0.97	y = 0.0104x + 0.5099	1.3
50 to 200	300	0.99	y = 0.0306x + 0.9124	1.1
1 to 50	500	0.99	y = 0.0419x + 0.5066	1.1

Table 6.5.3.1A - Linear relationship between peak height and concentration for the proposed FIA system for different preconcentration times.

Different preconcentration times were evaluated to cover samples containing different amounts of phenol. The results obtained are given in Table 6.5.3.1A. The correlation coefficients clearly indicated a linear relationship between the peak height and concentration for the three different ranges outlined. The proposed FIA system is suitable for the determination of phenol ranging from 1 - 600 mg/*l* by using the appropriate preconcentration time.

The proposed FIA system gave a linear calibration for the determination of o-cresol in the range 50 - 1 000 mg/*l* with a preconcentration time of 300 sec and a relationship between the peak height (y) and o-cresol concentration (x), in mg/*l* of $y = 0.003604x + 0.6208$; $r^2 = 0.98$.

A linear calibration curve with a relationship between the peak height (y) and m-cresol concentration (x), in mg/*l* of $y = 0.00617x + 0.5733$; $r^2 = 0.99$ was obtained for m-cresol in the range 25 - 1 000 mg/*l* with a preconcentration time of 300 sec.

6.5.3.2 Accuracy

Method	Proposed FIA system (mg/l)	Standard 4-AAP method (mg/l)	GC analysis (mg/l)
phenol	-	-	170.5
o-cresol	-	-	23.5
m-cresol	-	-	0
Total phenol	200.6	196.5	194.0

Table 6.5.3.2A - Comparison of the results of a light oil sample between the proposed FIA system, a standard 4-AAP method and a standard GC-method employed in industry.

The accuracy of the proposed FIA system was tested by comparing the results of a number of representative light oil samples with a standard manual 4-AAP method and with the results of a standard GC procedure employed in industry. A good agreement between the different methods was observed as illustrated from the results on an example of a representative light oil sample given in Table 6.5.3.2A.

6.5.3.3 Standard addition

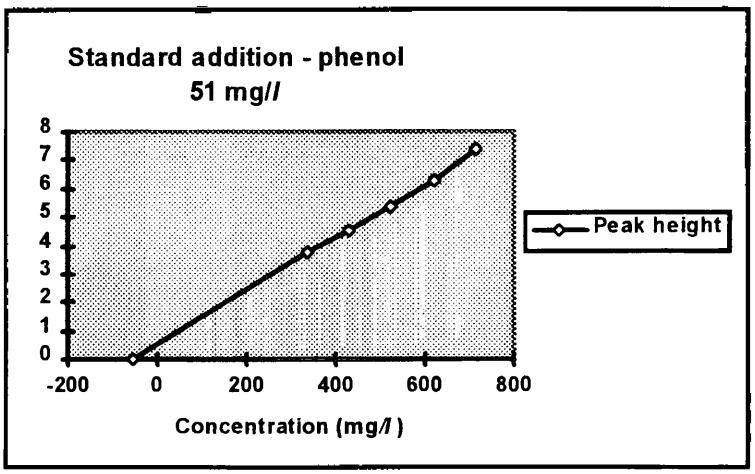

Figure 6.5.3.3A

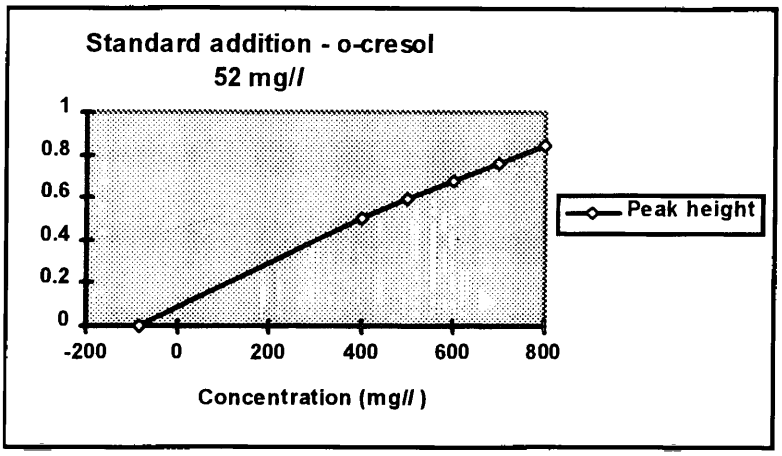

Figure 6.5.3.3B

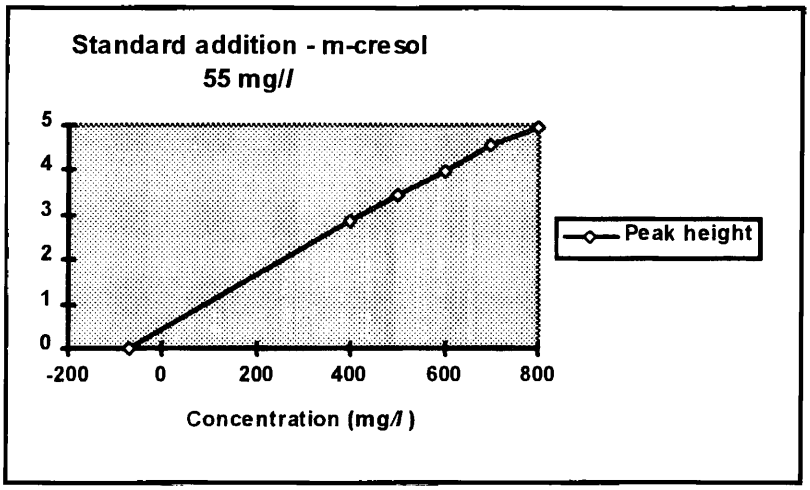

Figure 6.5.3.3C

The accuracy of the proposed system was evaluated for the different calibration curves by spiking representative light oil samples with phenol, o-cresol and m-cresol. Average recoveries of 97.9% for phenol, 99.8% for o-cresol and 101.1% for m-cresol were obtained which indicated the suitability of the system.

6.5.3.4 Precision

The relative standard deviation for 14 repetitions of standard analyte solutions in the linear ranges was better than 1.3%.

6.5.3.5 Detection limit

The calculated detection limits were 0.09 mg/*l* for phenol, 0.18 mg/*l* for o-cresol and 0.02 mg/*l* for m-cresol. These detection limits were calculated using the formula:

$$Detection.\lim it = \frac{3(S_k)K}{100}$$

where S_k = the relative standard deviation for the lowest concentration

K = the mean peak height of the lowest concentration

A safety factor of 25% was used in the calculation of the detection limit.

6.5.3.6 Sample interaction

Industrial light oil samples were analyzed in a random order to test carry over effects. Sample interaction was calculated as less than 2.0% for the system. The sample interaction was calculated using the equation:

$$Interaction = \frac{100(A_3 - A_1)}{A_2}$$

where A_1 = the true peak height of a sample containing a low concentration of analyte

A_2 = the true peak height of a sample containing ten times more analyte

A_3 = the peak height of a sample containing the same amount of analyte as A_1.

6.5.3.7 Interferences

Interferences on the 4-AAP method are well documented [12,17,26,27] and only relevant interfering species were investigated. 4-Aminoantipyrine reacts with primary, secondary and tertiary amines under acidic conditions, but did not interfere in the proposed system due to the repellent nature of the hydrophilic membrane and the basic 4-AAP reagent used.

Carbonyls were also repelled by the hydrophilic membrane, did not diffuse through the membrane and therefore did not interfere. Compounds like 5-hydroxy-1,3-dimethylbenzene, 3-hydroxy-1,4-dimethylbenzene, thymol, carvacrol and o-hydroxydiphenyl may interfere with the determination of phenol. The amounts of these compounds in light oils were negligibly small and therefore did not pose any threat to the proposed FIA system.

6.5.3.8 Sample frequency

The sample throughput is 12 samples per hour. The sample frequency is determined by the preconcentration time necessary for the specific analysis.

6.5.4 Conclusion

An in-line flow injection extraction preconcentration procedure for the determination of total phenols in oil was developed. The reaction between phenolic compounds and 4-aminoantipyrine in the presence of $K_2S_2O_8$ as oxidizing reagent was used. The phenols were extracted and preconcentrated from a xylene solution by using a more selective hydrophilic Spectrapor membrane that also removed interferences. The phenols deprotonated after diffusion to the basic acceptor stream and the preconcentrated phenolate was injected into a carrier stream containing 4-aminoantipyrine as colour reagent. The carrier stream then merged with the oxidant stream, followed by detection at 500 nm. The system was suitable for the determination of total phenols in oil at a sampling rate of 12 samples per hour with an RSD of better than 1.3%. The detection limit was 0.09 mg/*l* for phenol, 0.18 mg/*l* for *o*-cresol and 0.02 mg/*l* for *m*-cresol. The results of the proposed system compared favourably with a standard manual 4-AAP method and a standard GC procedure.

6.6 References

1. Růžička J, Hansen EH (eds.), Flow Injection Analysis, 2nd Edn., Wiley, New York, 1988.
2. Valcárcel M, Luque de Castro MD, Flow Injection Analysis. Principles and Applications, Ellis Horwood, Chichester, 1987.
3. van Staden JF, ***Fresenius J. Anal. Chem.***, **352**, 1995, 271.
4. Lazaro F, Luque de Castro MD, ***Analysis***, **16**, 1988, 216.
5. Frenzel W, ***Laboratory Robotics and Automation***, **5**, 1993, 245.
6. Barnes DE, van Staden JF, ***Anal. Chim. Acta***, **261**,1992, 441.
7. Barnes DE, Taylor MJC, Marshall GD, van Staden JF, ***Anal. Chim. Acta***, **274**, 1993, 283.
8. Barnes DE, Marshall GD, van Staden JF, ***Separation Science and Technology***, **30**, 1995, 751.
9. McMurry J, ***Organic Chemistry***, 2nd Edn, Brooks/Cole Publishing Company, California, 1988.
10. Emerson EJ, ***J. Org. Chem.***, **8**, 1943, 417.
11. Ochynski FW, ***Analyst***, **85**, 1960, 278.
12. Friedstad HO, Ott EE, Gunther FA, **"Automated Colorimetric Micro Determination of Phenol by Oxidative Coupling with 3-Methyl-2-benzothiazolinone Hydrazone"**, 1969.
13. Nasser TAK, Saleem M, ***J. Chem. Soc. Pak.***, **4**, 1982, 33.
14. Norwitz G, Keliher PH, ***Anal. Chim. Acta***, **144**, 1982, 273.
15. Fogg AG, Ali MA, Abdalla MA, ***Analyst***, **108**, 1983, 840.
16. Buckman NG, Hill JO, Magee RJ, ***Microchem. J.***, **28**, 1983, 470.
17. Mohler EF, Jacob LN, ***Anal. Chem.***, **29**, 1957, 1369.
18. Möller J, Martin M, ***Fresenius J. Anal. Chem.***, **329**, 1988, 728.
19. Gonzalo ER, Pavón JLP, Ruzicka J, Christian GD, ***Anal. Chim. Acta***, **259**, 1992, 37.
20. van Staden JF, Hattingh CJ, ***Anal. Chim. Acta***, **308**, 1995, 214.
21. van Staden JF, Hattingh CJ, ***Anal. Chim. Acta***, **308**, 1995, 222.
22. van Staden JF, Hattingh CJ, ***J. Anal. At. Spectrom.***, **10**, 1995, 727.

23. Marshall GD, van Staden JF, ***Anal. Instrum.***, **20**, 1992, 79.

24. Melcher RG, ***Anal. Chim. Acta***, **214**, 1988, 299.

25. Barnes DE, ***Supported Liquid Membranes in Flow Systems***, PhD-thesis, University of Pretoria, 1993.

26. Emerson E, Beacham HH, Beegle LC, ***J. Org. Chem.***, **8**, 1943, 417.

27. ***Standard methods for the examination of water and waste water***, 16th Edn, American Public Health Association, Washington DC, 1985.

CHAPTER 7

DETERMINATION OF KETONES AND ALDEHYDES IN WATER AND OILS

7.1 Introduction

Carbonyls and other oxygenates are sometimes present as undesirable compounds in certain hydrocarbon production streams and final products in petroleum refining processes. The reactivity of the >C=O group in certain process streams is of great concern due to their influence on reaction conditions and formation of unwelcome side products. This leads to a decrease in efficiency of industrial processes involved and contributes to an increase in production costs. Manufacturers in the petroleum industry also strive to produce final products that meet certain specifications. There is therefore a pressure to control the total carbonyl content in certain process streams and hydrocarbon products in industrial plants. Thus a need exists for suitable robust analysers that can monitor total carbonyl levels in the petroleum industry. The concept of flow injection analysis has established itself as an analytical technique that, when automated, is suitable for increasing sample output [1,2].

7.2 Uses of ketones and aldehydes

Ketones and aldehydes are among the most important of all compounds [3]. In nature many living systems require aldehydes or ketones and in the chemical industry they are synthesized in great quantities for use as solvents and starting materials for other products. Formaldehyde is synthesized for use in building insulation materials and in adhesive resins that bind particle board and plywood. These materials may be toxic. Acetone is widely used as a solvent.

Formaldehyde is synthesized industrially by catalytic hydrogenation of methanol, but this method is of little use in the laboratory because of the high temperatures required. Acetone is prepared by dehydrogenation of 2-propanol.

7.3 Properties of ketones and aldehydes

The carbonyl functional group is planar and the carbon-oxygen double bond is polar. The carbonyl polarity causes aldehydes and ketones to be weakly associated, resulting in higher boiling points than alkanes of similar molecular mass. Ketones and aldehydes cannot form hydrogen bonds, resulting in lower boiling points than that of alcohols. Formaldehyde is a gas at room temperature, but the other simple aldehydes and ketones are liquid. Aldehydes and ketones undergo the following reactions: oxidation (with the Jones' reagent, Tollens' reagent, hot nitric acid or aqueous sulphuric acid) and nucleophilic addition (to form a tetrahedral alkoxide ion intermediate). The nucleophilic addition reactions to a ketone or aldehyde can be used to synthesize a wide range of compounds: alcohols, cyanohydrins, imines, enamines, alkanes, acetals and alkenes.

7.4 Choice of analytical method

A number of procedures have been developed for the determination of carbonyl compounds. Volumetric determination of total carbonyls in organic solvents is amongst the most popular methods used in the petroleum industry. The method is, however, not very suitable for application in flow injection analysers and a more suitable method was found.

Carbonyl compounds are determined as 2,4-dinitrophenylhydrazine (DNPH) and in a strong basic medium to form dark red anions. The unreacted DNPH forms a dark red product that should decompose rapidly. The mechanism for this reaction was investigated, but is still unknown [4]. The reaction is time consuming and a faster, more simple reaction for determining carbonyls will provide better control and a higher sample throughput, especially in a flow injection system.

Chloramin-T in concentrated sulphuric acid reacts with carbonyl compounds dissolved in ethanol, to form red compounds [5]. This reaction is most effective when used as a spot test, as it is very important to use concentrated sulphuric acid for the reaction to take place. The presence and exothermic nature of concentrated sulphuric acid as one of the reagents makes this method unsuitable for application in a flow injection analyser. Ethanolamine and carbonyls react in the presence of formic acid to form yellow products [6]. This reaction is also very exothermic and water cannot be introduced in this reaction system, as it decomposes the imine and the yellow product is not formed.

A thermochromic reaction between 2-hydroxy-1-naphthaldehyde and aliphatic ketones occurs in methanoic solution when HCl gas is bubbling through the solution [7]. The product is extracted from the solution by using *o*-dichlorobenzene. This reaction is only sensitive for the $CH_3COCH_2^-$ grouping and cannot be used for formaldehyde and acetaldehyde. Another drawback of the reaction is the absolute dependence of the reaction on anhydrous methanol; the presence of moisture decreases the efficiency of the reaction drastically. Purple products form when *m*-dinitrobenzol reacts with monoketones in the presence of potassium hydroxide in methanol [8]. The reaction does not seem very suitable for flow injection analysis due to the kinetic dependence on temperature. The reaction mixture has to be heated to 80°C for 3 minutes.

2,3-Dimethyl-2,3-bis-(hydroxylamino)-butane can be used in a spot test for aldehydes and ketones [9]. This involves the formation of an anhydrous product that can be converted to a free radical by the addition of sodium periodate or lead oxide. The stable free radicals are intensely coloured. It is not clear if the ketones undergo the same reaction as the aldehydes, the colour reagent has to be recrystallized before use and the reaction is slow. Ketones can also be detected by reacting them with 1-chloro-2,4-dinitrobenzene in the presence of an anion-exchange resin in the OH^- form [10].

Aldehydes do not interfere with this reaction, but the reactivity of the carbonyl group is affected by steric hindrance. Carbonyl compounds can be detected spectrophotometrically through oximation and subsequent charge-transfer complexation reactions [11]. The sample preparation is extremely laborious and time-consuming.

Of all the reactions surveyed, the reaction between carbonyl compounds and vanillin seems to be the most suitable for application in a flow injection system [12]. Carbonyls react with vanillin in the presence of sodium hydroxide to form condensation products that can be detected spectrophotometrically at 414 nm.

The vanillin method has several advantages in comparison to the above mentioned methods. Vanillin is soluble in water, stable in solution for weeks and the reaction between vanillin and carbonyls are relatively fast and simple. This method can be used for the detection of methylketones and aldehydes in aqueous solution.

The following reaction between carbonyls and vanillin, in the presence of sodium hydroxide as catalyst, was used for the spectrophotometric determination of carbonyls in water and organic solvents:

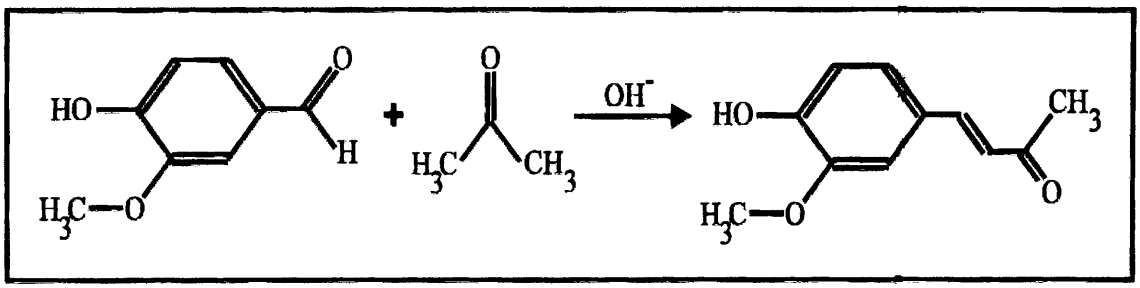

Figure 7.4A - Chemical reaction used in determination of acetone and other carbonyls.

7.5 Determination of ketones and aldehydes in water by flow injection analysis

7.5.1 Experimental

7.5.1.1 Reagents and solutions

A stock solution containing 1 000 mg/*l* of acetone was prepared by dissolving the appropriate amount of acetone (Merck) in deionized water. Working standard solutions were prepared by suitable dilution of the stock solution with deionized water. The vanillin reagent solution was prepared by dissolving 9.0 g vanillin in 1 *l* deionized water. The sodium hydroxide solution was prepared by dissolving 525.0 g of NaOH in 1 *l* deionized water.

7.5.1.2 Apparatus

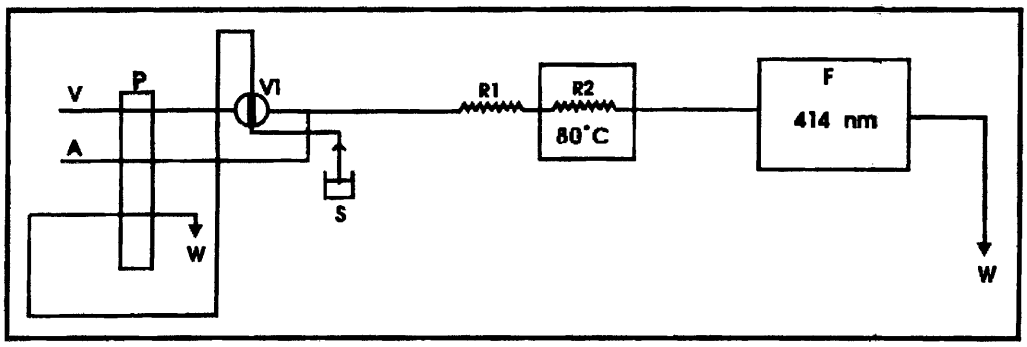

Figure 7.5.1.2A - Flow system used for determination of carbonyls in water.

P = pump
V = vanillin
A = sodium hydroxide solution
S = sample
W = waste
V_1 = valve
R_1 and R_2 = reactors
F = detector

The flow system (Fig. 7.5.1.2A) was constructed from the following components: a Gilson Minipuls peristaltic pump, a VICI 10-port multi-functional sampling valve and a Unicam 8625 UV/visible spectrophotometer equipped with a 10-mm Hellma flow-through cell (volume 80 μl) with a debubbler for detection at 414 nm.

Data acquisition and device control were achieved using a PC30-B interface board (Eagle Electric, Cape Town, South Africa) and an assembled distribution board (MINTEK, Randburg, South Africa). The FlowTEK [13] software package (obtainable from MINTEK) for computer-aided flow analysis was used throughout for device control and data acquisition.

The system consisted of two lines: the vanillin carrier stream and the NaOH stream. The sample was injected into the aqueous vanillin carrier by a 10-port VICI multi-position sampling valve. Teflon transmission tubing with 0.76 mm id for the manifold and Acidflex pump tubing were used.

7.5.1.3 Procedure

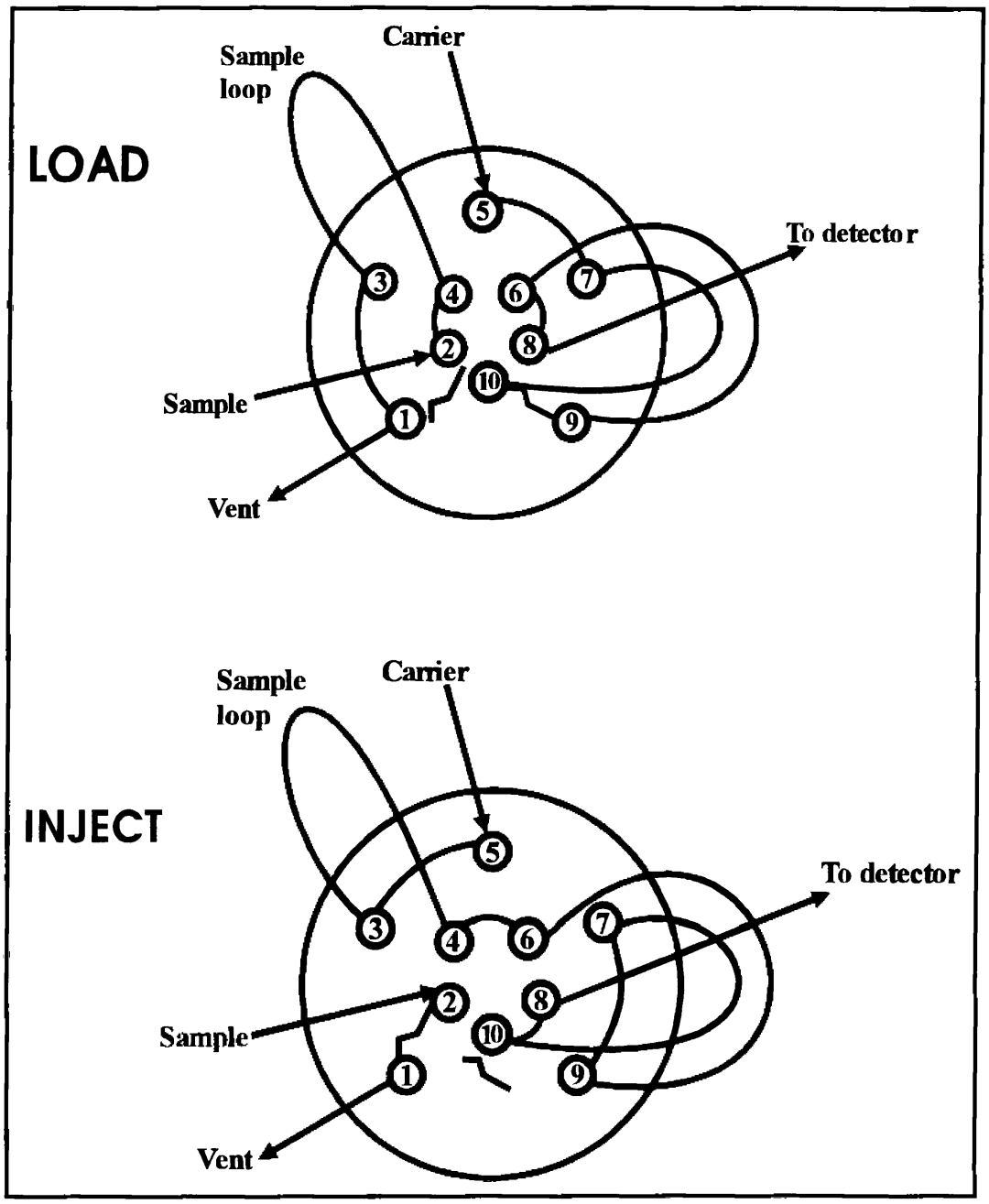

Figure 7.5.1.3A - Valve configuration.

The valve configuration is outlined in Fig. 7.5.1.2A. The sample loop was rinsed with the sample for 10 seconds while the valve was set on the **LOAD** position.

The valve was switched to the **INJECT** position for 5 seconds to introduce the sample into the carrier stream. The valve was then switched back to the **LOAD** position and remained there until the next sample run.

The sample zone was then transported to the reaction coil in the water bath where the sample and reagents were mixed and heated for the reaction to proceed and the reaction product was pumped to the detector. The outlet from the detector was pumped at a constant flow rate to waste. This was done to maintain a constant flow rate throughout the system and to avoid back pressure problems. The warm aqueous mixture of vanillin and NaOH was used as blank for the analysis.

Compound	**Wavelength (nm)**		**Compound**	**Wavelength (nm)**	
	Water	**Vanillin and NaOH**		**Water**	**Vanillin and NaOH**
acetaldehyde	346	425	5-nonanone	346	424
acetone	346	425	pentanal	346	427
butanone	346	425	formaldehyde	-	433
hexyl ketone	346	418	octanal	346	430
2-heptanone	346	430	3-nonanone	346	430
3-heptanone	346	425	nonanal	346	425
heptanal	349	433	4-heptanone	346	418
2-octanone	346	430	3-methyl butyraldehyde	346	433
2-nonanone	346	425	vanillin	280	-
decanal	346	433	2-decanone	346	421

Table 7.5.1.3A - Wavelengths of maximum absorbencies for different carbonyl compounds with (a) water and (b) the vanillin and NaOH mixtures as blank.

The wavelength of maximum absorbance for the yellow coloured reaction products of different carbonyls were determined against two different background solutions. Water was used as blank for the first method, while the second determination was done by using the vanillin and NaOH mixture as blank. The wavelengths of maximum absorbencies for different carbonyl compounds are given in Table 7.5.1.3A.

It was clear from the results given in Table 7.5.1.3A that due to solvent effects the absorption maxima tended to shift in wavelength. Two regions were observed: 346 nm for reaction products with water as solvent and in the vicinity of 418 to 433 nm for reaction products dissolved in an alkaline vanillin solution.

Although the more sensitive absorption maximum was at 346 nm, a prerequisite for the formation of the condensation products at a reasonable reaction rate was the presence of vanillin in a concentrated sodium hydroxide solution medium.

The wavelength scans showed a high background absorption at wavelengths higher than 425 nm. That is the reason why 414 nm, a lower wavelength than the average absorption maximum, was chosen for the analysis.

7.5.2 Method optimization

7.5.2.1 Physical parameters

7.5.2.1.1 Flow rate

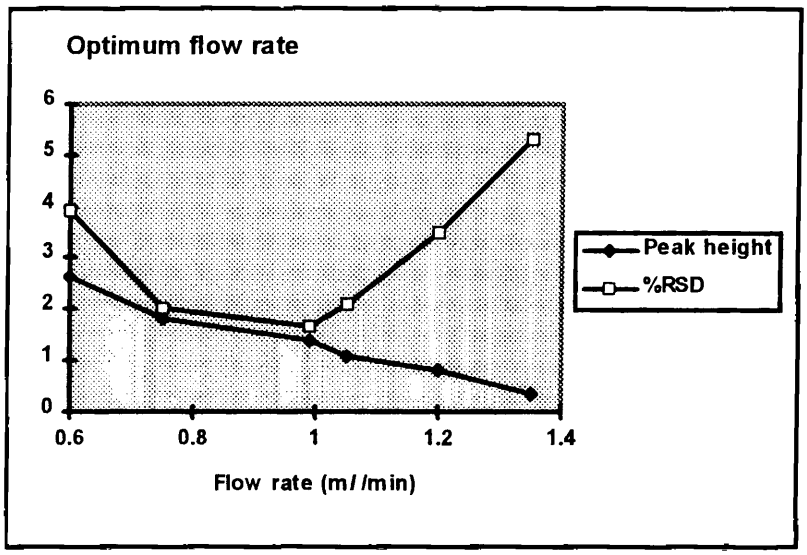

Figure 7.5.2.1.1A - Optimum flow rate.

The physical parameters had a remarkable influence on the response and precision and particular attention was given to them in the system design. Flow rates between 0.6 and 1.35 ml/min. were evaluated and the results obtained are illustrated in Fig. 7.5.2.1.1A.

Two factors contributed to the performance of the system in this regard; dispersion and reaction kinetics. Optimum reaction conditions and dispersion were reached with a flow rate of 0.75 ml/min. where the maximum response and the best RSD of 2.0% were achieved.

7.5.2.1.2 Sample volume

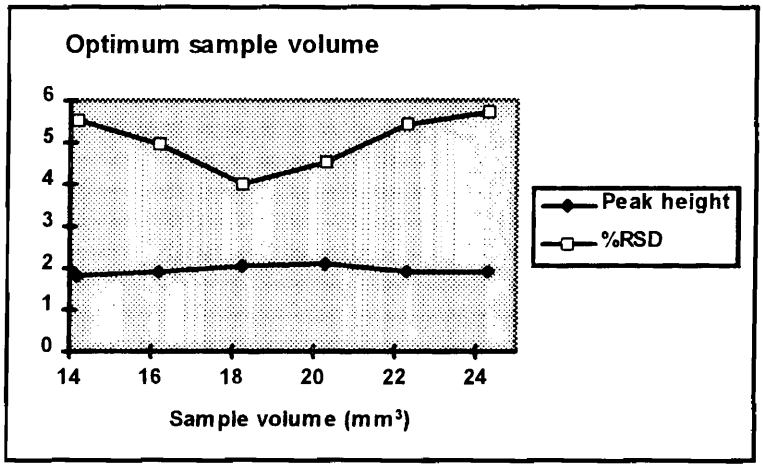

Figure 7.5.2.1.2A - Optimum sample volume.

The dispersion of the sample depended upon the zone length injected, which was also controlled by the internal diameter of the tubing used. These factors contributed to peak broadening and had to be considered in the optimization of the sample volume. A sample volume between 14 and 24 μl was evaluated and the optimum sample volume was 18 μl with a best RSD of 4.0%. Too large sample volumes resulted in insufficient mixing of the analyte with the reagent solutions before detection.

7.5.2.1.3 Line length

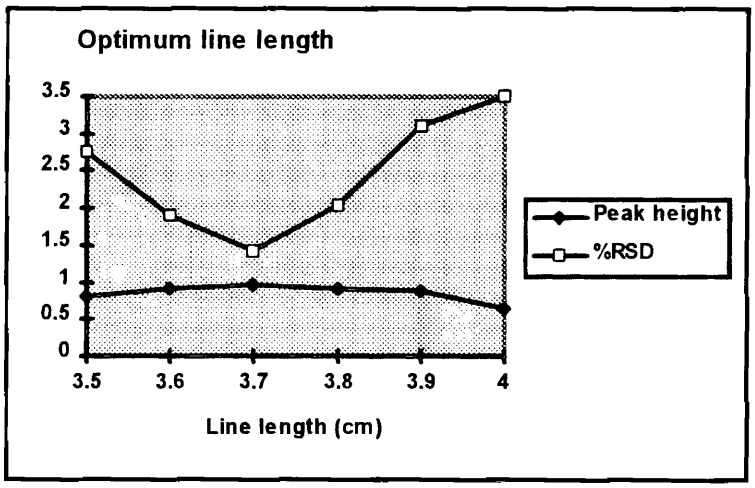

Figure 7.5.2.1.3A - Optimum line length.

Line lengths of between 3.5 and 4.0 m were evaluated. The results obtained are illustrated in Fig. 7.5.2.1.3A. A line length of 3.7 m resulted in optimum contact time for the analyte and reagents with a RSD of 1.4% and was selected for the proposed system.

7.5.2.1.4 Coil diameter

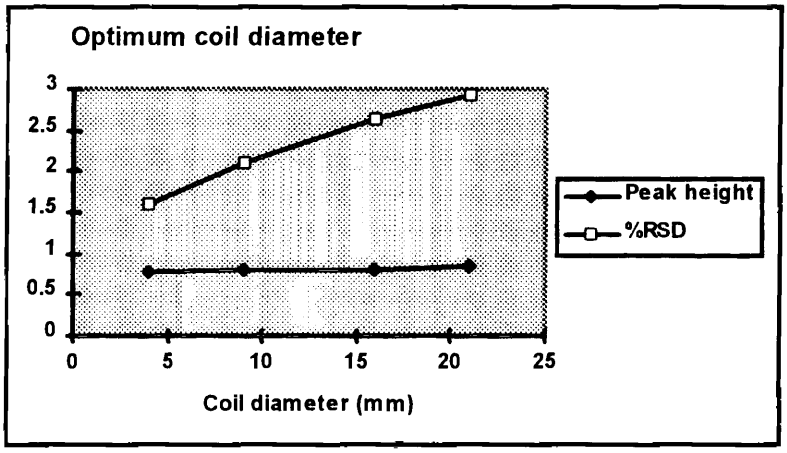

Figure 7.5.2.1.4A - Optimum reaction coil diameter.

The optimum coil diameter for the reaction coil was 4 mm (RSD = 1.6%). A smaller coil diameter resulted in an increase in radial dispersion and a decrease in axial dispersion.

7.5.2.2 Chemical parameters

7.5.2.2.1 NaOH concentration

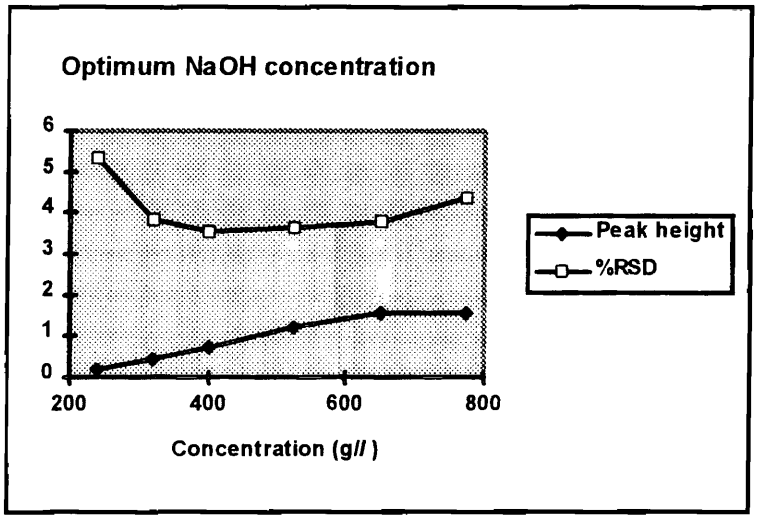

Figure 7.5.2.2.1A - Optimum NaOH concentration.

The method is based on a derivatisation reaction of the carbonyl compounds with vanillin in alkaline medium. The sodium hydroxide acts as catalyst for the aldol condensation reaction and the success of the reaction depends on the amount of sodium hydroxide present in the chemical manifold.

It was clear that the rate of the chemical reaction improved with the inclusion of more sodium hydroxide into the reaction system until a limit was reached around 700 g/*l*. The use of a highly concentrated sodium hydroxide solution (concentrations higher than 525 g/*l*) will result in unnecessary waste of NaOH, as can be seen in Fig. 7.5.2.2.1A. An optimum NaOH concentration of 525 g/*l* (RSD = 3.6%) was selected for the proposed system.

7.5.2.2.2 Vanillin concentration

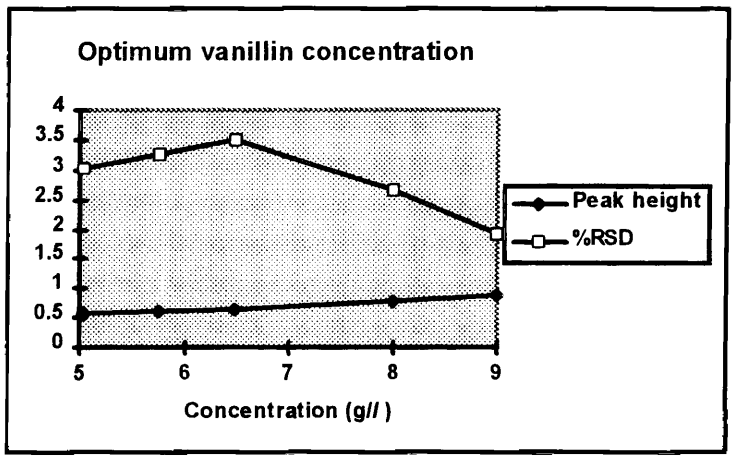

Figure 7.5.2.2.2A - Optimum vanillin concentration.

As the vanillin is an essential part of the resulting light absorbing product, the higher the concentration of the vanillin, the higher the response. Vanillin concentrations between 5 and 9 g/l were evaluated and the results are depicted in Fig. 7.5.2.2.2A.

There was a steady increase in response with an increase of vanillin concentration. A concentration of 9 g/l seemed to be the saturation point of vanillin in water. This concentration gave the best response and a RSD of 1.9% and was used as optimum concentration.

7.5.2.2.3 Temperature

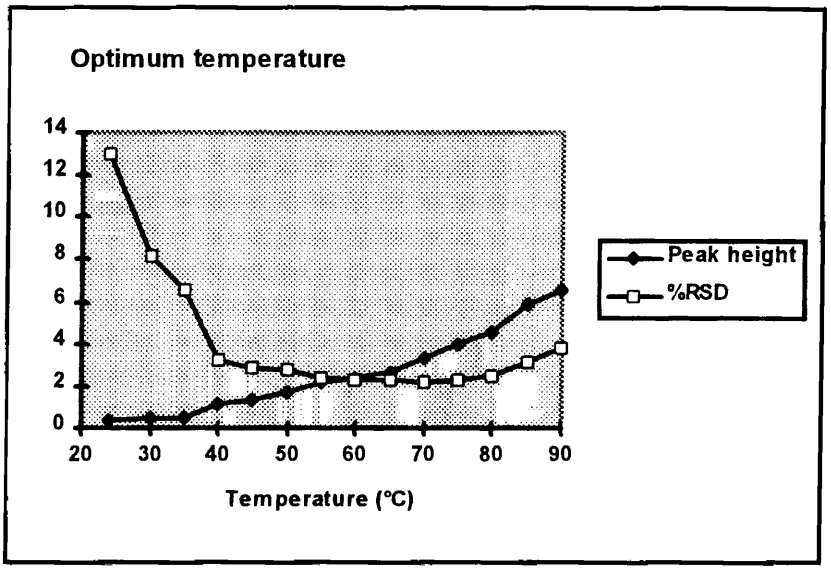

Figure 7.5.2.2.3A - Optimum temperature.

The rate of the reaction is temperature dependent. A waterbath was used for temperature control and the influence of temperature between 24 and 90°C on the reaction rate was investigated. The reaction rate increased with an increase in temperature. An optimum temperature of 80°C was selected (RSD = 2.5%).

7.5.3 Evaluation of the method

7.5.3.1 Linearity

The response linearity of the proposed flow injection system for the spectrophotometric determination of total carbonyls was evaluated under the optimum conditions.

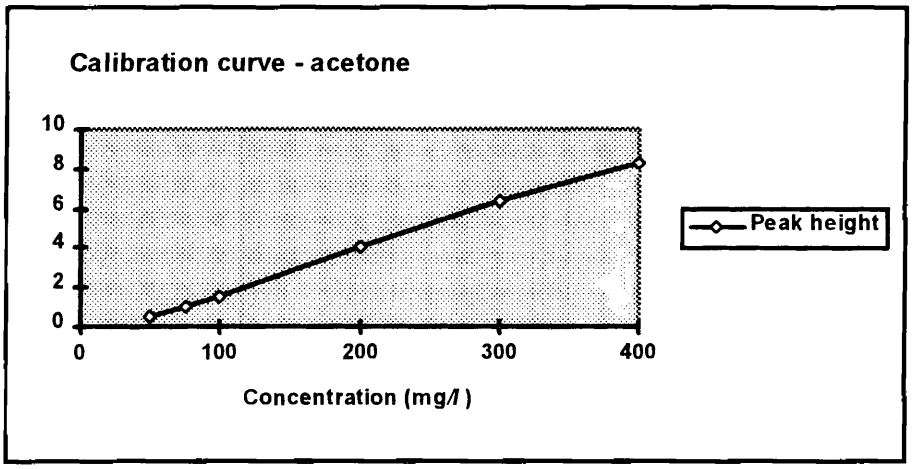

Figure 7.5.3.1A - Calibration curve for acetone.

Compound	Relationship between peak height (y) and concentration (x) in mg/*l*	Correlation coefficient (r^2)
formaldehyde	y = 0.000327x + 0.685	0.952
butanone	y = 0.000517x + 0.725	0.998
2-heptanone	y = 0.000138x + 0.815	0.995
pentanal	y = 0.000138x + 0.816	0.995
acetaldehyde	y = 0.00236x + 0.997	0.991
3-heptanone	y = 0.00040x + 0.420	0.957

Table 7.5.3.1A - Linear relationship between peak height and concentration for the determination of different carbonyls in the range 250 - 1 000 mg/*l* for the proposed FIA system.

Calibration experiments were conducted with a number of water soluble carbonyl compounds (Table 7.5.3.1A) in the concentration range between 0 and 1 000 mg/*l*. The calibration graph for acetone, depicted in Fig. 7.5.3.1A, is linear for acetone concentrations between 50 and 400 mg/*l* (r^2 = 0.998, n = 6) with a linear relationship between the peak height and the acetone concentration (x) expressed as y = 0.0225x - 0.5656.

The linear relationship between the peak height (y) and concentration (x) for the different carbonyls in the range 250 to 1 000 mg/*l* is given in Table 7.5.3.1A. The larger ketones did react, but the reactivity decreased with an increase in the length of the carbon chain, and the system was not adjusted accordingly.

7.5.3.2 Accuracy

The accuracy of the method was determined by comparing the results obtained by the proposed FIA system and a standard volumetric method for standard acetone samples in the range 250 to 1 000 mg/*l* in water. The results revealed an excellent agreement between the two methods. As an example, a 400 mg/*l* acetone solution was analysed by making use of the proposed FIA method and the average result was 417 mg/*l*, which indicated the suitability of the system.

7.5.3.3 Standard addition

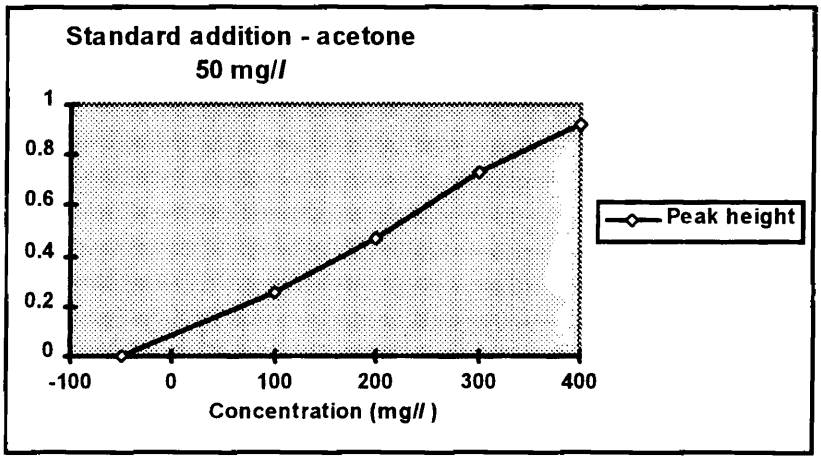

Figure 7.5.3.3A

The accuracy of the method was determined by standard addition to acetone samples and the percentage recovery for acetone was 99% (Fig. 7.5.3.3A).

7.5.3.4 Precision

The precision of the method was evaluated by doing 14 repetitions of a standard analyte solution in the linear range. The relative standard deviation for acetone was between 1.25% and 1.8%. The RSD for other carbonyl compounds was better than 2.0%.

7.5.3.5 Detection limit

Compound	Detection Limit (mg/*l*)
formaldehyde	0.183
butanone	0.116
2-heptanone	0.435
pentanal	0.435
acetaldehyde	0.254
acetone	0.267
3-heptanone	0.150

Table 7.5.3.5A - Detection limits for different carbonyl compounds.

The detection limits for the different carbonyls were calculated by using the formula

$$\det ection.\lim it = \frac{[3s_b + I_b] - k}{m}$$

where s_b = the standard deviation of the background signal

I_b = the relative peak height of the background signal

k = the intercept of the calibration curve

m = the slope of the calibration curve

7.5.3.6 Sample interaction

The sample interaction (carry-over effect) between samples was determined by analyzing a sample with a low analyte content, followed by one with a high analyte concentration which was again followed by a sample with the same low analyte content as the first sample. The sample interaction between samples as calculated was less than 1%.

7.5.3.7 Interferences

As can be seen from Table 7.5.3.1A, the low molecular mass ketones and aldehydes will interfere with the analysis of a specific ketone or aldehyde if the sample is composed of a mixture of different carbonyls. Imhof and Bosset [12] have done an intensive study on the molar absorptivities of a number of carbonyl compounds.

7.5.3.8 Sample frequency

The sample throughput is 30.5 samples per hour.

7.5.4 Conclusion

The determination of carbonyls in water by flow injection analysis was investigated. The approach is based on the condensation reaction between carbonyls and vanillin in the presence of a strong alkaline sodium hydroxide medium. The carbonyls, dissolved in water, were mixed and heated and detected spectrophotometrically at 414 nm. Parameters affecting the performance of the analyser were studied. The proposed analyser is fully computerized and is able to monitor carbonyls in samples at a frequency of 30.5 samples per hour with a relative standard deviation of less than 2.0%. The calibration graphs are linear between 50 and 400 mg/*l* for acetone and between 250 and 1 000 mg/*l* for other carbonyls.

7.6 Determination of ketones and aldehydes in oil by flow injection analysis

7.6.1 Experimental

7.6.1.1 Reagents and solutions

All samples were kindly provided by Sasol. A stock solution containing 1 000 mg/*l* of acetone was prepared by dissolving the appropriate amount of acetone (Merck) in xylene solution. Working standard solutions were prepared by suitable dilution of the stock solution with the same xylene. The vanillin reagent solution was prepared by dissolving 9.0 g of vanillin in 1 *l* deionized water. The sodium hydroxide solution was prepared by dissolving 400.0 g of NaOH in 1 *l* deionized water.

7.6.1.2 Apparatus

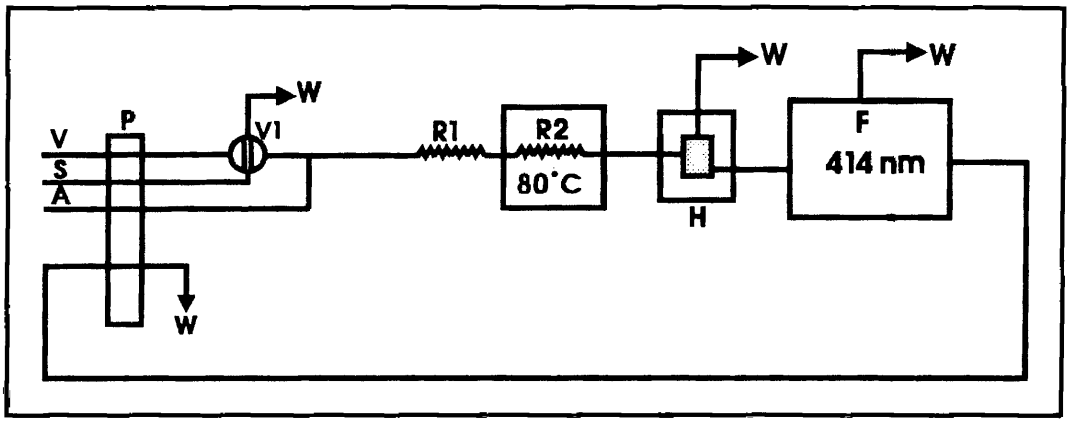

Figure 7.6.1.2A - FIA system used for determination of carbonyls in hydrocarbons by reaction with vanillin.

V = vanillin solution
A = sodium hydroxide solution
R_1, R_2 = reactors
F = detector
V_1 = valve
S = sample
W = waste
H = phase separator
P = peristaltic pump

The flow system depicted in Fig. 7.6.1.2A was constructed from the following components: a Gilson Minipuls peristaltic pump, a VICI 10-port multi-functional sampling valve, a homemade phase separator and a Unicam 8625 UV/VIS spectrophotometer equipped with a 10-mm Hellma flow-through cell (volume 80 μl) with a debubbler for detection at 414 nm.

Data acquisition and device control were achieved using a PC30-B interface board (Eagle Electric, Cape Town, South Africa) and an assembled distribution board (MINTEK, Randburg, South Africa). The FlowTEK [13] software package (obtainable from MINTEK) for computer-aided flow analysis was used throughout for device control and data acquisition.

The system consisted of two lines: the vanillin carrier stream and the NaOH stream. The sample was injected into the aqueous vanillin carrier stream by a 10-port VICI multi-position sampling valve. Teflon transmission tubing with 0.76 mm id. for the manifold and Acidflex pump tubing were used.

7.6.1.3 Procedure

The valve configuration is outlined in Fig. 7.5.1.3A. The sample loop was rinsed with the sample for 10 seconds while the valve was set on the **LOAD** position. The valve was switched to the **INJECT** position for 5 seconds to introduce the sample into the carrier stream. The valve was then switched back to the **LOAD** position and remained there until the next sample run. The sample zone was then transported to the reaction coil in the water bath where the sample and reagents were mixed and heated for the reaction to proceed. The water and xylene phases separated in a phase separator and a part of the aqueous phase, containing the reaction product was then pumped to the detector. The outlet sample from the detector was pumped at a constant flow rate to waste. This was done to regulate the separation in the phase separator for optimum separation between the two phases and to maintain a constant flow rate through the system. The warm aqueous mixture of vanillin and NaOH was used as blank for the analysis.

7.6.2 Method optimization

7.6.2.1 Physical parameters

7.6.2.1.1 Phase separation

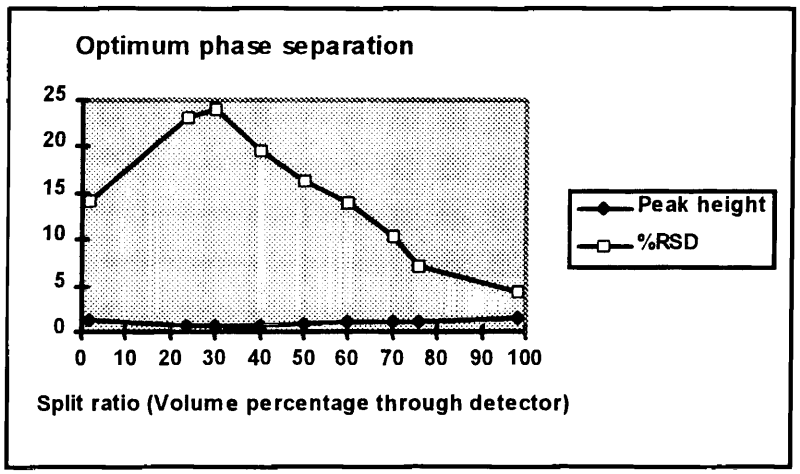

Figure 7.6.2.1.1A - Results of split ratio between aqueous and organic phases investigated.

It was clear from the initial experiments that successful separation of the aqueous phase (containing the reaction products in an alkaline vanillin solution) from the organic phase in the phase separator before detection, would be a limiting factor in employing the proposed system at a high degree of sensitivity, accuracy and precision. A split ratio between 0 and 100% was investigated and the results as volume percentages of the aqueous phase through the detector are given in Fig. 7.6.2.1.1A. The results show that the optimum sensitivity and the lowest %RSD were obtained when 98.1% (v/v) of the aqueous reaction products was pumped through the detector.

The phase separator's performance was tested in different positions in the system. Test runs were also done in order to decide the use of a two-point flow cell or debubbler flow cell. When the phases were separated before the sample entered the water bath, the separation was not successful, resulting in xylene gas bubbles in the flow system.

When the phases were separated just before detection, the bubbles were also removed from the system, but there was a high background absorption of xylene dissolved in the water. The best results were obtained when the phases were separated just before detection and when the debubbler flow cell was used, instead of the two point flow cell. This resulted in double phase separation and debubbling, but higher peaks and lower %RSD values were obtained.

7.6.2.1.2 Flow rate

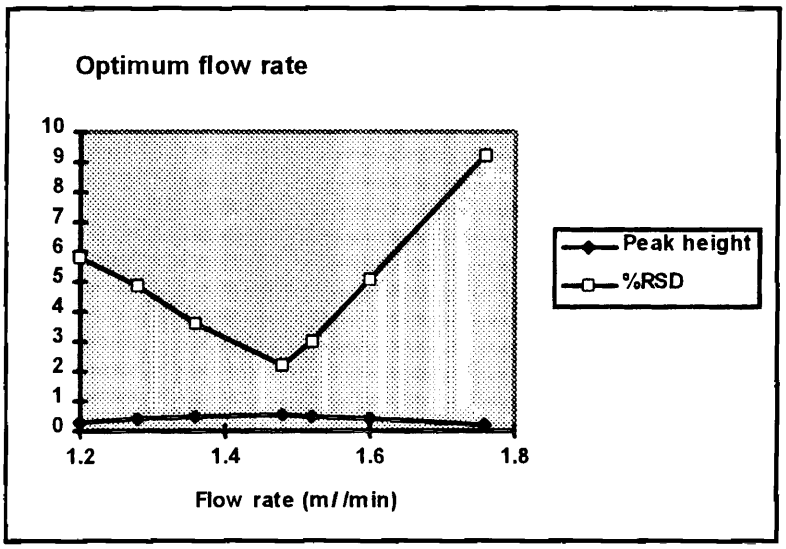

Figure 7.6.2.1.1A - Optimum flow rate.

Flow rates between 1.1 and 1.8 ml/min. were evaluated and the results obtained are illustrated in Fig. 7.6.2.1.2. Two factors contributed to the performance of the system in this regard; dispersion and reaction kinetics. Optimum reaction conditions and dispersion were reached with a flow rate of 1.48 ml/min. where the maximum response and the best RSD of 2.2% were achieved.

7.6.2.1.3 Sample volume

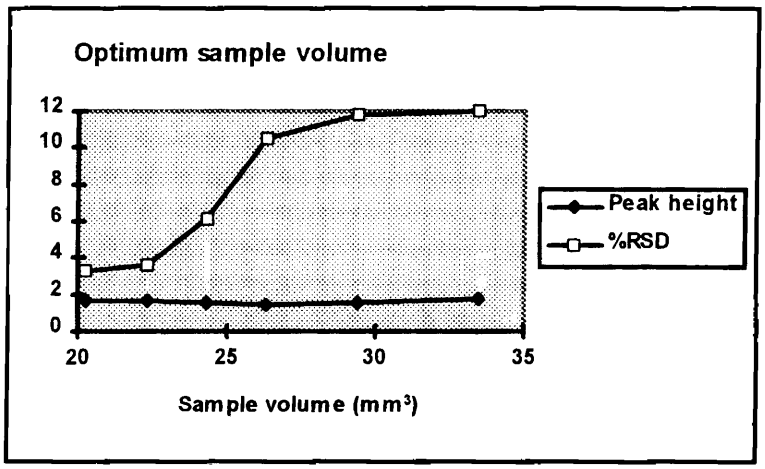

Figure 7.6.2.1.3A - Optimum sample volume.

The injected sample was in the organic phase and the merging of the organic phase sample with the aqueous carrier stream depended on the contact area between the sample and carrier stream, which played a crucial role in the mixing and extraction of the analyte into the aqueous phase on its path to the detector. The dispersion of the sample therefore depended upon the zone length injected, that was controlled by the internal diameter of the tubing used. These factors all contributed to peak broadening and had to be considered in the optimisation of sample volume.

Sample volumes between 20 and 34 μl were evaluated (Fig. 7.6.2.1.3A) and there were two regions where the response reached a maximum. It was found that high sample volumes resulted in insufficient extraction and mixing of the analyte with the aqueous reagent solutions before detection.

Although the response increased due to the increased amount of sample, reaching an optimum response at 34 μl, the % RSD also increased. The optimum sample volume was obtained at 20.3 μl with a best RSD of 3.3%.

7.6.2.1.4 Line length

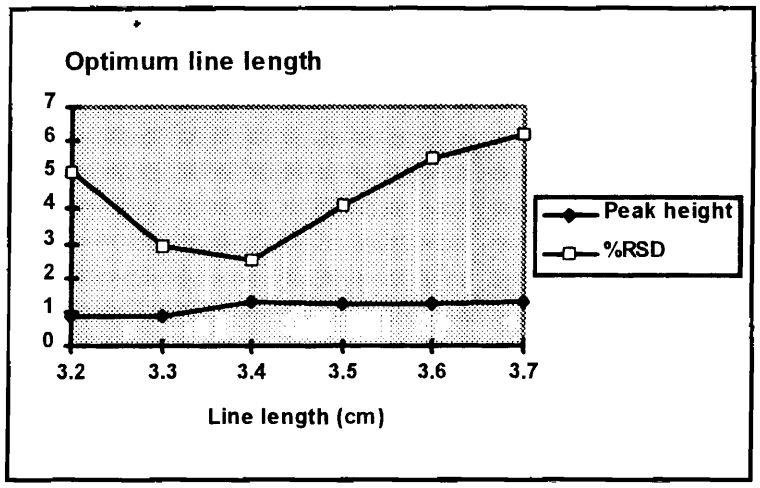

Figure 7.6.2.1.4A - Optimum line length.

Line lengths of between 3.1 and 3.7 m were evaluated. The results obtained are illustrated in Fig. 7.6.2.1.4A. A line length of 3.4 m resulted in optimum contact time for the analyte and reagents with a RSD of 2.5% and was selected for the proposed system.

7.6.2.2 Chemical parameters

7.6.2.2.1 NaOH concentration

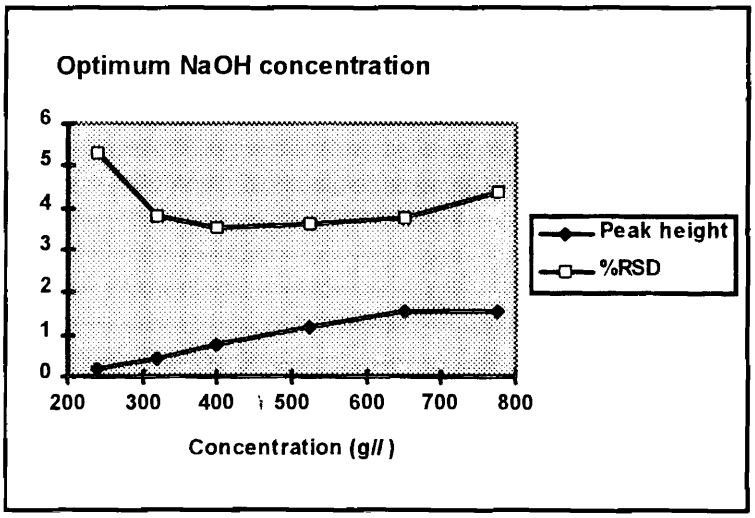

Figure 7.6.2.2.1A - Optimum NaOH concentration.

The method is based on a derivatisation reaction of the carbonyl compounds with vanillin in an alkaline medium. The sodium hydroxide acts as catalyst for the aldol condensation reaction and the success of the reaction depends on the amount of sodium hydroxide present in the chemical manifold. It was clear that the rate of the reaction improved with the inclusion of more sodium hydroxide into the reaction system until a limit was reached around 700 g/*l*. The use of highly concentrated sodium hydroxide (more concentrated than 400 g/*l*) will result in unnecessary waste of NaOH, as can be seen on the graph (Fig. 7.6.2.2.1A). An optimum NaOH concentration of 400 g/*l* (RSD = 3.5%) was selected for the proposed system.

7.6.2.2.2 Vanillin concentration

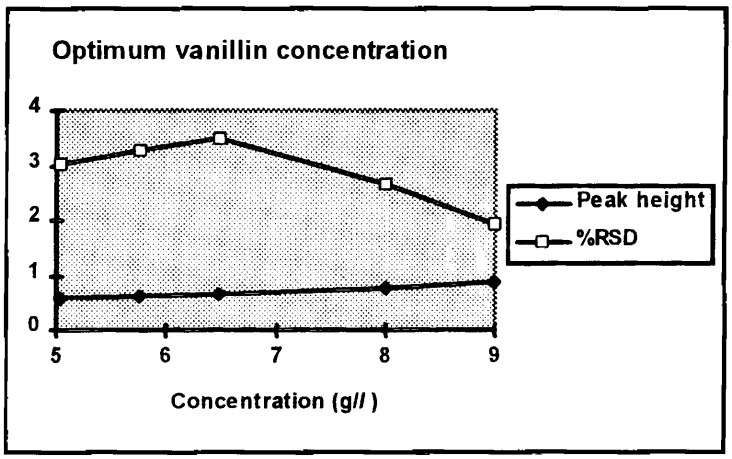

Figure 7.6.2.2.2A - Optimum vanillin concentration.

As the vanillin is an essential part of the resulting light absorbing product, the higher the concentration of the vanillin, the higher the response. Vanillin concentrations between 5 and 9 g/*l* were evaluated and the results are depicted in Fig. 7.6.2.2.2A. There was a steady increase in response with an increase of the vanillin concentration. A concentration of 9 g/*l* seemed to be the saturation point of vanillin in water. This concentration gave the best response and a RSD of 1.9% and was used as optimum concentration.

7.6.2.2.3 Temperature

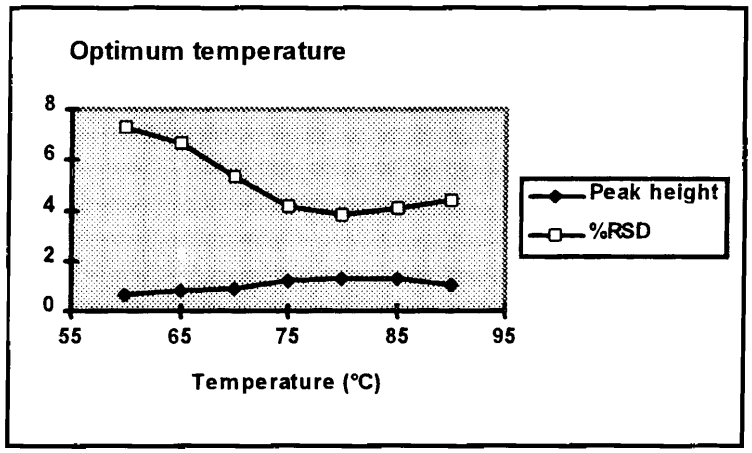

Figure 7.6.2.2.3A - Optimum temperature.

The rate of the reaction is temperature dependent. A waterbath was used for temperature control and the influence of temperature between 60 and 90°C on the reaction rate was investigated. The reaction rate increased until 80°C where the graph reacted a plateau (Fig. 7.6.2.2.3A). The optimum temperature of 80°C gave the best %RSD value.

7.6.3 Evaluation of the method

7.6.3.1 Linearity

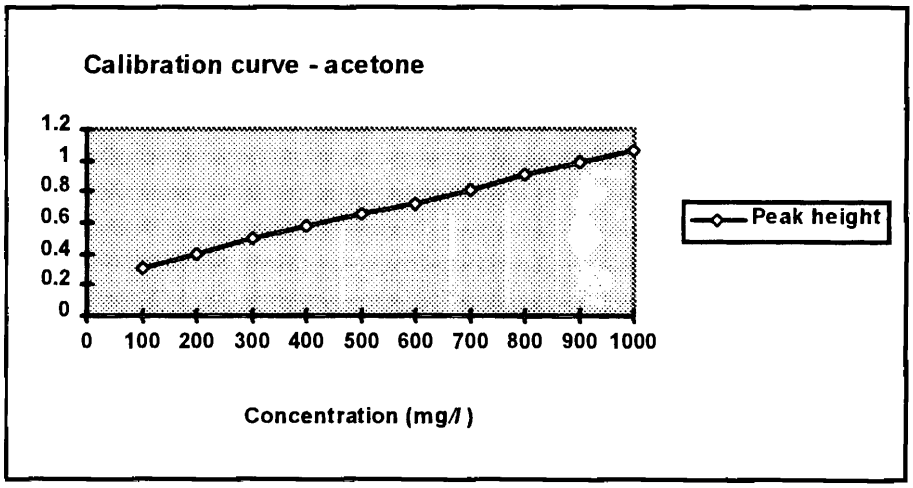

Figure 7.6.3.1A - Calibration graph for acetone in xylene.

Compound	Relationship between peak height (y) and concentration (x) in mg/*l*	Correlation coefficient (r^2)
acetaldehyde	y = 0.00226x + 0.551	0.99
2-butanone	y = 0.000108x + 0.705	0.99
hexyl ketone	y = 0.000234x + 0.534	0.98
3-heptanone	y = 0.000147x + 0.519	0.98
decanal	y = 0.000156x + 0.478	0.99
heptanal	y = 0.000327x + 0.472	0.98

Table 7.6.3.1A - Linear relationship between peak height and concentration for the determination of different carbonyls in the range 250 - 1 000 mg/*l* for the proposed FIA system.

The response linearity of the proposed flow injection system for the spectrophotometric determination of total carbonyls was evaluated under the optimum conditions. Calibration experiments were conducted with a large number of carbonyl compounds in the concentration range between 0 and 1 000 mg/*l*. The calibration graph for acetone (Fig. 7.6.3.1A) is linear for acetone concentrations between 100 and 1 000 mg/*l* (r^2 = 0.998, n = 6) with a linear relationship between the peak height (y) and the acetone concentration (x) expressed as y = 0.000826x + 0.235.

The linear relationship between the peak height (y) and concentration for the different carbonyls in the range 250 to 1 000 mg/*l* is given in Table 7.6.3.1A.

7.6.3.2 Accuracy

It was realised that it would be difficult to compare data between standard methods and the proposed FIA system for mixtures of different total carbonyl mixtures in hydrocarbons, where the content and composition of the total carbonyls varied considerably.

The main purpose of the study was to develop a suitable robust analyser to control the carbonyl content in certain process streams and hydrocarbon products in the petroleum industry. The intent was to monitor any deviation in the levels and contents of the total carbonyls in specific streams or products. It was therefore assumed that the composition of the specific streams or products would remain within certain specifications that could be handled by the proposed system.

The accuracy of the method was determined comparing the results obtained by the proposed FIA system and a standard volumetric method for standard acetone samples in the range 100 to 1 000 mg/*l* in xylene. The results revealed an excellent agreement between the two methods. As an example, a 200 mg/*l* acetone solution was analysed by making use of the proposed FIA method and the average result was 220 mg/*l*, which indicated the suitability of the system.

7.6.3.3 Standard addition

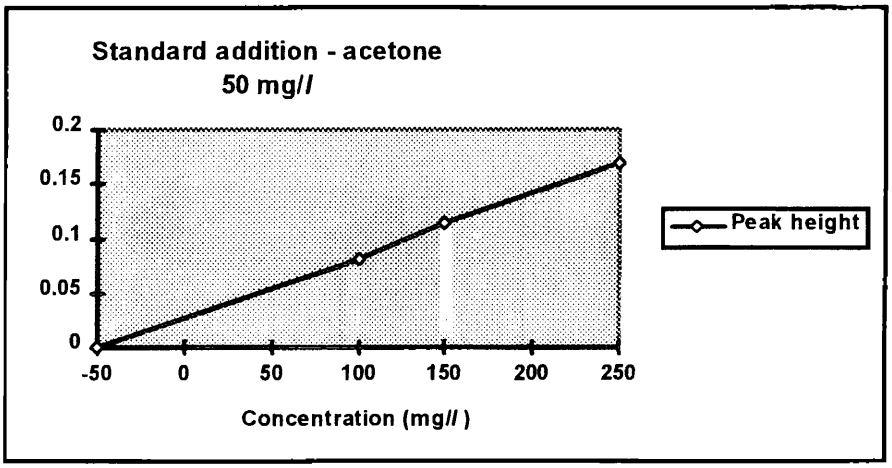

Figure 7.6.3.3A

The accuracy of the method was determined by standard addition to acetone samples in xylene (Fig. 7.6.3.3A). The percentage recovery for acetone was 99%.

7.6.3.4 Precision

The precision of the method was evaluated by doing 14 repetitions of a standard analyte solution in the linear range. The relative standard deviation for acetone was between 1.5% and 1.9%. The RSD for other carbonyl compounds was better than 2.5%.

7.6.3.5 Detection limit

Carbonyl compound	Detection limit (mg/*l*)
acetaldehyde	2.66
2-butanone	5.58
hexyl ketone	2.57
3-heptanone	4.09
decanal	3.84
heptanal	1.83
3-methyl butyraldehyde	5.40
formaldehyde	1.73
3-nonanone	6.74
3-octanone	3.60
pentanal	3.17
nonanal	2.88
2-decanone	3.61
4-heptanone	3.81

Table 7.6.3.5A - Detection limits for different carbonyl compounds.

The detection limits for the individual carbonyl compounds as calculated, are given in Table 7.6.3.5A.

7.6.3.6 Sample interaction

The sample interaction (carry-over effect) between samples was determined by analysing a sample with a low analyte content, followed by one with a high analyte concentration that was again followed by a sample with the same analyte content as the first sample. The sample interaction between samples as calculated was less than 3%.

7.6.3.7 Interferences

Carbonyl compound	Response relative to acetone
2-methyl butyraldehyde	0.150
formaldehyde	0.419
3-nonanone	0.434
3-octanone	0.532
pentanal	0.437
nonanal	0.397
2-decanone	0.497
4-heptanone	0.525

Table 7.6.3.7A - Relative responses to acetone for different carbonyl solutions dissolved in xylene (1 000 mg/l) tested under the same conditions as were used for acetone.

The larger ketones did react, but the reactivity decreased with an increase in the length of the carbon chain, and the system was not adjusted accordingly. Imhof and Bosset [12] have previously done an intensive study on the molar absorptivities of a number of carbonyl compounds. The responses of the carbonyls were compared relative to acetone in this study. The different carbonyls were tested under the same reaction conditions as were used for acetone.

The relative responses for 1 000 mg/l solutions of the different carbonyls are given in Table 7.6.3.7A. It is clear from Table 7.6.3.7A that the composition of the samples had to be taken into account in evaluation of the proposed system. The proposed FIA system was critically evaluated to see if it can be used as a robust analyser that can monitor total carbonyls in industry. As the composition of the different carbonyls may change in samples, this may have an effect on the response of the analyser.

7.6.3.8 Sample frequency

The sample throughput was 15.3 samples per hour.

7.6.4 Conclusion

The determination of carbonyls in xylene by flow injection analysis was investigated. The carbonyls, in an organic phase, were introduced into an aqueous carrier stream, mixed and extracted in a phase separator before the reaction products in the aqueous phase was detected spectrophotometrically at 414 nm. Parameters affecting the performance of the analyser were studied. The proposed analyser is fully computerized and is able to monitor carbonyls in samples at a frequency of 15.3 samples per hour with a relative standard deviation of less than 2.5%. The calibration graphs are linear in the range 100 to 1 000 mg/l and between 250 and 1 000 mg/l for other carbonyls. The detection limits for the individual carbonyls are given.

7.7 References

1. Růžička J, Hansen EH (eds), ***Flow Injection Analysis***, 2nd Edn, John Wiley and Sons, New York, 1988.
2. Valcárcel M, Luque de Castro MD, ***Flow Injection Analysis. Principles and Applications***, Ellis Horwood, Chichester, 1987.
3. McMurry J, ***Organic Chemistry***, 2nd Edn., Brooks/Cole Publishing Company, California, 1988.
4. Dasgupta PK, Zhang G, Schulze S, Marx JN, ***Anal. Chem.***, **66**, 1994, 1965.
5. Bajaj KL, Ahuja KL, ***Analusis***, **8**, 1980, 35.
6. Bajaj KL, ***Talanta***, **23**, 1976, 77.
7. Sawicki E, ***Chemist-Analyst***, **48**, 1959 4.
8. Anger V, Ofri S, ***Z. Anal. Chem.***, **206**, 1964, 185.
9. Munson JW, Hodgkis T, ***Microchemical Journal***, **20**, 1975, 39.
10. Qureshi SZ, Izzatullah, ***Talanta***, **24**, 1977, 529.
11. Belal S, El Kheir AA, Ayad MM, Al Adl SA, ***Analyst***, **111**, 1986, 1039.
12. Imhof R, Bosset JO, ***Mitt. Gebiete Lebensm. Hyg.***, **88**, 1989, 409.
13. Marshall GD, van Staden JF, ***Anal. Instrum.***, **20**, 1992, 79.

CHAPTER 8

DETERMINATION OF ALCOHOLS IN WINE, BEER, WATER AND OIL BY FLOW-INJECTION ANALYSIS

8.1 Introduction

Alcohols occur widely in nature and have many industrial and pharmaceutical applications. Alcohols are present in certain hydrocarbon production streams and final products in petroleum refining processes. Manufacturers in the petroleum industry strive to produce final products that meet certain specifications. The alcohol content in certain process streams and hydrocarbon products in industrial plants has to be controlled. Flow injection analysis has established itself as an analytical technique that is suitable for increasing sample output [1,2].

8.2 Uses of alcohols

Ethanol can be used as a fuel additive, an industrial solvent and a beverage. Ethanol is produced by fermentation of grains and sugars, but this method provides only 5% of the ethanol produced industrially. Today ethanol is mainly produced by acid-catalyzed hydration of ethylene. Menthol is an alcohol that is isolated from peppermint oil and is used as a flavouring and perfumery agent. Cholesterol, a steroidal alcohol, is a causative agent in heart disease. Methanol was prepared by heating wood in the absence of air, but today it is a manufactured by catalytic reduction of carbon monoxide with hydrogen gas.

Methanol is toxic to humans and causes blindness in low doses and death in large amounts. Industrially it is used as a solvent and as a starting material for production of formaldehyde and acetic acid.

8.3 Properties of alcohols

Alcohols are compounds that have hydroxyl groups bonded to saturated, *sp*3-hybridized carbon atoms. This definition of alcohols exclude compounds like phenol (where the hydroxyl group is bonded to an aromatic ring) and enols (where the hydroxyl groups are bonded to a vinylic carbon). The chemistry of phenols, alcohols and enols is quite different.

Alcohols can be thought of as organic derivatives of water in which one of the hydrogens has been replaced by an organic group. The R-O-H bond angle has an approximately tetrahedral value (109° in methanol).

The reason for the high boiling points for alcohols (1-buthanol's boiling point is 117.5°C) is that alcohols are highly associated in solution because of hydrogen bonds.

Alcohols are weakly acidic (pK_a for ethanol is 16.00). When electron-withdrawing groups stabilize the secondary or tertiary alcohol, the pK_a value is lower, resulting in a stronger acidic alcohol. The solvation effect of water surrounding a sterically accessible oxygen atom of unhindered alcohols also results in the alcohol being a stronger acid. Alcohols are much weaker than carboxylic acids and do not react with weak bases (amines, bicarbonate ions or metal hydroxides), but they will react with strong bases like sodium amide, sodium hydride alkyllithium reagents and Grignard reagents. Alcohols can be dehydrated to yield alkenes, they can be converted into alkyl halides or tosylates and alcohols can be oxidized to yield carboxylic acids or ketones.

8.4 Choice of analytical method

Alcohol in wine can be determined by oxidizing the alcohol with potassium dichromate and then measuring the chromic ion spectrophotometrically [3]. The sample preparation step is time-consuming, as the samples have to be distilled and then heated again for the oxidation step.

A nickel oxide electrode was used for the determination of ethanol in an air-stream [4]. The electrode was not selective enough and an air stream purge and trap method had to be used. Low-molecular-mass alcohols, aldehydes and amines reacted at the nickel oxide electrode and interferences could still not be ruled out completely.

Alcohol can be determined enzymatically by using flow-injection analysis [5]. The determination is based on the catalytic oxidation of alcohol by alcohol dehydrogenase (ADH) in the presence of the coenzyme NAD^+.

A triple-pulse potential waveform at platinum electrodes was used to determine simple alcohols amperometrically [6]. The loss of activity for noble-metal electrodes, from adsorbed organic compounds was overcome by the use of a triple-step pulsed-potential waveform. This method can be used to determine methanol, ethanol and ethylene glycol.

Alcohol dehydrogenase was immobilised by reaction with glutaraldehyde onto silica gel, which was packed in a column in a flow system [7]. Ethanol was determined by catalysis of the reaction with NAD^+ and the NADH produced was detected amperometrically. The peak current was a non-linear function of ethanol concentration.

An oxidase-electrode (without the immobilisation of the enzyme) in a flow-injection system was used for the determination of ethanol in beverages [8]. A layer of cigarette paper was impregnated with the alcohol oxidase solution. The half life of the entrapped enzyme was 5 days.

The violet complex of vanadium(V)-N-phenyl benzohydroxamate in chloroform is susceptible to traces of alcohols, which change the colour of the complex to pale yellow [9]. Phenols and cresols interfere with the determination of alcohols.

A four channel FIA-system was developed for the on-line process monitoring of an anaerobic bacterial ethanol fermentation with Zymomonas Mobilis in a fluidized bed reactor [10]. Parallel configured gas diffusion and membrane dialysis were used. The glucose, ethanol, acetaldehyde and L-lactate were detected at a fluorescence detector.

A gas sensor was used to detect ethanol in biological liquids [11]. Methanol and isopropyl alcohol interfered with this determination.

Most of the methods to determine ethanol made use of enzymes [12-38]. Immobilised enzymes had to be used, which can be expensive and the stability of the reactors has to be checked regularly.

Ethanol was determined by using flow-injection enthalpimetry [39]. The calibration graph was curved and the enthalpimetric signals for the lower concentration region consisted of double peaks.

Alcohol can be oxidised by a dichromate membrane and determined by the reduction of the excess dichromate with ferrous ion in a flow system [40]. The use of a gas-diffusion separation unit made the analysis of beer and wine possible, by ruling out the interference of coexisting species, such as sugars, organic acids and amino acids.

The total alcohol content in a sample can be determined by using acetic anhydride to esterificate the alcohol [41]. The excess acetic anhydride is titrated with a standard volumetric ethanolic potassium hydroxide solution in the presence of phenolphthalein as indicator. This method is time consuming and the use of pyridine is not recommended due to its toxicity and unpleasant odour.

Ruthenium dioxide-modified electrodes can be used for the detection of simple alcohols [42]. The responses of methanol, ethanol and 1-propanol are small relative to glycerol when detected with these electrodes.

The alcohol content of alcoholic drinks can be determined by making use of the dissociation of the bis(O,O'-dipropyl dithiophosphato)nickel(II) complex in water-ethanol mixed solvents [43]. Precipitation occurred upon the addition of pure ethanol to the drinks and this caused negative errors due to adsorption between the precipitate and the nickel(II) complex.

Ethanol can be determined colorimetrically by coupling the alcohol with diazotized *p*-aminobenzoic acid [44]. In this investigation, the in-line synthesis of diazotized *p*-aminobenzoic acid and the second in-line synthesis of the coupled ethanol diazotized *p*-aminobenzoic acid product, were investigated. The following reaction was used to determine different alcohols in water:

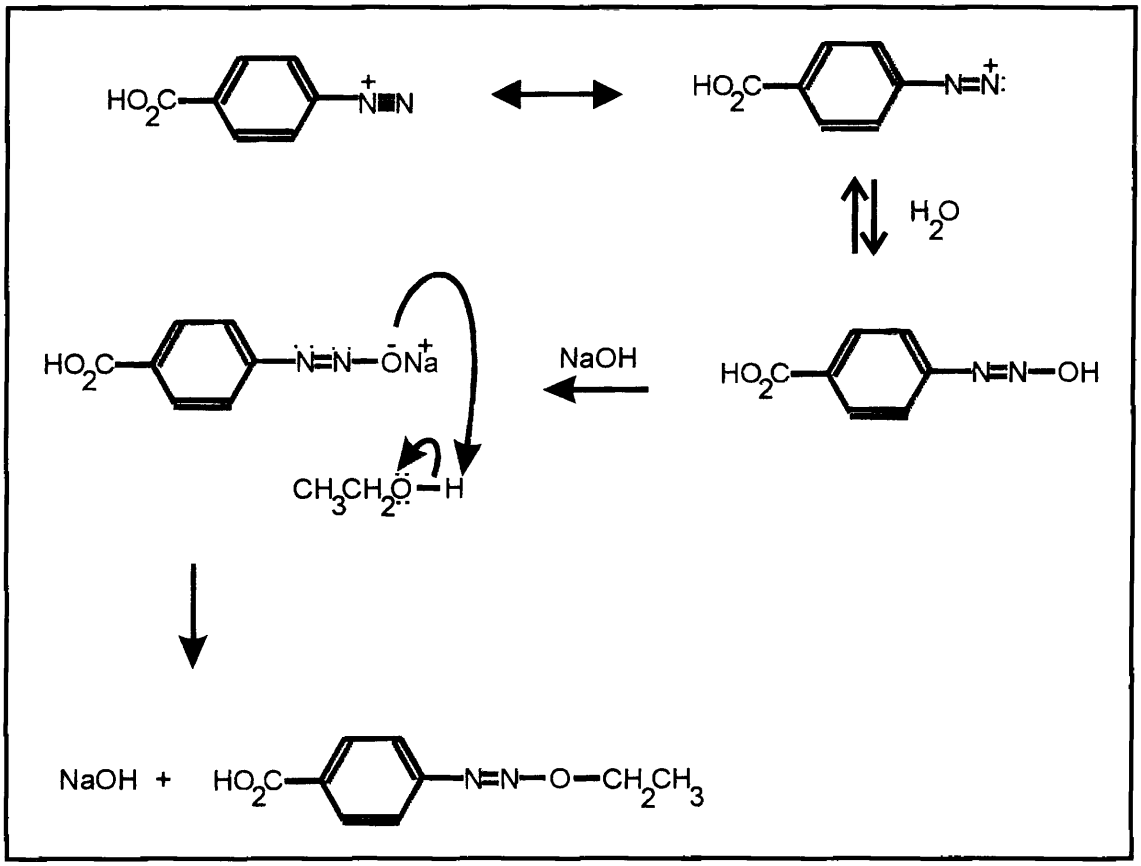

Figure 8.4A - Chemical reaction used for the determination of alcohols in water and oil.

The diazotized *p*-aminobenzoic acid was synthesised in-line by mixing a *p*-aminobenzoic acid solution and a sodium nitrite solution. This stream then merged with a sodium hydroxide stream to form the carrier stream. The alcohol sample was then injected in this carrier stream, followed by detection at 420 nm.

8.5 Determination of alcohols in water by flow-injection analysis

8.5.1 Experimental

8.5.1.1 Reagents and solutions

A stock solution of ethanol containing 1 000 mg/*l* was prepared by mixing the appropriate amount of ethanol (Merck) with deionized water. Working standard solutions were prepared by suitable dilution of the stock solution with deionized water. A 0.5 mol/*l* aqueous solution of hydrochloric acid was prepared.

The *p*-aminobenzoic acid solution was prepared daily by dissolving 3.75 g of the salt in 250 m*l* 0.5 mol/*l* hydrochloric acid. The sodium nitrite solution was freshly prepared by dissolving 18.75 g of the salt in 250 ml deionized water. The NaOH solution was prepared by dissolving 300 g of the salt in 1 *l* deionized water.

8.5.1.2 Apparatus

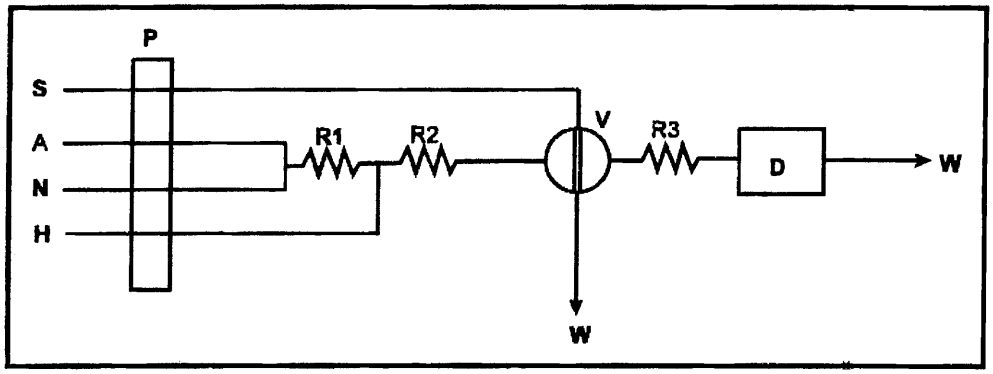

Figure 8.5.1.2A - Flow injection system constructed for the determination of alcohol in water.

S = sample
A = *p*-aminobenzoic acid
N = $NaNO_2$
H = NaOH
P = pump
V = valve
W = waste
D = detector
R1, R2, R3 = reactors

The flow injection system outlined in Fig. 8.5.1.2A was constructed from the following components: a Gilson Minipuls peristaltic pump (used to pump the reagents), a VICI Valco 10-port multi-functional sampling valve and a Unicam 8625 UV-visible spectrophotometer equipped with a 10-mm Hellma debubbler flow-through cell (volume 80 µl) for detection at 420 nm.

Data acquisition and device control were achieved using a PC30-B interface board (Eagle Electric, Cape Town, South Africa) and an assembled distribution board (MINTEK, Randburg, South Africa). The FlowTEK [45] software package (obtainable from MINTEK) for computer-aided flow analysis was used throughout for device control and data acquisition.

The system consists of four lines: the sodium nitrite stream, *p*-aminobenzoic acid stream, the sodium hydroxide stream and the sample stream. Teflon tubing (0.76 mm i.d.) was used. Acidflex tubing was used to pump the reagents.

8.5.1.3 Procedure

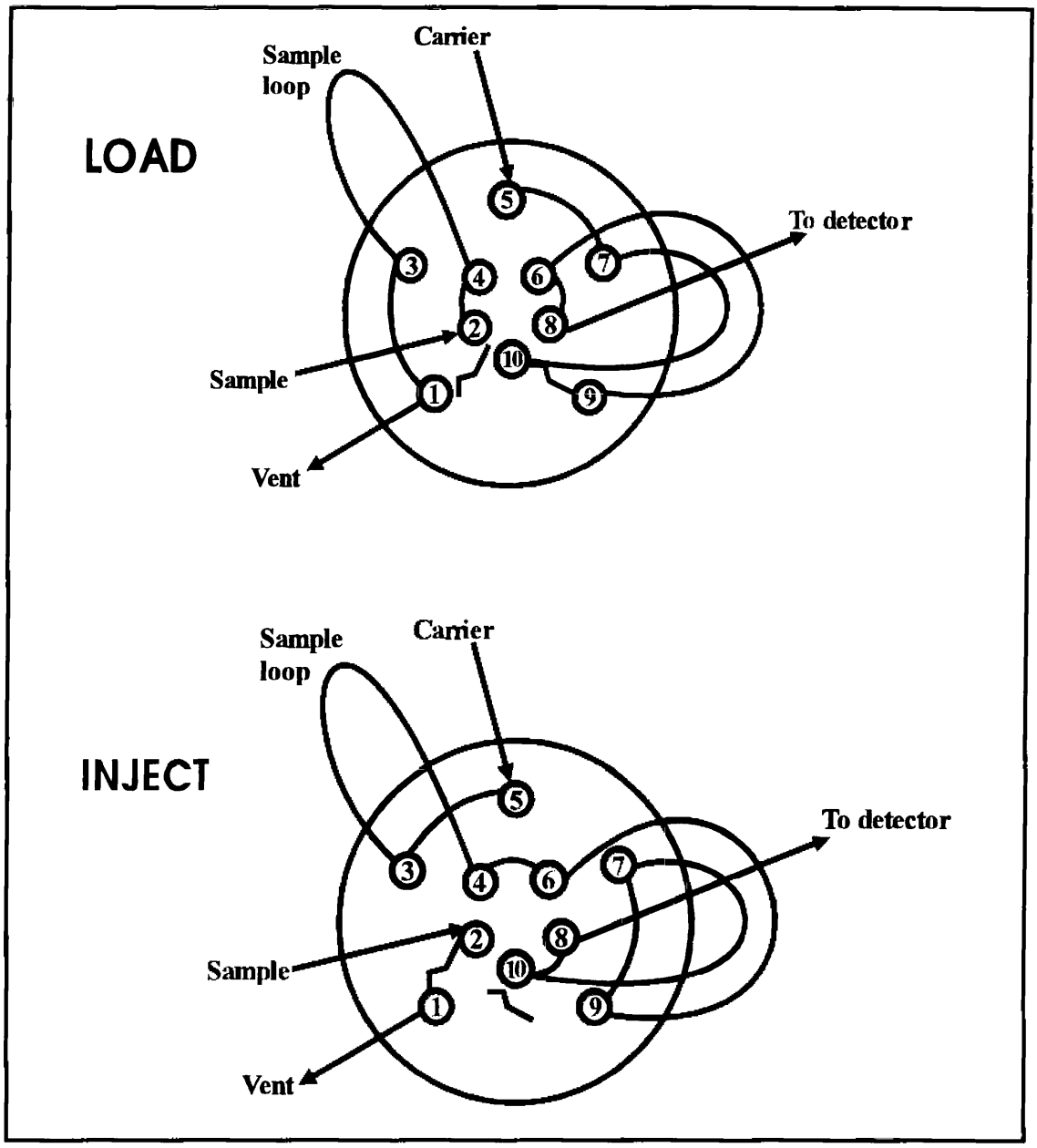

Figure 8.5.1.3A - Valve configuration.

All the reagents and samples were cooled to less than 5°C with ice before using them in the analysis. The sodium nitrite solution was mixed with the *p*-aminobenzoic acid solution in a cooled mixing coil. The sodium hydroxide solution merged with this mixture and was mixed in a mixing coil to form the final carrier stream.

The valve was switched to the inject position for 5 seconds to inject the alcohol in water sample in the carrier stream. The valve then switched to the load position to rinse the sample loop with the next sample, while the injected sample was rinsed to the detector by the carrier stream. The carrier stream, consisting of the sodium nitrite, *p*-aminobenzoic acid and sodium hydroxide mixture, was used as blank for the analysis.

Wavelength scans of the maximum absorbance for the yellow coloured reaction product for ethanol gave a wavelength of 418 nm when the diasotized *p*-aminobenzoic acid and NaOH mixture was used as background. When water was used as background for the same scan, the wavelength of maximum absorbence was 301 nm. A wavelength of 420 nm was selected as optimum wavelength to determine the ethanol in water for two reasons. Firstly, the design of the system was done in such a way that the diasotized *p*-aminobenzoic acid and NaOH mixture had to be used as background and secondly there was a high background absorption at wavelengths just lower than 418 nm.

The temperature was not optimised, as the reagents had to be cooled down with ice to a temperature of less than 5°C. A diasotized compound is used in this determination, this temperature must be maintained throughout the system. A rise in temperature causes the diazotized compound to decompose, forming nitrogen gas bubbles in the flow system. This caused an obvious loss in sensitivity of the ethanol determination. Temperatures lower than 0°C causes the reagents to freeze and the reaction coils could only be cooled down while there was a flow of water or reagents in the system.

8.5.2 Method optimization

8.5.2.1 Physical parameters

8.5.2.1.1 Flow rate

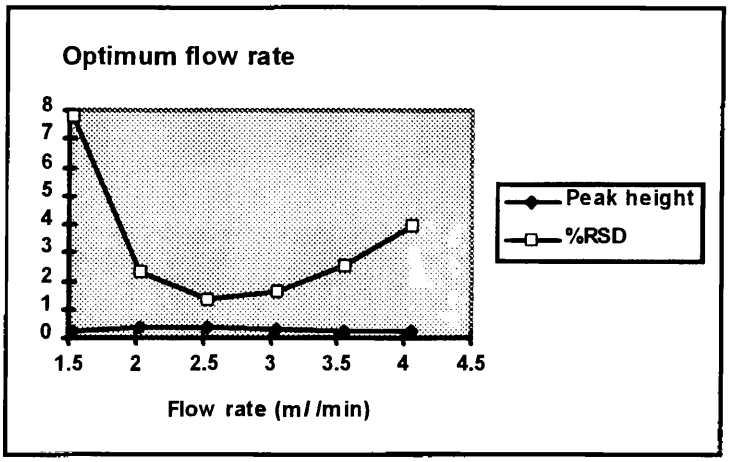

Figure 8.5.2.1.1A - Optimum flow rate.

Several factors that influence the response and %RSD values of the ethanol determination, were optimised and the optimum conditions were chosen so that the highest response and lowest %RSD values could be obtained.

The results illustrated in Fig. 8.5.2.1.1A clearly indicate an optimum flow rate of 2.58 ml/min for the carrier stream. Although the dispersion decreased with an increasing flow rate, resulting in an increase in peak height, the %RSD also increased for higher flow rates.

8.5.2.1.2 Sample volume

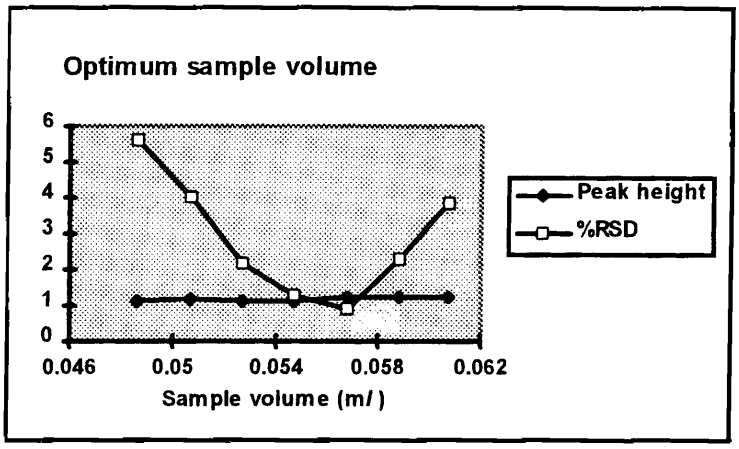

Figure 8.5.2.1.2A - Optimum sample volume.

The sampling volume of the alcohol analyte plays a crucial role in the response and precision of the proposed system. Sampling volumes between 49 and 61 µl were investigated. The results obtained are given in Fig. 8.5.2.1.2A. The response increased with an increase in sample volume. The optimum sample volume of 57 µl gave the best precision and was selected for the proposed system.

8.5.2.1.3 Line length

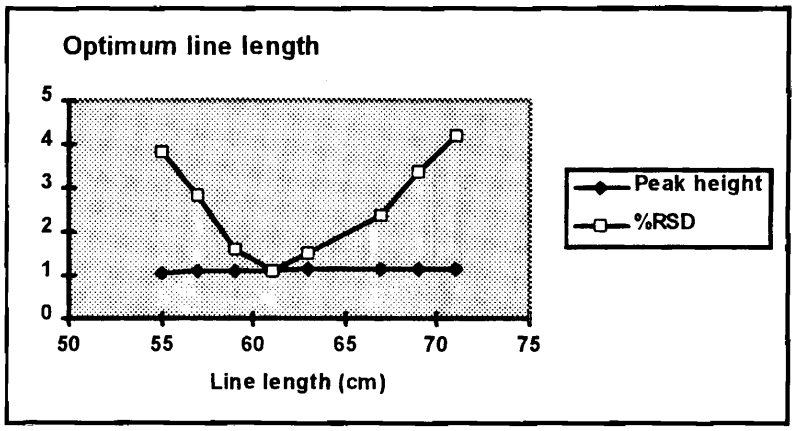

Figure 8.5.2.1.3A - Optimum line length.

Reaction development of the final reaction product started the moment the alcohol was injected into the carrier stream. Mixing and final colour development occurred in the reactor mixing coil R (Fig. 8.5.2.1A) before the final product was transported to the detector. Line lengths between 55 and 71 cm were evaluated.

The results obtained are illustrated in Fig. 8.5.2.1.3A. An optimum reactor length of 61 cm was chosen, as it gave the best precision.

As the diazotizing of the *p*-aminobenzoic acid is an immediate reaction for all practical purposes, only a short reaction coil was used to mix the $NaNO_2$ and *p*-aminobenzoic acid.

8.5.2.2 Chemical parameters

8.5.2.2.1 Volume percentage $NaNO_2$ in the $NaNO_2$ *p*-amino benzoic acid mixture

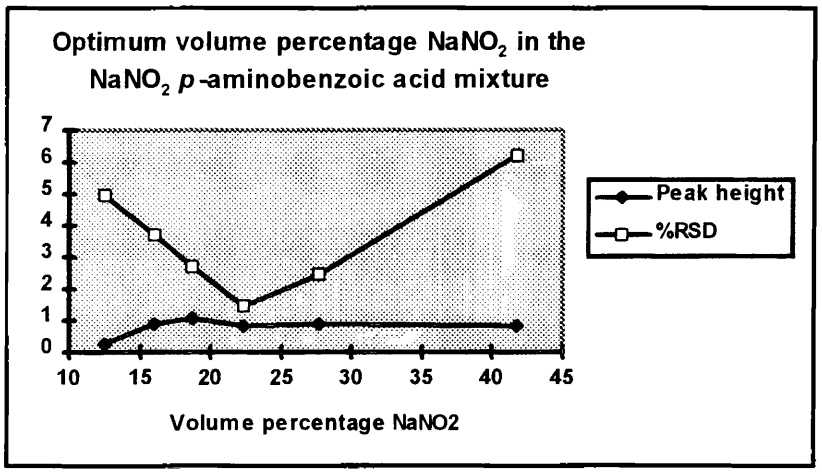

Figure 8.5.2.2.1A - Optimisation of the synthesis of the reagent used in this analysis.

As the colour reagent, diazotized *p*-aminobenzoic acid, was synthesized in-line, this synthesis needed to be optimised to ensure the highest yield possible and this yield had to be repeatable. Any fluctuations in the yield of the colour reagent caused a higher %RSD in the second reaction, which was the final reaction product.

The volume percentage of $NaNO_2$ in the $NaNO_2$ *p*-aminobenzoic acid mixture was optimised and 22.3% $NaNO_2$ was the optimum, as can be seen in Fig. 8.5.2.2.1A. This was achieved by pumping the $NaNO_2$ with a flow rate of 0 28 m*l*/min. A higher volume percentage $NaNO_2$ resulted in an increase in peak height, but volume percentages higher than 18.7% had no significant influence on the peak height. A volume percentage of 22.3% $NaNO_2$ was chosen as optimum, as it resulted in the lowest %RSD values for the ethanol determination.

8.5.2.2.2 $NaNO_2$ concentration

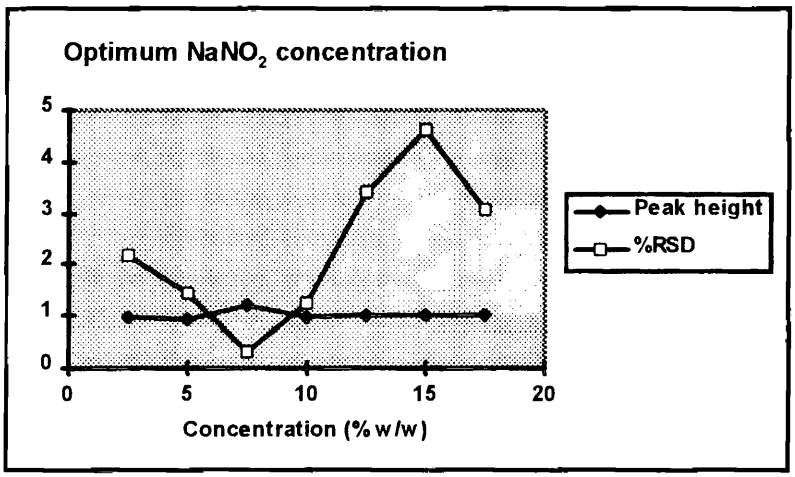

Figure 8.5.2.2.2A - Optimum sodium nitrite concentration.

The optimum concentration of the $NaNO_2$ solution was 7.5 % (w/w), as can be seen in Fig. 8.5.2.2.2A. Diluted $NaNO_2$ solutions resulted in less diazotized *p*-aminobenzoic acid formed and this caused a decrease in the peak height of the ethanol diazotized *p*-aminobenzoic acid product.

8.5.2.2.3 *p*-aminobenzoic acid concentration

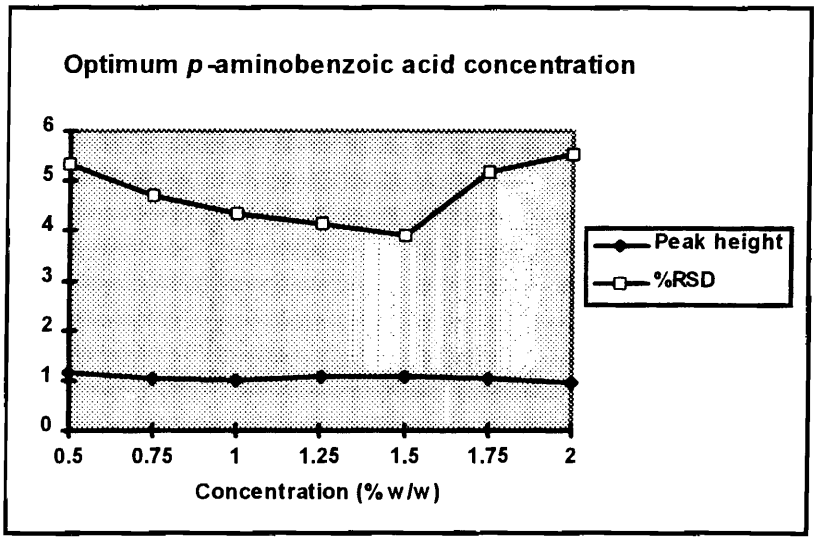

Figure 8.5.2.2.3A - Optimum concentration of *p*-aminobenzoic acid.

The optimum concentration of the *p*-aminobenzoic acid solution was 1.5% (w/w) (Fig. 8.5.2.2.3A). This concentration gave the lowest %RSD values. Diluting the *p*-aminobenzoic acid solution resulted in a decrease in peak height, but using a very concentrated solution would be a waste of reagent, as it clearly did not cause a significant increase in peak height.

8.5.2.2.4 NaOH concentration

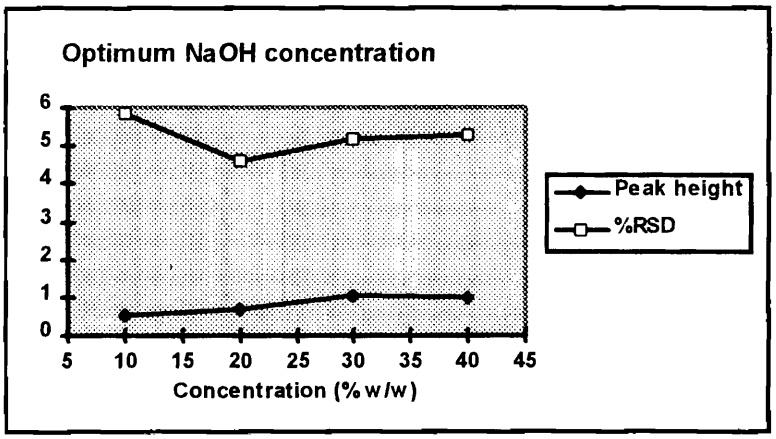

Figure 8.5.2.2.4A - Optimum NaOH concentration.

The concentration of the NaOH solution is crucial in the synthesis of the colour reagent, diasotized *p*-aminobenzoic acid (Fig. 8.4A). The optimum concentration of the NaOH is 30% (w/w) (Fig. 8.5.2.2.4A). Higher concentrations will probably cause an increase in peak height, but the NaOH solutions with concentrations of higher than 30% (w/w) are cloudy and gives higher response values than the reaction product.

8.5.3 Evaluation of the method

8.5.3.1 Linearity

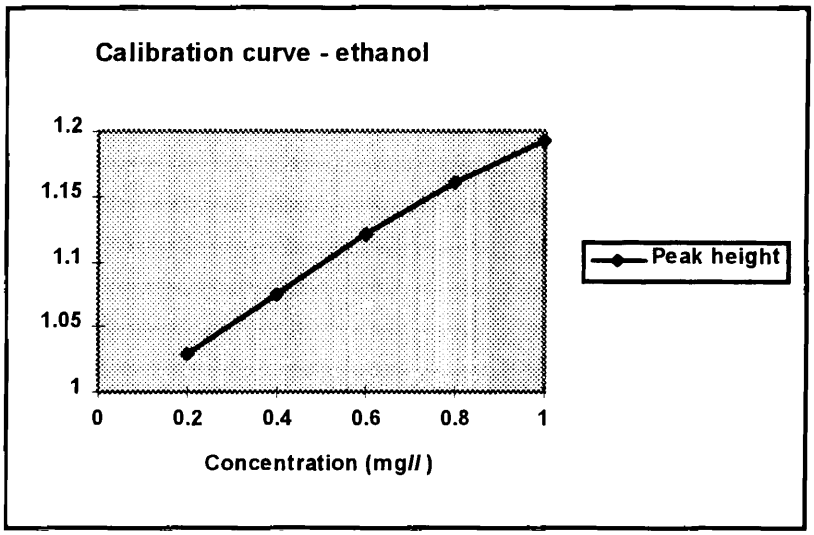

Figure 8.5.3.1A - Calibration curve for ethanol dissolved in water.

Alcohol	Range (mg/*l*)	Correlation coefficient	Relationship between peak height (y) and alcohol concentration (x) in mg/*l*	Relative standard deviation (%)
ethanol	0.2 to 1	0.99	y = 0.204x + 0.988	1.3
methanol	0.5 to 1	0.99	y = 0.102x + 1.054	1.5
1-propanol	0.5 to 1	0.98	y = 0.386x + 0.895	1.3
buthanol	0.5 to 1	0.94	y = 0.142x + 1.084	1.4
iso-propanol	0.5 to 1	0.99	y = 0.166x + 1.2386	1.5

Table 8.5.3.1A - Linear relationship between peak height and concentration for the proposed FIA system for different alcohols.

The proposed FIA system gave a linear calibration for the determination of different alcohols, as the correlation coefficients clearly indicate a linear relationship between the peak height and concentration for the different alcohols.

8.5.3.2 Accuracy

The accuracy of the proposed FIA system was tested by comparing the results of a number of representative samples with the results of a standard procedure employed in industry. A good agreement between the different methods was observed as illustrated from the results on an example of a representative sample given in Table 2. Very dilute solutions of the samples were analyzed, which can explain the difference in the results of wine sample number 3.

Sample	Proposed FIA system (mg/*l*)	Standard method of analysis (mg/*l*)
wine 1	106 920	110 000
wine 2	109 917	115 000
wine 3	97 291	120 000
beer 1	40 775	50 000

Table 8.5.3.2A - Comparison of the results of a sample between the proposed FIA system and a standard method employed in industry.

8.5.3.3 Standard addition

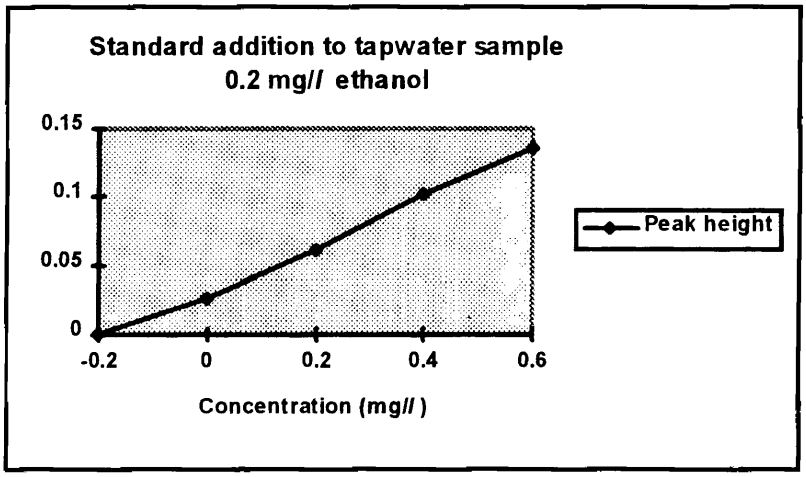

Figure 8.5.3.3A - Standard addition to tapwater sample.

The accuracy of the method was tested by standard addition. Tapwater containing 0.2 mg/*l* ethanol was analised by standard addition and the percentage recovery was 100.2 %.

8.5.3.4 Precision

The relative standard deviation for 14 repetitions of standard analyte solutions in the linear ranges was better than 1.1%..

8.5.3.5 Detection limit

Alcohol	Detection limit (mg/*l*)
methanol	0.068
1-propanol	0.025
buthanol	0.094
iso-propanol	0.110

Table 8.5.3.5 - Detection limits of different alcohols.

The detection limits were calculated using the equation described in 7.5.3.5.

8.5.3.6 Sample interaction

Samples were analysed in a random order to test carry over effects. Sample interaction was calculated as less than 3.0% for the system

8.5.3.7 Interferences

Relevant interfering species were investigated. The diazotized *p*-aminobenzoic acid reacts with methanol, ethanol, 1-propanol, butanol and iso-propanol. Although it was documented that these species do not interfere with the ethanol determination, it was found that small amounts do interfere, since the proposed method is very sensitive [44]. Compounds like ethyl acetate, acetic acid and acetone do not interfere with the analysis.

8.5.3.8 Sample frequency

The sample throughput was 43 samples per hour.

8.5.4 Conclusion

A procedure for the determination of alcohols in water, wine and beer is described. The reaction between alcohol and diazotized *p*-aminobenzoic acid was used. The diazotized *p*-aminobenzoic acid was synthesised in-line by mixing a *p*-aminobenzoic acid solution with a sodium nitrite solution. This stream then merged with a sodium hydroxide stream to form the carrier stream. The alcohol sample was then injected in this carrier stream, followed by detection at 420 nm.

The system is suitable for the determination of alcohol in water, wine and beer at a sampling rate of 43 samples per hour with an RSD of better than 1.1%. The detection limit is 0.03 mg/*l* for ethanol, 0.068 mg/*l* for methanol, 0.025 mg/*l* for 1-propanol, 0.094 mg/*l* for butanol and 0.110 mg/*l* for 2-propanol. The results of the proposed system compared favourably with a standard GC procedure.

8.6 Determination of alcohols in oil by flow-injection analysis

8.6.1 Experimental

8.6.1.1 Reagents and solutions

All oil samples were kindly provided by Sasol. A stock solution of ethanol containing 1 000 mg/*l* was prepared by mixing the appropriate amount of ethanol with xylene. Working standard solutions were prepared by suitable dilution of the stock solution with xylene.

A 0.5 mol/*l* aqueous solution of hydrochloric acid was prepared. The *p*-aminobenzoic acid solution was freshly prepared by dissolving 3.75 g of the salt in 250 m*l* 0.5 mol/*l* hydrochloric acid. The sodium nitrite solution was freshly prepared by dissolving 18.75 g of the salt in 250 m*l* deionized water. The NaOH solution was prepared by dissolving 300 g of the salt in 1*l* deionized water.

8.6.1.2 Apparatus

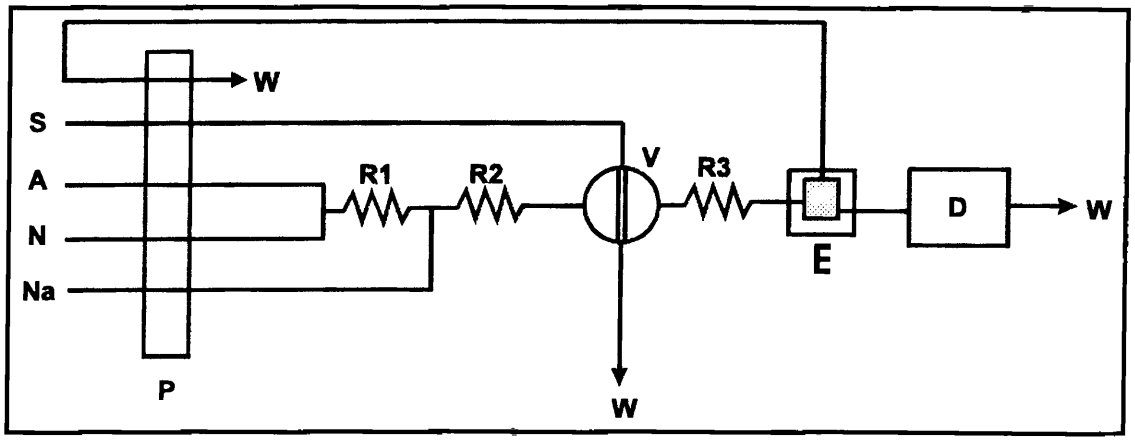

Figure 8.6.1.2A - Flow injection system used for the determination of ethanol in oils.

S = sample
A = *p*-aminobenzoic acid
N = $NaNO_2$ solution
Na = NaOH solution
P = peristaltic pump
V = valve
W = waste
D = detector
R_1, R_2, R_3 = reactors
E = phase separator

The flow injection system outlined in Fig. 8.6.1.2A was constructed from the following components: a Gilson Minipuls peristaltic pump (used to pump the reagents), a VICI Valco 10-port multi-functional sampling valve and a Unicam 8625 UV-visible spectrophotometer equipped with a 10-mm Hellma debubbler flow-through cell (volume 80 µl) for detection at 420 nm. Data acquisition and device control were achieved using a PC30-B interface board (Eagle Electric, Cape Town, South Africa) and an assembled distribution board (MINTEK, Randburg, South Africa). The FlowTEK [45] software package (obtainable from MINTEK) for computer-aided flow analysis was used throughout for device control and data acquisition.

The system consists of four lines: the sodium nitrite stream, *p*-aminobenzoic acid stream, the sodium hydroxide stream and the sample stream. Teflon tubing (0.76 mm i.d.) was used. Acidflex tubing was used to pump the reagents.

8.6.1.3 Procedure

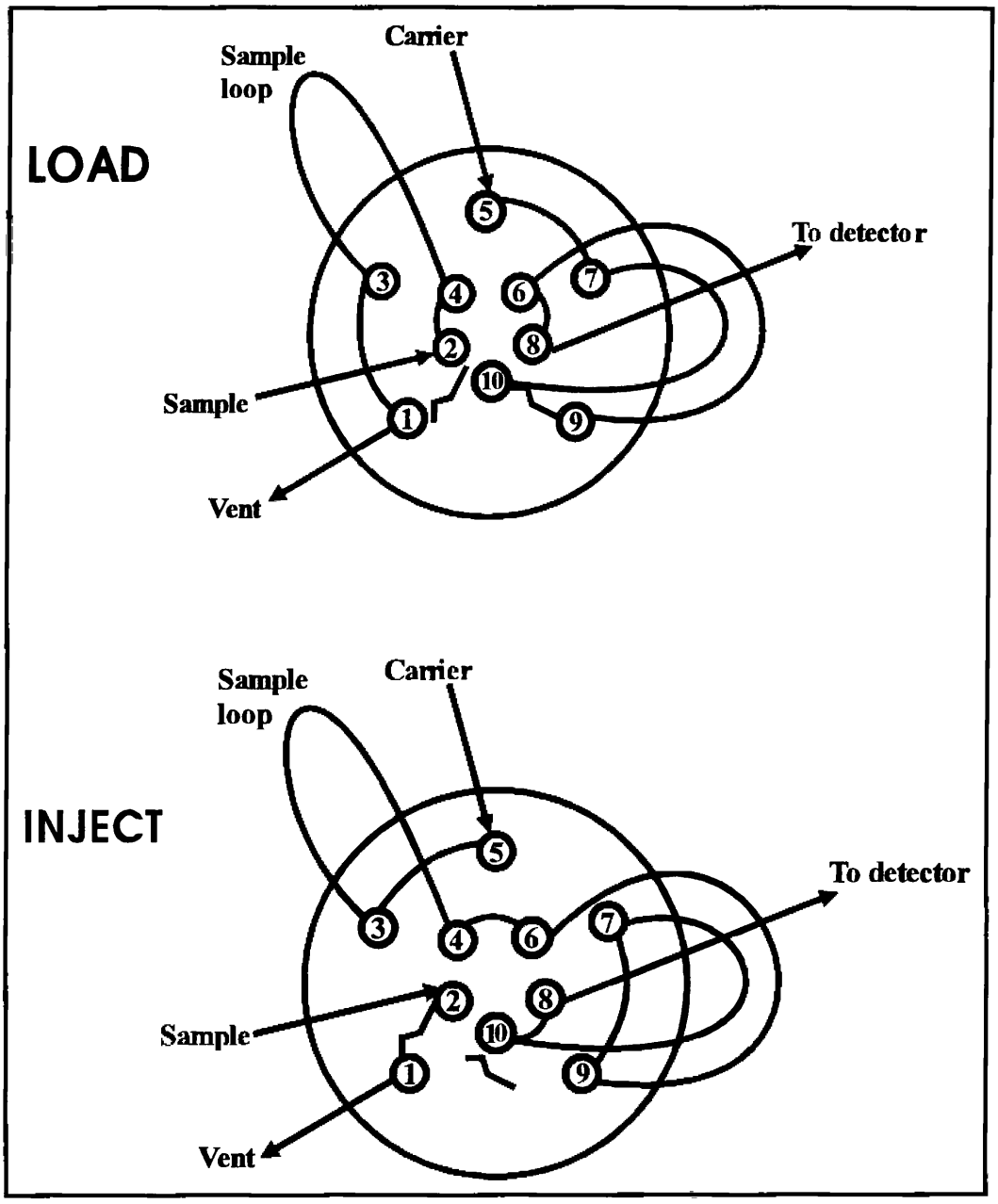

Figure 8.6.1.3A

All the reagents and samples were cooled to less than 5°C with ice before the alcohol determination was started. The sodium nitrite solution was mixed with the *p*-aminobenzoic acid solution in a cooled mixing coil. The sodium hydroxide solution merged with this mixture and was mixed in a cooled mixing coil to form the final carrier stream.

The valve was switched to the **INJECT** position for 5 seconds to inject the alcohol in xylene sample in the carrier stream (Fig. 8.6.1.3A). The valve then switched to the **LOAD** position to rinse the sample loop with the next sample, while the injected sample was rinsed to the reactor and extractor, followed by detection at 420nm. The carrier stream was used as blank for the analysis.

Wavelength scans of the maximum absorbance for the yellow coloured reaction product for ethanol gave a wavelength of 418 nm. A wavelength of 420 nm was selected as optimum to determine the ethanol in oil.

8.6.2 Method optimization

8.6.2.1 Physical parameters

8.6.2.1.1 Flow rate

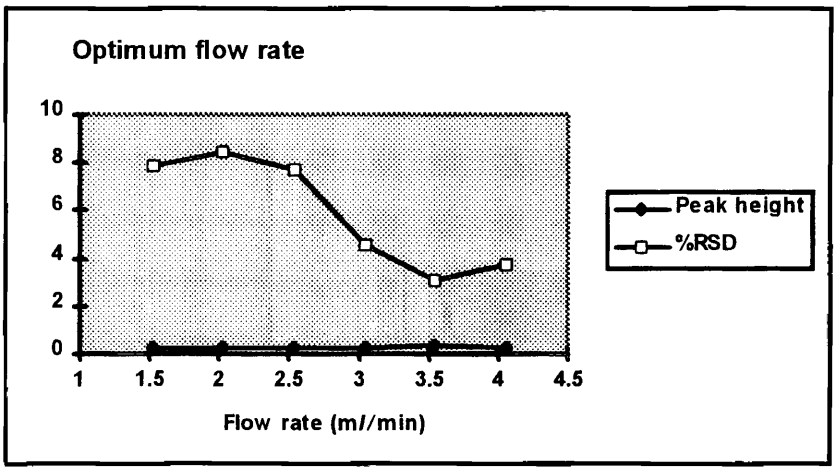

Figure 8.6.2.1.1A - Optimum flow rate.

Several factors that influence the response and %RSD values of the ethanol determination, were optimized and the optimum conditions were chosen so that the highest response and lowest %RSD values could be obtained.

The results in Fig. 8.6.2.1.1A clearly indicates an optimum flow rate of 2.58 ml/min for the carrier stream. Although the dispersion decreased with an increasing flow rate, resulting in an increase in peak height, the %RSD also increased for higher flow rates.

8.6.2.1.2 Sample volume

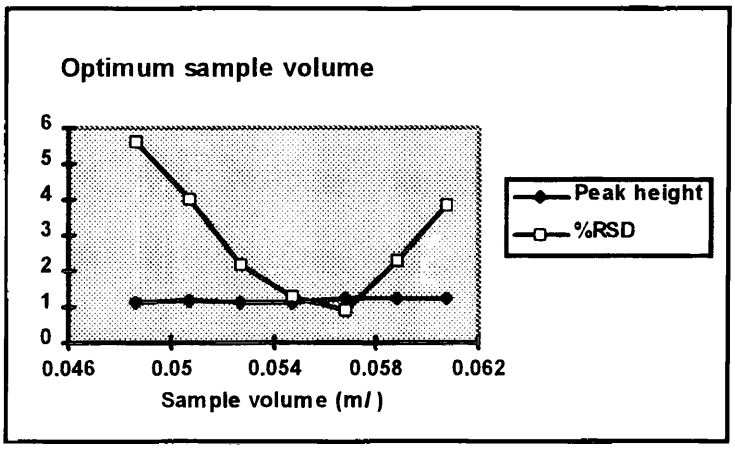

Figure 8.6.2.1.2A - Optimum sample volume.

The sampling volume of the alcohol analyte plays a crucial role in the response and precision of the proposed system. Sampling volumes between 49 and 61 µl were investigated. The results obtained are given in Fig. 8.6.2.1.2A. The response increased with an increase in sample volume. The optimum sample volume of 57 µl gave the best precision and was selected for the proposed system.

8.6.2.1.3 Line length

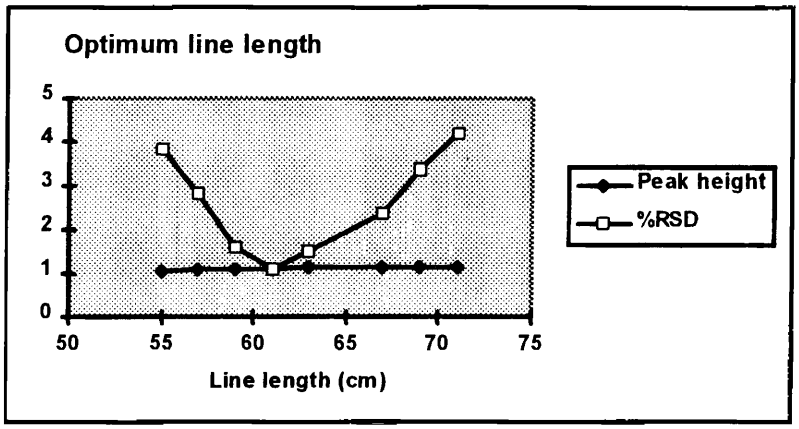

Figure 8.6.2.1.3A - Optimum reactor length.

Reaction development started the moment the alcohol was injected into the carrier stream. Mixing and final colour development occured in the reactor mixing coil R (Fig. 8.6.1.2A), before the final product was transported to the detector. Line lengths between 55 and 71 cm were evaluated. The results obtained are illustrated in Fig. 8.6.2.1.3A. An optimum reactor length of 61 cm was chosen, as it gave the best precision. As the diazotizing of the *p*-aminobenzoic acid is an immediate reaction for all practical purposes, only a short reaction coil was used to mix the $NaNO_2$ and *p*-aminobenzoic acid.

The temperature was not optimized, as the reagents had to be cooled down with ice to a temperature of less than 5°C. As a diazotized compoud is used in this determination, this temperature must be maintained throughout the system. A rise in temperature causes the diazotized compound to decompose, forming nitrogen gas bubbles in the flow system. This causes an obvious loss in sensitivity of the ethanol determination. A temperature of lower than 0°C causes the reagents to freeze and the reaction coils could only be cooled down once there was a flow of water or reagents in the system.

8.6.2.2 Chemical parameters

8.6.2.2.1 Volume percentage of $NaNO_2$ in the $NaNO_2$ *p*-aminobenzoic acid mixture

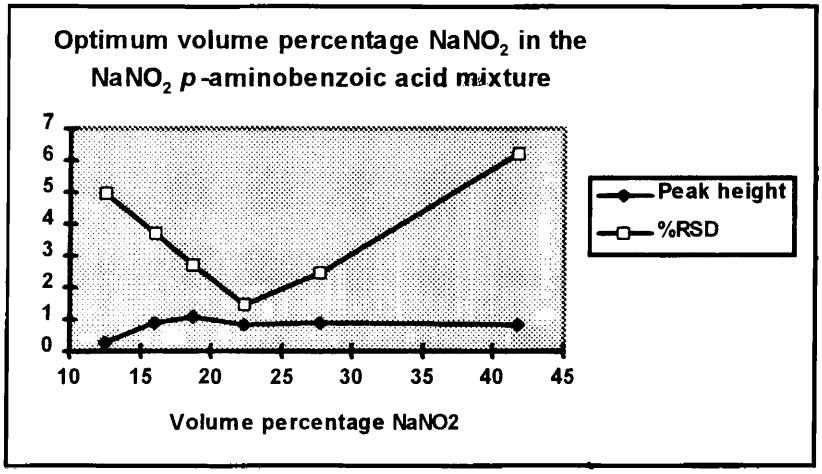

Figure 8.6.2.2.1A.

As the "colour reagent", diazotized *p*-aminobenzoic acid, was synthesized in-line, this synthesis needed to be optimized to ensure the highest yield possible, but this yield had to be repeatable. Any fluctuations in the yield of the colour reagent caused a higher %RSD in the second reaction, which was the determination of ethanol.

The volume percentage of $NaNO_2$ in the $NaNO_2$ *p*-aminobenzoic acid mixture was optimized and 22.3% $NaNO_2$ was the optimum, as can be seen in Fig. 8.6.2.2.1A. This was achieved by pumping the $NaNO_2$ with a flow rate of 0.28 m*l*/min.

A higher volume percentage of $NaNO_2$ resulted in an increase in peak height, but volume percentages of higher than 18.7% had no significant influence on the peak height. A volume percentage of 22.3% $NaNO_2$ was chosen as optimum, as it resulted in the lowest %RSD values for the ethanol determination.

8.6.2.2.2 $NaNO_2$ concentration

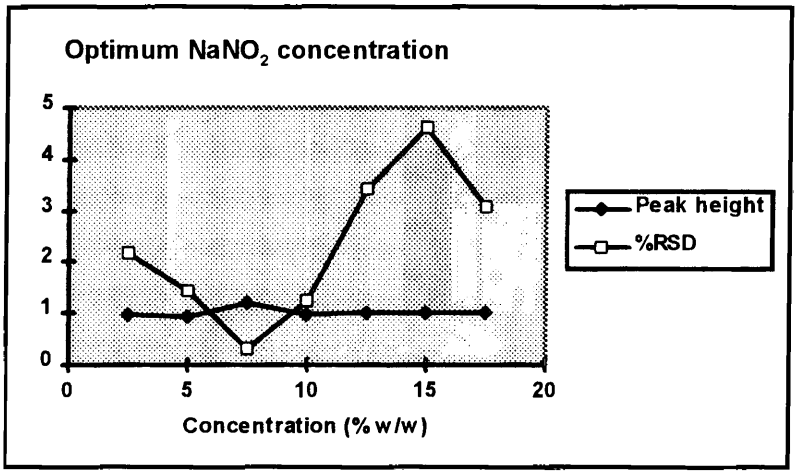

Figure 8.6.2.2.2A - Optimum $NaNO_2$ concentration.

The concentration of the $NaNO_2$ solution was optimized and found to be 7.5 % (w/w), as can be seen in Fig. 8.6.2.2.2A. Diluted $NaNO_2$ solutions resulted in less diasotized *p*-aminobenzoic acid formed and a decrease in the peak height of the ethanol diazotized *p*-aminobenzoic acid product.

8.6.2.2.3 *p*-aminobenzoic acid concentration

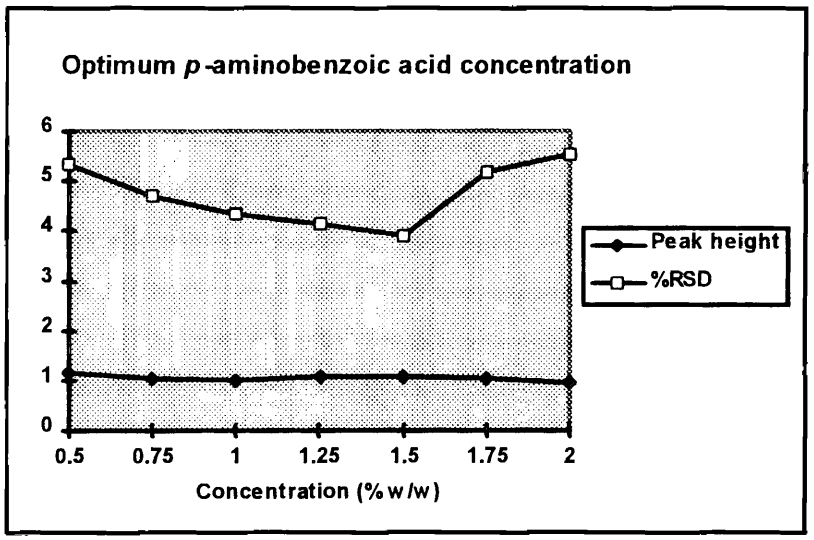

Figure 8.6.2.2.3A - Optimum *p*-aminobenzoic acid concentration.

The optimum concentration of the *p*-aminobenzoic acid solution was 1.5% (w/w) (Fig. 8.6.2.2.3A). This concentration gave the lowest %RSD values. Diluting the *p*-aminobenzoic acid solution resulted in a decrease in peak height, but using very concentrated solution would be a waste of reagent, as it clearly didn't cause a significant increase in peak height.

8.6.2.2.4 NaOH concentration

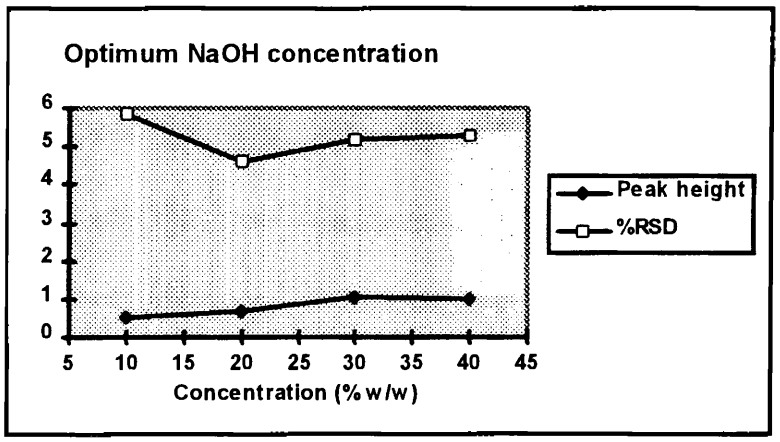

Figure 8.6.2.2.4A - Optimum NaOH concentration.

The concentration of the NaOH solution is crucial in the synthesis of the colour reagent, diasotized *p*-aminobenzoic acid. The optimum concentration of the NaOH solution is 30% (w/w) (Fig. 8.6.2.2.4A).

Higher concentrations will probably cause an increase in peak height, but the NaOH solutions with concentrations of higher than 30% (w/w) are cloudy and have higher absorbencies than the reaction product.

8.6.3 Evaluation of the method

8.6.3.1 Linearity

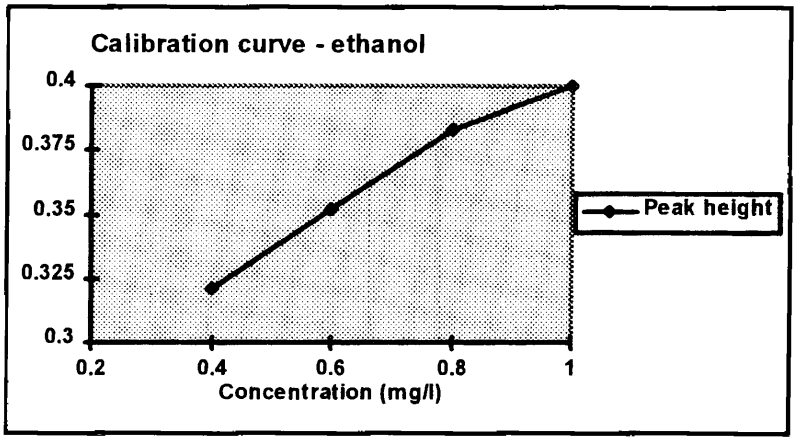

Figure 8.6.3.1A

The proposed FIA system gave a linear calibration for the determination of different alcohols, as the correlation coefficients clearly indicate a linear relationship between the peak height and concentration for the different alcohols (Fig. 8.6.3.1A).

Alcohol	Range (mg/l)	Correlation coefficient	Relationship between peak height (y) and alcohol concentration (x) in mg/l	Relative standard deviation (%)
ethanol	0.4 to 1	0.99	y = 0.155x + 0.259	2.0
methanol	0.5 to 1	0.96	y = 0.195x + 0.076	2.1
1-propanol	0.5 to 1	0.98	y = 0.244x + 0.080	2.0
buthanol	0.5 to 1	0.96	y = 0.059x + 0.212	2.2
iso-propanol	0.5 to 1	0.99	y = 0.034x + 0.220	2.1

Table 8.6.3.1A - Linear relationship between peak height and concentration for the proposed FIA system for different alcohols.

8.6.3.2 Accuracy

The accuracy of the proposed FIA system was tested by comparing the results of a number of representative samples with the results of a standard GC procedure employed in industry. A good agreement between the different methods was observed as illustrated from the results on an example of a representative sample given in Table 8.6.3.2A and B.

Method	Proposed FIA system (% w/w)	GC analysis (% w/w)
ethanol	-	<0.02
propanol	-	0.1
buthanol	-	0.25
pentanol	-	0.58
hexanol	-	0.76
heptanol	-	0.86
octanol	-	0.81
nonanol	-	0.69
decanol	-	0.53
undekanol	-	0.31
dodecanol	-	0.16
tridecanol	-	0.08
tetradecanol	-	0.03
pentadecanol	-	0.02
Total alcohols	7.8	5.17

Table 8.6.3.2A - Comparison of the results of a synthetic oil sample between the proposed FIA system and a standard GC-method employed in industry.

Method	Proposed FIA system (% w/w)	Standard alcohol method (% w/w)	Standard GC method (% w/w) (primary and secondary alcohols)
Total alcohols	3.4	3.1	2.9

Table 8.6.3.2B - Comparison of the result of a FT-liquid oil sample between the proposed FIA system, a standard alcohol determination (used in industry) method and a standard GC-method in industry.

8.6.3.3 Standard addition

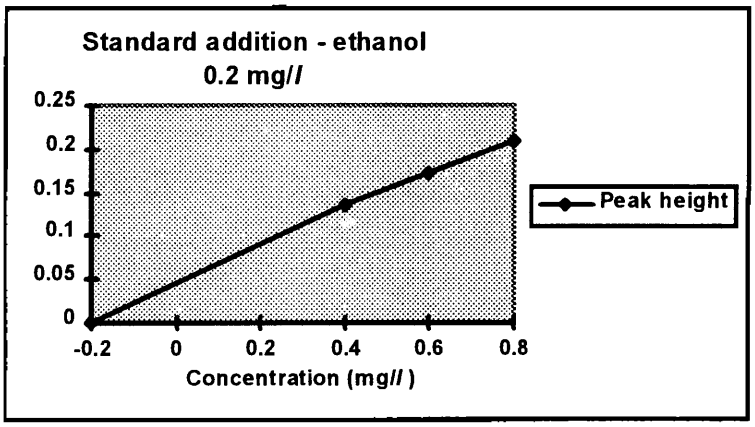

Figure 8.6.3.3A

The accuracy of the method was determined by standard addition to ethanol samples in xylene. The percentage recovery for ethanol was 99%.

8.6.3.4 Precision

The relative standard deviation for 14 repetitions of standard analyte solutions in the linear ranges was better than 2.0 %.

8.6.3.5 Detection limit

Alcohol	Detection limit (mg/*l*)
ethanol	0.039
methanol	0.032
1-propanol	0.025
buthanol	0.011
iso-propanol	0.019

Table 8.6.3.5A - Detection limits of different alcohol compounds.

The detection limits for the different alcohols with the proposed FIA system were calculated using the equation in section 7.5.3.5 (Table 8.6.3.5A).

8.6.3.6 Sample interaction

Samples were analysed in a random order to test carry over effects. Sample interaction was calculated as less than 2.0 % for the system

8.6.3.7 Interferences

Relevant interfering species were investigated (Table 8.6.3.1A). The diazotized *p*-aminobenzoic acid reacts with methanol, ethanol, 1-propanol, butanol and iso-propanol. Although it was documented that these species do not interfere with the ethanol determination, it was found that small amounts do interfere, since the proposed method is very sensitive [44]. Compounds like ethyl acetate, acetic acid and acetone do not interfere with the analysis.

8.6.3.8 Sample frequency

The sample throughput was 40 samples per hour.

8.6.4 Conclusion

A procedure for the determination of alcohols in xylene is described. The reaction between alcohols and diazotized *p*-aminobenzoic acid was used. The diazotized *p*-aminobenzoic acid was synthesized in-line by mixing a *p*-aminobenzoic acid solution with a sodium nitrite solution. This stream then merged with a sodium hydroxide stream to form the carrier stream. The alcohol sample was injected in this carrier stream.

The alcohol was extracted from the xylene by mixing the sample with the aqueous carrier stream and the xylene was then seperated from the aqueous stream, using an extractor. The carrier stream containing the alcohol condensation product was then pumped to the detector.

The system is suitable for the determination of alcohols in oil at a sampling rate of 40 samples per hour with an RSD of better than 2.0%. The detection limit was 0.039 mg/*l* for ethanol, 0.032 mg/*l* for methanol, 0.025 mg/*l* for 1-propanol, 0.011 mg/*l* for butanol and 0.019 mg/*l* for 2-propanol. The results of the proposed system compared favourably with a standard GC procedure.

8.7 References

1. Růžička J, Hansen EH (eds.), ***Flow Injection Analysis***, 2nd Edn, John Wiley and Sons, New York, 1988.
2. Valcárcel M, Luque de Castro MD, ***Flow Injection Analysis. Principles and Applications***, Ellis Horwood, Chichester, 1987.
3. Crowell EA, Ough CS, ***Am. J. Enol. Vitic.***, **30**, 1, 1978, 61.
4. Morrison TN, Schick KG, Huber CO, ***Analytica Chimica Acta***, **120**, 1980, 75.
5. Worsfold PJ, Růžička J, Hansen H, ***Analyst***, **106**, 1981, 1309.
6. Hughes S, Meschi PL, Johnson DC, ***Analytica Chimica Acta***, **132**, 1981, 1.
7. Yao T, Kobayashi Y, Musha S, ***Analytica Chimica Acta***, **139**, 1982, 363.
8. Schelter-Graf A, Huck H, Schmidt H, ***Z Lebensm Unters Forsch***, **177**, 1983, 356.
9. Sahu BR, Tandon U, ***J. Indian Chem. Soc.***, **60**, 1983, 615.
10. Joksch B, Eberhardt R, Spohn U, Weuster D, Wandrey C (FIA 280
11. Giles HG, Renaud GE, Meggiorini S, ***Alcoholism: Clinical and Experimental Research***, **10**, 5, 1986, 521.
12. Nabi A, Worsfold PJ, ***Analyst***, **111**, 1986, 531.
13. Belghith H, Romette J, Thomas D, ***Biotechnology and Bioengineering***, **30**, 1986, 1001.
14. Lázaro F, Luque de Castro MD, Valcárcel M, ***Anal. Chem.***, **59**, 1987, 1859.
15. Fernández A, Luque de Castro MD, Valcárcel M, ***Fresenius Z. Anal. Chem.***, **327**, 1987, 552.
16. Linares P, Ruz J, Luque de Castro MD, Valcárcel M, ***Journal of Pharmaceutical & Biomedical Analysis***, **5**, 7, 1987, 701.
17. Ruz J, Luque de Castro M, Valcárcel M, ***Analyst***, **112**, 1987, 259.
18. Ruz J, Luque de Castro M, Valcárcel M, ***Microchemical Journal***, **36**, 1987, 316.
19. Maquieira A, Luque de Castro M, Valcárcel M, ***Microchemical Journal***, **36**, 1987, 309.
20. Almuaibed AM, Townshend A, ***Analytica Chimica Acta***, **214**, 1988, 161.
21. Ukeda H, Imabayashi M, Matsumoto K, Osajima Y, ***Agric. Biol. Chem.***, **53**, 11, 1989, 2909.

22. Künnecke W, Schmid RD, ***GBF Monographs***, **13**, 1989, 303.

23. Künnecke W, Schmid RD, ***Dechema Biotechnology Conferences 3 - VCH Verlagsgesellschaft***, 1989, 751.

24. Kubiak WW, Wang J, ***Analytica Chimica Acta***, **221**, 1989, 43.

25. Künnecke W, Schmid RD, ***Analytica Chimica Acta***, **234**, 1990, 213.

26. Maeder G, Veuthey J, Pelletier M, Haerdi W, ***Analytica Chimica Acta***, **231**, 1990, 115.

27. Künnecke W, Schmid RD, ***Journal of Biotechnology***, **14**, 1990, 127.

28. Matsumoto K, Matsubara H, Hamada M, Ukeda H, Osajima Y, ***Journal of Biotechnology***, **14**, 1990, 115.

29. Wangsa J, Danielson ND, ***Electroanalysis***, **3**, 1991, 625.

30. de Boer J, Postema F, Plijter-Groendijk H, Korf J, ***Clinical and preclinical applications***, 1991, 445.

31. Ukeda H, Nakada Y, Matsumoto K, Osajima Y, ***GBF Monographs***, **14**, 1991, 203.

32. Matsumoto K, Matsubara H, Hamada M, Osajima Y, ***Nippon Shokuhin Kogyo Gakkaishi***, **38**, 8, 1991, 699.

33. Xiangfang X, Suleiman A, Guilbault GG, ***Analytica Chimica Acta***, **266**, 1992, 325.

34. Jortani SA, Poklis A, ***Journal of Analytical Toxicology***, **16**, 1992, 368.

35. Förster E, Silva M, Otto M, Pérez-Bendito D, ***Talanta***, **40**, 6, 1993, 855.

36. Kullick T, Beyer M, Henning J, Lerch T, Quack R, Zeitz A, Hitzmann B, Scheper T, Schügerl K, ***Analytica Chimica Acta***, **296**, 1994, 263.

37. Mattos IL, Fernandez-Romero JM, Luque de Castro MD, Valcárcel M, ***Analyst***, **120**, 1995, 179.

38. Mohns J, Künnecke W, ***Analytica Chimica Acta***, **305**, 1995, 241.

39. de Oliveira WA, Pasquini C, ***Analyst***, **113**, 1988, 359.

40. Ohura H, Imato T, Asano Y, Yamasaki S, Ishibashi N, ***Analytical Sciences***, **6**, 1990, 541.

41. ***British Standard BSI***, 1991, 4583.

42. Leech D, Wang J, Smyth MR, ***Electroanalysis***, **3**, 1991, 37.

43. Sasaki Y, Tagashira S, Murakami Y, Kai S, ***Analytical Sciences***, **9**, 1993, 483.

44. Rahim SA, Geeso SG, ***Talanta***, **39**, 11, 1992, 1489.

45. Marshall GD, van Staden JF, ***Anal. Instrum.***, **20**, 1992, 79.

CHAPTER 9

FINAL CONCLUSION

Flow-injection analysis is a powerful tool for substituting tedious manual procedures and to revolutionize conventional operations in the analytical laboratory. FIA is the most advanced form of solution manipulation available to analytical chemists for the mixing of sample, reagents and reaction products and their transport to the measurement point.

FIA has a simple basis, its equipment is not expensive and rapid, accurate and precise results are produced by this versatile method. The researcher can adapt a specific FIA system easily to suit a different application. This technique can be used to obtain excellent and fast results without using glassware and without exposing the analyst to toxic reagents. Reagents and samples are safe from atmospheric gases and contamination.

Phenols, alcohols and carbonyls are present in the light oil mixtures in the Synthol process. The concentration of these compounds present influence some of the synthesis processes. At the moment these type of samples are analysed by gaschromatography.

Gaschromatography is used for detailed, precise analyses, but is time consuming. Conventional methods of analysing these samples are time consuming. Often a fast analysis, which gives a global estimate of the concentration of a compound, is necessary. FIA has an exceptionally high sample throughput and is ideal for fast assays.

In this project methods for determining phenol, carbonyls and alcohols in light oil mixtures were automated and the prospects for application as process analysers were investigated. These different methods were critically evaluated to determine the accuracy, precision, linearity, detection limit, sample interaction, interferences and sample frequency. The results indicated that these systems are suitable for use as process analyzers.

The use of a dialyser in the determination of phenol is an advantage. It is used for the separation of the phenol from a complex sample mixture and this phenol is concentrated. Dialysis is a slow process, but very accurate and precise, especially in this specific application.

Liquid-liquid extraction was used in the determination of ketones and aldehydes in oil, as well as in the determination of ethanol in oil. This was done to remove interferences and to preconcentrate the analyte. With these specific applications, the samples were in organic solutions, and by automating the extraction process, the analyst did not have to cope with the (toxic) odours from the organic solutions used.

The application of these methods as process analysers will give additional information about product streams and this has become imperative in modern manufacturing processes. Timely composition data of the product streams will ensure better quality control of products as required by the consumer, lower quality costs and will give more information on impurities, solvents and wastewater.